3-21-2017

Interference Mitigation, Resource Allocation and Channel Control Techniques for 4G and Beyond Systems

Mustafa Harun Yilmaz
University of South Florida, myilmaz@mail.usf.edu

Interference Mitigation, Resource Allocation and Channel Control Techniques for 4G and Beyond Systems

by

Mustafa Harun Yılmaz

A dissertation submitted in partial fulfillment
of the requirements for the degree of
Doctor of Philosophy
Department of Electrical Engineering
College of Engineering
University of South Florida

Major Professor: Hüseyin Arslan, Ph.D.
Richard D. Gitlin, Sc.D.
Thomas Weller, Ph.D.
Dmitry B. Goldgof, Ph.D.
Mohamed M. Abdallah, Ph.D.

Date of Approval:
February 24, 2017

Keywords: Cognitive Radio, Game Theory, Scheduling, Filtered Multitones, Heterogeneous Networks

DEDICATION

To my family

ACKNOWLEDGMENTS

First, I would give my special thanks to my advisor, Dr. Hüseyin Arslan for his guidance, encouragement, and continuous support throughout my Ph.D. I would like to thank my friends who helped me out in any issue during my Ph.D. in Wireless Communication and Signal Processing group. Also, I would like to thank all my colleagues at the University of South Florida and staff in our department, Electrical Engineering.

I would like also to thank Dr. Khalid A. Qaraqe, Dr. Hassan M. El-Sallabi and especially Dr. Mohamed M. Abdallah from Texas A&M University at Qatar and my friends in Tampa, Florida.

My sincere appreciation goes to my parents for their moral support throughout my Ph.D.

And, my deepest gratitude goes to my wife from my heart for all of her sacrifice, support and patience during my doctorate. I could have never completed this Ph.D. without her and my sweetie son & daughter.

TABLE OF CONTENTS

LIST OF TABLES iv

LIST OF FIGURES v

ABSTRACT viii

CHAPTER 1: INTRODUCTION 1
- 1.1 A Review of the Main Concepts in the Dissertation 3
  - 1.1.1 Game Theory 4
  - 1.1.2 Supermodular Games 5
  - 1.1.3 Potential Games 6
  - 1.1.4 Resource Allocation 7
  - 1.1.5 Reconfigurable Antennas 8
  - 1.1.6 Partially Overlapping Tones 10
- 1.2 Dissertation Outline 10
  - 1.2.1 Chapter 2: Random Subcarrier Allocation with Supermodular Game in Cognitive Heterogeneous Networks 10
  - 1.2.2 Chapter 3: Joint Subcarrier and Antenna State Selection for Cognitive Heterogeneous Networks with Reconfigurable Antennas 11
  - 1.2.3 Chapter 4: Partially Overlapping Filtered Multitone with Reconfigurable Antennas in Heterogeneous Networks 12
  - 1.2.4 Chapter 5: Resource Allocation with Partially Overlapping Filtered Multitone in Heterogeneous Networks 13
  - 1.2.5 Chapter 6: Millimeter-Wave Wireless Channel Control Using Spatially Adaptive Antenna Arrays 13

CHAPTER 2: RANDOM SUBCARRIER ALLOCATION IN COGNITIVE HETEROGENEOUS NETWORKS WITH SUPERMODULAR GAME 15
- 2.1 System Model 17
- 2.2 Game Theoretical Model 18
  - 2.2.1 Supermodular Game Formulation 20
  - 2.2.2 Random Subcarrier Allocation Scheme 21
- 2.3 Performance Evaluation 22
  - 2.3.1 Capacity Level Analysis 24
  - 2.3.2 Throughput Analysis 25

CHAPTER 3: JOINT SUBCARRIER AND ANTENNA STATE SELECTION FOR COGNITIVE HETEROGENEOUS NETWORKS WITH RECONFIGURABLE ANTENNAS 28
3.1 System Model 32
3.1.1 Power Control 33
3.1.2 Reconfigurable Antenna Structure 34
3.2 Problem Formulation 35
3.2.1 Potential Game Formulation 36
3.2.2 Nash Equilibrium Convergence 38
3.3 Solution Framework and Nash Equilibrium Convergence 39
3.3.1 Step 1: Candidate Antenna State Set 39
3.3.2 Step 2: Joint Subcarrier Allocation and Antenna State Selection 40
3.4 Performance Evaluations 42

CHAPTER 4: PARTIALLY OVERLAPPING FILTERED MULTITONE WITH RECONFIGURABLE ANTENNAS IN HETEROGENEOUS NETWORKS 50
4.1 System Model 54
4.1.1 Transmission Model 54
4.1.2 Channel Model 54
4.1.3 Reception Model 56
4.2 Problem Formulation 57
4.2.1 Potential Game Formulation 58
4.2.2 Convergence to Nash Equilibrium 59
4.2.3 FSR and Antenna State Selection Scheme 59
4.3 Performance Evaluation 61
4.3.1 POFMT for Various Filter Roll-off and Dispersion Parameter Values 62
4.3.2 POFMT for Various Subcarrier Spacing 63
4.3.3 POFMT with Reconfigurable Antenna 65

CHAPTER 5: RESOURCE ALLOCATION WITH PARTIALLY OVERLAPPING FILTERED MULTITONE IN HETEROGENEOUS NETWORKS 67
5.1 System Model 69
5.2 Problem Formulation 70
5.2.1 Subcarrier and Frequency Shift Ratio Selection Scheme 72
5.2.2 Potential Game Formulation 72
5.2.3 Convergence to Nash Equilibrium 74
5.3 Performance Evaluation 74

CHAPTER 6: MILLIMETER-WAVE WIRELESS CHANNEL CONTROL USING SPATIALLY ADAPTIVE ANTENNA ARRAYS 76
6.1 System Model 77
6.2 Spatially Adaptive Antenna Array 79
6.3 Performance Evaluation 82

CHAPTER 7: CONCLUSION AND OPEN ISSUES 86

REFERENCES 90

APPENDICES 95
Appendix A: Copyright Permissions 96
Appendix B: List of Acronyms 100

ABOUT THE AUTHOR End Page

LIST OF TABLES

Table 2.1	Random subcarrier allocation algorithm	22
Table 2.2	Simulation parameters	23
Table 3.1	Subcarrier allocation algorithm with random state selection	43
Table 3.2	Simulation parameters	43
Table 3.3	Path loss models	44
Table 3.4	Percentage difference in RS & BeS algorithms	44
Table 3.5	Feedback loads for RS & BeS	45
Table 3.6	Capacity gains in terms of mean&meadian level for RS & BeS	47
Table 3.7	The maximum number of SUs who would perform the highest capacity in the network for RS & BeS	49
Table 4.1	FSR and antenna state selection scheme	60
Table 4.2	Simulation parameters	62
Table 5.1	Subcarrier and FSR selection scheme	74

LIST OF FIGURES

Figure 1.1	Heterogeneous network structure with SUs, PUs, SBSs and PBSs.	3
Figure 1.2	Resource allocation can either be in consecutive or random order.	7
Figure 1.3	RAs consist of antenna elements with which the states can be formed.	9
Figure 1.4	Users U_1 and U_2 fully overlap in (a) and (b).	11
Figure 2.1	System view.	17
Figure 2.2	Mean utility values in each iteration.	24
Figure 2.3	Capacity level vs. CDF for the whole system.	25
Figure 2.4	Mean capacity level becomes the same in the NE.	26
Figure 2.5	Total throughput increases 1.05Mbps in both algorithms when they reach the NE.	26
Figure 3.1	Cognitive heterogeneous network structure.	33
Figure 3.2	Based on the geographic location of PBS and SBS, SU selects the states which would cause the least interference onto PBS and provide the highest possible signal strength onto SBS.	41
Figure 3.3	The BeS algorithm outperforms the RS algorithm and it can provides a level of performance close to the exhaustive search algorithm.	42
Figure 3.4	When the antenna state selection is not adaptive, i.e., it is fixed for all users, the capacity difference in terms of percentage from 2S case to 6S case in 50% level is 37.2% and 33.8% in RS and BeS algorithms, respectively.	45
Figure 3.5	Users reach the NE in each case.	46
Figure 3.6	When state selection is adaptive for all users, the mean capacity difference from 2S case to 6S case is %3.2 and %2.2 in the RS and BeS algorithms, respectively.	47
Figure 3.7	Capacity values in APSS approach with two states are very close to ones in FPSS approach with six states.	48

Figure 3.8 When the number of SUs increases, the total capacity also increases. 48

Figure 3.9 When the beam width is 60°, the maximum mean capacity level is obtained. 49

Figure 4.1 Users i and j fully overlap in (a). 51

Figure 4.2 System view. 55

Figure 4.3 (a)When subcarrier spacing is constant, increasing the filter roll-off decreases the SINR gain in orthogonal waveforms. 63

Figure 4.4 (a)When filter roll-off is constant, increasing the subcarrier spacing increases the SINR gain in orthogonal waveforms. 64

Figure 4.5 (a)When filter control parameter is constant, increasing the subcarrier spacing increases the SINR gain in non-orthogonal waveforms. 65

Figure 4.6 (a)When RAs are used within POT concept, the system gain can be increased further in orthogonal schemes. 66

Figure 4.7 (a)When RAs are used within POT concept, the system gain can be increased further in non-orthogonal schemes. 66

Figure 5.1 (a) Both users allocate the same resources at the same time. 68

Figure 5.2 A player searches for the consecutive subcarriers which give the highest utility by sliding the subcarrier set (SS) through all the available ones. 71

Figure 5.3 (a)The resource allocation with POFMT outperforms the resource allocation with OFDM. 75

Figure 6.1 Base station (BS) changes position of the antenna array to maximize signal power and reduce fading. 77

Figure 6.2 (a) 5 element linear patch antenna array that can perform spatial, i.e., position adaptation using microfluidics; (b) Substrate stack-up in which an RT5880LZ PCB is located inside a microfluidic channel (formed by bonding PDMS mold onto RT5880 PCB with 6 μm thick BCB layer). 80

Figure 6.3 Layout details of the antenna, feed network, and grounding vias (units: mm). 80

Figure 6.4 (a) S_{21} performance of the feed network for: (a) various overlap length f_{ov} values (reference plane is taken for feed transition); (b) no grounding pads and vias (c) with grounding pads and vias (d) different array positions d (reference plane is taken for feed loss evaluation). 82

Figure 6.5 Simulated x-z plane realized gain patterns of the antenna array at various d positions for progressive phase shifts of (a) $\beta = 0$, (b) $\beta = \pi/4$, (c) $\beta = -\pi/4$, and (d) $\beta = 7\pi/8$. 83

Figure 6.6 (a) Link capacity vs. spatial adaptation range; (b) SIR gains of wireless systems utilizing different types of antennas at BSs; (c) Mean SIR gains of each individual user within the wireless systems. 85

ABSTRACT

The usage of the wireless communication technologies have been increasing due to the benefits they provide in our daily life. These technologies are used in various fields such as military communication, public safety, cellular communication. The current systems might not be sufficient to meet the increasing demand. Therefore, the new solutions such as the usage of smart antennas have been proposed to satisfy this demand. Among different solutions, cognitive heterogeneous networks (HetNets) have been recently introduced as a promising one to meet the high user demand. In cognitive Hetnets, there are secondary base stations (SBSs) with secondary users (SUs) and primary base stations (PBSs) with primary users (PUs) in a given area without any coordination between SBS-SBS and SBS-PBS.

Due to the physical coexistence of SBSs and the lack of available spectrum, interference caused by the SBSs becomes a significant issue. Therefore, there is a need for the techniques that allow users to share the same spectrum while maintaining the required performance level for each user by adopting interference mitigation techniques. In this dissertation, we focus on resource allocation, interference coordination/mitigation and channel control techniques in 4G and beyond systems.

As resource allocation techniques, we propose two studies. In the first study, we present the random subcarrier selection algorithm which is that each SU selects a specific number of subcarriers determined by its needs. In comparison where, at each iteration of the game, the SU searches all the subcarriers to maximize its payoff, our algorithm is based on selecting the subcarriers randomly and checks only those subcarriers that achieve higher payoff. In the second study, we utilize the reconfigurable antennas (RAs) which allows wireless devices to alter their antenna states determined by different radiation patterns to maximize received signal strength, and present the joint subcarrier and antenna state selection algorithm. SU selects the subcarriers whose capacity values are the

highest among the available ones. Since SUs employ RAs, i.e., multiple antenna states, they obtain the reports for all subcarriers from each antenna states, and select the state with the subcarriers which provide the highest capacity gain.

As interference coordination/mitigation technique, we propose a game theoretical partially overlapping filtered multitone (POFMT) scheme. Partially overlapping is performed in both frequency and space domains. While intentional carrier frequency shift is introduced in frequency, RAs are utilized to achieve partially overlapping in space domain. Within a game theoretical framework, when SUs search for the frequency shift ratio, they also select the antenna state to increase the system utility.

We also combine the resource allocation technique with POTs and present the game theoretical resource allocation with POFMT. To achieve the resource allocation, an SBS slides a group of consecutive subcarriers through all available ones and computes the utility for each selected subcarriers. It picks the consecutive ones which give the highest capacity result.

Our results show that our algorithms reach Nash equilibrium and increase the system gain substantially in terms of the corresponding utility.

As channel control technique, we propose a wireless channel control using spatially adaptive antenna arrays. This technique simultaneously utilizes beam-steering and spatial adaptation to enhance the wireless channel gain and system capacity. While the interference is reduced via beam-steering feature of proposed antenna, the wireless channel can be controlled by spatially moving the antenna in one axis. Simulated realized gain patterns at various array positions and phase shifter states are subsequently utilized in link and system level simulations to demonstrate the advantages of the proposed concept. It is shown that the system gain can be increased with the spatial adaptation capability of the antenna.

CHAPTER 1

INTRODUCTION

Wireless technologies have gained important place in our daily life. Due to their indisputable advantages, wireless communications are employed in various fields such as in cellular, vehicle-to-vehicle, machine-to-machine, in-vivo communications. However, along with this increasing usage in wireless technologies, a scarcity problem exists in the spectrum due to being limited source. To solve this problem, various solutions have been proposed such as the usage of smart antennas, directing some of the traffic to WiFi networks, developing new content compression techniques [1]. Besides these solutions, establishing a new type of network called cognitive heterogeneous networks (HetNets) has also been presented as a promising solution for spectrum scarcity. Such networks include the deployment of networks with small footprint called small cells within the large footprint networks called macrocells. At this point, it worths mentioning that the term small cell is used to express various types of cells which can be given as follows.

- *Microcell:* Microcells are deployed to cover the areas where the coverage of macrocell is not sufficient. Micro base stations (BSs) are operator deployed with a coverage area from 200m to 2km. They can be utilized for indoor and outdoor environments.

- *Picocell:* Picocells are deployed to improve the indoor coverage such as in airports, hospitals. The cell radius of picocells can be from 100m to 200m with a lower transmission power, which is typically 250mW-to-1mW, than macrocell or microcell. Similar to microcells, pico BSs are also operator deployed.

- *Femtocell:* Femtocell, also called as home node B, is a technology with a low power usage, which is 1mW-to-250mW, that can provide the high data rate for the end user that cannot be covered by the closest macro BS due to bad channel conditions. In terms of access

mode, it can either be open, close or hybrid [2]. In open access mode, femto BS (FBS) can be used by femto user equipment (FUE) and macro user equipment (MUE) while it is used only FUE in close access mode. On the other hand, in hybrid access mode, it is used by both FUE and MUE, however, most of the resources are typically allocated to the FUE due to its higher priority in accessing the FBS. Femto BSs are user deployed with a coverage area from 10m to 100m.

Within a cognitive radio concept, small cells are named as secondary networks which consist of secondary users (SUs) and secondary base stations (SBSs), and macrocells are named as primary networks which are formed with primary users (PUs) and primary base stations (PBSs) as seen in Figure 1.1. While the PUs have a right to use the spectrum as licensed users, SUs as unlicensed users are required to access the spectrum by utilizing some cognitive approaches which can be categorized as underlay, overlay and interweave approaches.

1. *Underlay Approach:* The SUs are allowed to share the spectrum with the PUs under limited interference constraint. In this constraint, the power transmitted by the SUs must guarantee that the interference at the PUs is below a predetermined threshold which is defined as the interference temperature (IT).

2. *Overlay Approach:* SUs are allowed to use the licensed spectrum with PU simultaneously by performing special coding techniques without reducing its transmission power.

3. *Interweave Approach:* SU performs the spectrum sensing to determine which bands are in idle position, i.e., not used by the PU. When it finds the idle bands, SU allocates those resources for its transmission.

Although HetNets have been proposed as a solution to spectrum scarcity, some challenges have been emerged in the deployment of these networks. Such challenges can be summarized as follows.

- How to perform interference coordination/mitigation?
- How to perform resource allocation?

- How to perform handover between PBS - SBS or SBS - SBS?
- How to manage the mobility?
- How to handle back-haul scalability?
- How to perform synchronization?

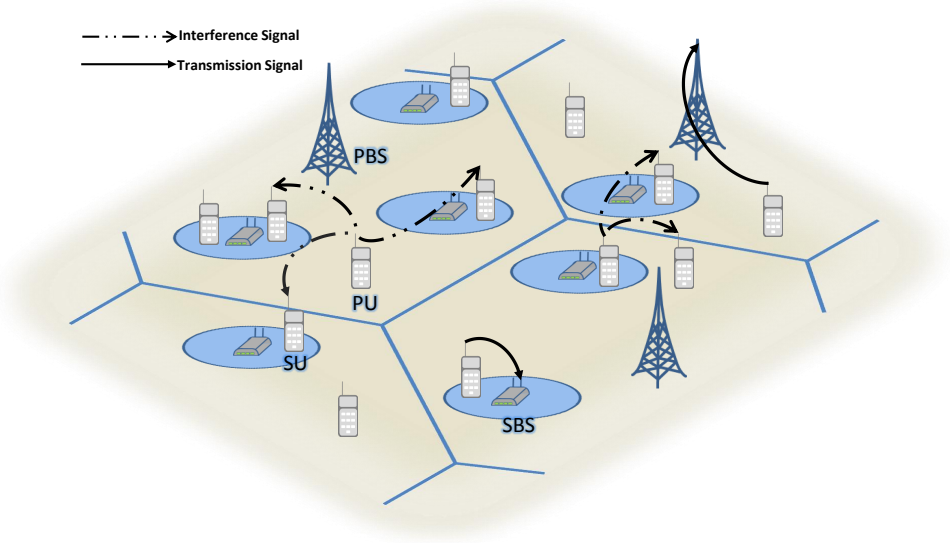

Figure 1.1 Heterogeneous network structure with SUs, PUs, SBSs and PBSs.

In cognitive HetNets, the secondary networks serve the purpose of providing reliable communication links to the indoor users. However, these networks suffer from interference among SUs and PUs since they share the spectrum. Therefore, among the corresponding challenges, in this dissertation, we focus on the interference coordination/mitigation, resource allocation and channel control techniques in 4G and beyond systems.

1.1 A Review of the Main Concepts in the Dissertation

In this dissertation, we focus on the following concepts. In each subsection, while we explain the concepts, we also provide the related works about the corresponding concept if applicable.

1.1.1 Game Theory

Game theory (GT) is a science of the strategic thinking. We can define the strategic thinking in a way that it is to make a plan by considering the plans of others as well. It is a social phenomenon and used by the military in general. While the roots of GT are based upon older times, a seminal work had been performed by John Von Neumann and Oskar Morgenstern in 1944 [3]. After this study, John Nash introduced a notion of equilibrium point for the non-cooperative games in 1951 [4]. After the mid 1950s, GT has been widely used in wireless communication literature.

GT is a mathematical tool and investigates the interaction between, at least, two nodes/users where there exist two types of games; cooperative and non-cooperative games. While cooperative games construct a game with the coalitions which refer to a subgroup of a group of users, non-cooperative games construct a game with independently acting users. An important difference between these two games is the availability of the payoffs of the other players at each player. In cooperative games, users in a subgroup know what the others do, but in non-cooperative games, such information is not available.

Since the cognitive HetNets consist of the uncoordinated networks, non-cooperative games are utilized to solve the interference problem. These games are defined with three components:

1. *Player:* Players are the decision-makers in a given game and denoted with i, $i \in \mathcal{I}$ where $\mathcal{I}$ is the set of players in a game. The games are played among the players.

2. *Strategy:* Strategies are the alternatives for the decision-makers and denoted with s_i for player i.

3. *Utility function:* Payoff (utility function) is the set of possible outcomes which are assigned a number, so, the player can select one towards its benefits and denoted with U_i for player i.

After defining these three components, it is important to define another phenomenon which is the Nash equilibrium (NE) which can be described as an equilibrium point where the players

have no incentive to change their strategies and can be defined as

$$U_i(s_i^*, s_{-i}^*) \geq U_i(s_i, s_{-i}^*)$$
$$\forall i \in \mathcal{I}, \forall s_i, s_{-i} \in S \tag{1.1}$$

where S indicates the set of strategy profiles for player i and every other player $-i$ and '*' indicates the equilibrium point.

In the literature, selection of the highest utility is expressed with the best response correspondence. The aim is to maximize the utility by playing with the most profitable strategy for each player. This approach of playing game is reached the players to the NE. The best response correspondence is defined as

$$\mathcal{B}_i(s_{-i}) \in \arg\max_{s_i \in S_i} U_i(s_i, s_{-i}) \tag{1.2}$$

Different types of games can be utilized to prove the NE existence. In this dissertation, we employed the supermodular and potential games.

1.1.2 Supermodular Games

Supermodular game is a type of non-cooperative game. The characterization of supermodular game is defined with strategic complementarities. In other words, when one player changes his strategy towards his benefit, other players also have an incentive to do the same towards their benefit, e.g. better/higher signal-to-interference-plus-noise ratio (SINR) under the constant transmission power.

Definition 1 *A game $\mathcal{G}$ is considered as supermodular game if, $\forall i \in \mathcal{I}$,*

1. *S_i is a compact set of $\mathbb{R}$,*
2. *U_i is semi-continuous in (s_i, s_{-i}),*
3. *U_i has increasing differences in (s_i, s_{-i}).*

To obtain the NE with supermodular games, these features need to be satisfied. For the last feature, we need to prove that $U_i(s_i, s_{-i})$ is twice continuously differentiable, i.e.,

$$\frac{\partial^2 U_i(s_i, s_{-i})}{\partial s_i \partial s_{-i}} \geq 0 \tag{1.3}$$

Two important properties are possessed by the supermodular games when the above features are satisfied [5]:

- There is at least one pure NE
- It has monotonically increasing property in its best responses.

1.1.3 Potential Games

A game is said to be a potential game defined with a potential function. When a player changes its strategy, the change in its utility function is reflected in the potential function. Various potential games are defined in [6]. Among those games, we utilized the ordinal potential games. The following definition can be found in [6] for the ordinal potential games.

Definition 2 *A game $\mathcal{G}$ is said to be an ordinal potential game if it admits an ordinal potential. A function V is an ordinal potential for $\mathcal{G}$ if for every $i \in \mathcal{I}$ and for every $s_{-i} \in S_{-i}$*

$$U_i(s_i', s_{-i}) - U_i(s_i, s_{-i}) > 0 \text{ iff } V(s_i', s_{-i}) - V(s_i, s_{-i}) > 0$$
$$\forall s_i, s_i' \in S_i. \tag{1.4}$$

It is guaranteed that there is at least one pure NE in ordinal potential games. The NE convergence with potential games can be shown over the finite improvement path (FIP) [6], because this property guarantees NE convergence and indicates the increment of the utility function in each path.

1.1.4 Resource Allocation

In wireless communications, the resources are defined as the carrier frequencies. While this might be a single carrier with wide band, it can also be multiple carriers with narrow band for a given bandwidth. In orthogonal frequency-division multiple access (OFDMA), multicarrier structure is employed. A given band consists of subcarriers with equal bandwidth. In long term evolution (LTE) standards, each subcarrier has 15 KHz bandwidth, and 12 subcarriers form a resource block [7].

Basically, the resource allocation is to assign the symbols to carrier frequencies. In the literature, this can also be named as subcarrier allocation or scheduling. Figure 1.2 shows how to allocate the resources. In OFDMA, there are two ways for resource allocation; it can either be in consecutive order or random order based on the channel response of each subcarrier. The transmitter obtains the SINR reports from the receiver for each subcarrier and allocates the resources accordingly. If there are multiple receivers, the transmitter can perform the resource allocation with either maximum rate or proportional fair scheduling algorithms [8].

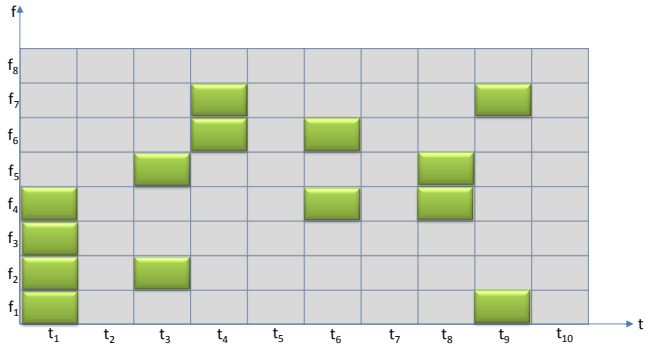

Figure 1.2 Resource allocation can either be in consecutive or random order.

Resource allocation in cognitive HetNets is commonly performed with game theoretical methods because GT provides the tools necessary to manage the interactions between players (users) in order to improve the performance of the network while maintaining the interference coordination between users. Different game theoretical methods, which can be categorized as cooperative and non-cooperative games, are used in the resource allocation literatures on cognitive HetNets. For example, in [9], cooperative games are utilized to achieve resource allocation where

the players establish coalitions. Stackelberg games as a non-cooperative framework are utilized in resource and power allocation studies in [10–14]. In [15], Bayesian auction games are introduced within the resource allocation literature. In [16–18], authors propose resource allocation techniques by utilizing potential games. Besides game theoretical techniques, optimization methods are also proposed in the literature to fulfill the resource allocation [19–22].

1.1.5 Reconfigurable Antennas

reconfigurable antennas (RAs) have been presented as an emerging technology due their physical sizes which make them to be feasibly employed at the user equipments (UEs) and their ability to provide different antenna radiation patterns for every antenna element using hardware techniques when compared to multiple-input multiple-output (MIMO) system. A simple RA structure can be seen in Fig 1.3. Reconfigurability of antenna adds a degree of freedom in terms of system capability to tackle the random nature of the wireless channel. This degree of freedom of reconfigurability depends on antenna structure and reconfigurability method. Theoretically, the number of degree of freedom depends on the number of states that an RA provides. For instance, if an RA has three radiation patterns of different point directions and be able to operate in two different frequency bands, it can be said that this RA has six degree of freedoms. The choice of a reconfiguration mechanism is based on the design space and performance level required. Antenna reconfigurability can be categorized into four different reconfigurability functions, namely, a)reconfiguring resonance frequency, which usually takes place by changing physical properties that alter surface current distribution, b) reconfiguring radiation pattern, which usually takes place by changing radiating edges, slots, or the feeding network, c) reconfiguring polarization state, which usually takes place via changing the surface structure or the feeding network, and d) combinations of reconfiguring the above characteristics, which usually takes place by using numerous techniques simultaneously [23]. By reconfiguring its frequency, RA can carry out spectrum allocation and frequency hopping to enhance the system capacity and can also reduce in-band frequency interference by reconfiguring its radiation pattern and polarization [24].

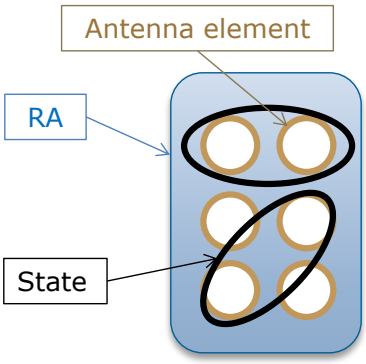

Figure 1.3 RAs consist of antenna elements with which the states can be formed.

Reconfigurable antenna states can be continuous or discrete. This depends on reconfiguration methods, e.g., RF switches as in reconfigurable pixel antenna or variable capacitor as tunable load. The continuous states has smooth changes in antenna impedance, which might be desirable in some applications but this will come at the cost of more complex circuitry and similarity between antenna states. The discrete number of states has a pre-selected antenna radiation pattern that have different properties due to large impedance variation between antenna states. The independence between antenna states is key feature that is required in the applications addressed in this dissertation.

In antenna design and operation of a reconfigurable antenna with discrete antenna states, a control circuit sends a set of ON-OFF combination of switches that correspond to each antenna state. This combination makes a particular current distribution on antenna surface that generates particular radiation pattern. So, if we have 8 antenna states, that means, the antenna system has 8 sets of combinations of ON-OFF switches which makes the antenna have particular pointing directions with particular beamwidth. Each antenna state represents a particular pointing direction (0°, 45°, 90°, 135°, 180°, 225°, 270°, and 315°) and corresponds to a particular current distribution density defined by a particular set of combination of ON-OFF switches.

These reconfigurable features of the RA have attracted the interest of the research community to improve the performance of wireless communication systems in different applications. For example, SU can select the best state of the RA that maximizes SINR or capacity [25]. RAs can

also be utilized to detect intruders to enhance security in communication systems [26]. For MIMO multiuser orthogonal frequency-division multiplexing (OFDM) system, RAs are utilized to increase the performance in terms of capacity of MIMO systems for slowly fading environments and in different multipath environment including rich and sparse [27–30]. In [31], the authors use RAs to achieve blind interference alignment by introducing channel fluctuations resulting in independent signal-to-noise ratio values at predetermined time instants via blind antenna switching.

1.1.6 Partially Overlapping Tones

One of the most important problems with the cognitive HetNets is the other user interference. Various solutions have been proposed to mitigate this problem. Partially overlapping tones (POTs) has also been introduced to reduce the interference coming from other users in cognitive HetNets [32]. Rather than utilizing the overlapping channels as in partially overlapping channels (POCs) techniques [33], intentional carrier frequency shift (CFS) is performed in the POTs concept. The main idea behind POTs can be explained over Figure1.4. The allocated resources to two uncoordinated users U_1 and U_2 are illustrated in Figure1.4a and Figure1.4b (dashed curve) where U_1 and U_2 are assigned at the same time. Before U_2 is provided with a frequency shift, both users fully overlap each other, i.e., they fully interfere with each other. To decrease the interference, U_2 introduces some CFS (solid curve) as shown in Figure1.4b. Partially overlapping scheme can therefore be achieved at the subcarrier level to reduce the cross interference as depicted in Figure1.4c.

1.2 Dissertation Outline

1.2.1 Chapter 2: Random Subcarrier Allocation with Supermodular Game in Cognitive Heterogeneous Networks

In this chapter, our main objective is to solve the problem of subcarrier allocation for the SU using supermodular games. Under certain conditions, the supermodular games guarantee at least one NE without the need of proving the quasi-concavity of utility functions or dealing with interior solutions [34]. In previous studies such as in [35] and [5], subcarriers are selected based

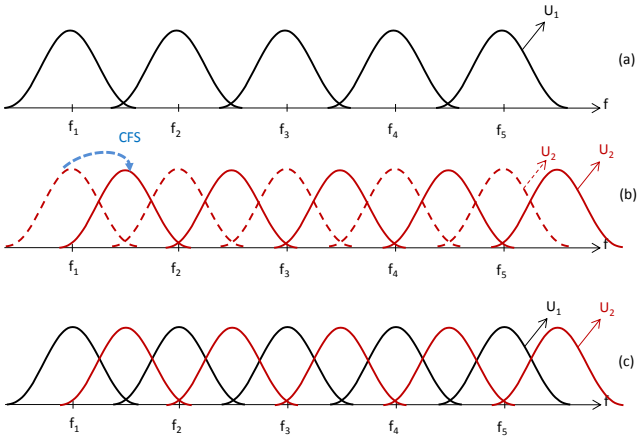

Figure 1.4 Users U_1 and U_2 fully overlap in (a) and (b). U_2 performs CFS to decrease the interference in (b). U_1 and U_2 partially overlap in (c).

on the payoff of each subcarrier via utilizing supermodular games. Each SU sweeps through the all subcarriers to determine the ones which have the highest payoff. If the payoff of the best selected subcarriers is larger than the ones which are selected in previous iteration, SU changes its subcarriers. While this approach has an advantage in terms of fast convergence rate, i.e. to reach the NE faster, it requires high feedback load. On the other hand, in random subcarrier allocation technique [36], each SU picks certain number of random subcarriers based on its need and only considers these subcarriers when making a decision. This has the advantage of limited feedback since only the number of subcarriers considered in each iteration is much less than considering all subcarriers. Our objective is to use this technique with supermodular games. This should provide lower feedback load against higher convergence rate. We will present analysis and simulation to show this trade-off among convergence and feedback load, and our results indicate that we can have significant reduction in feedback on the expense of convergence, which makes our algorithm beneficial in slowly varying channels.

1.2.2 Chapter 3: Joint Subcarrier and Antenna State Selection for Cognitive Heterogeneous Networks with Reconfigurable Antennas

In this chapter, we develop resource allocation technique for cognitive HetNets by exploiting RAs. Our objective is to use the capabilities of RAs to generate independent channel gains with

different parameters to improve the capacity of cognitive HetNets. We use game theory to solve this problem and, in particular, we model the problem as potential games to solve the problem of jointly finding the antenna state and subcarriers for each SU as these games can be shown to achieve NE for our utility function. Since the number of antenna states in RA can be large, this might increase the computational complexity in the system. To reduce the complexity, we divided our solution into two steps. In the first step, before playing the game, the players select the candidate antenna states set based on either of two different approaches. In the fixed prior state selection (FPSS) approach, all players have the same predetermined states (or radiation patterns). On the other hand, in the adaptive prior state selection (APSS) approach, players select the states based on the locations of BSs and the signal-to-interference-plus-noise ratio (SINR) measurements in each state. In the second step, after selecting a candidate set, the game starts to be played. We focus on two different algorithms in terms of RA state selection, namely random state selection (RS) and best selection (BeS). Both techniques are based on the best subcarriers selection in terms of their capacity measurements among all available subcarriers achieved by the SU. In the BeS algorithm, this process is performed for each state, while SBS sends capacity reports of the subcarriers for only one randomly selected state with the aim of reducing the feedback load (FL) in the RS algorithm. Our results show that, while RS gives lower FL than BeS for RAs with two states, it becomes higher when we consider more than three states in an RA. This is due to the fact that the RS scheme requires more iterations to converge to NE compared to the BeS scheme as the number of states increases. On the other hand, we are showing that as the number of antenna states in RAs increases, the capacity enhances further.

1.2.3 Chapter 4: Partially Overlapping Filtered Multitone with Reconfigurable Antennas in Heterogeneous Networks

In this chapter, partially overlapping filtered multitone (POFMT) with Reconfigurable antenna (RA)s is proposed within a game theoretical framework. In our previous study [37], we investigated the POFMT concept with only orthogonal waveforms in the system level without utilizing the RAs. In this chapter, non-orthogonal waveforms are introduced. Additionally, RAs are

also utilized to introduce the space domain partially overlapping and to further improve the system performance. A joint frequency shift ratio (FSR) and antenna state selection game is proposed. While SUs search for the FSR to reduce the interference from other SUs in the environment, they also determine the antenna state where the highest utility can be achieved for the relevant FSR. The existence of NE in this game is proved theoretically with potential games and simulations. As demonstrated with simulation results, POFMT scheme with RAs outperforms OFDM in terms of capacity with the expense of slightly lower spectral efficiency in the system.

1.2.4 Chapter 5: Resource Allocation with Partially Overlapping Filtered Multitone in Heterogeneous Networks

In this chapter, we develop a resource allocation technique for POFMT within a game theoretical framework in cognitive HetNets. We utilize the filtered multitone (FMT) which does not require the synchronization and cyclic prefix usage [38]. In downlink, SBSs as players perform the resource allocation by searching for the best subcarriers which are constrained to be in consecutive order. To perform subcarrier selection, SBS picks a certain number of subcarriers based on the total need of SU by starting from the first available subcarrier and computes the utility of the selected subcarriers. Then, it shifts the subcarriers intentionally to introduce the CFS and calculates the utility in this position, too. The SBS performs this operation throughout the all available subcarriers. After obtaining the capacity results for every position and subcarriers, SBS selects the one which provides the highest utility. With this scheme, the existence of NE is proved theoretically and by simulations. As indicated in simulation results, the proposed scheme outperforms OFDM with a slightly slower convergence rate.

1.2.5 Chapter 6: Millimeter-Wave Wireless Channel Control Using Spatially Adaptive Antenna Arrays

In this chapter, we introduce a wireless channel control concept based on spatially, i.e., position adaptive antenna arrays. This technique simultaneously utilizes beam-steering and spatial adaptation to enhance the wireless channel gain and system capacity. The concept is inspired by

the microfluidically reconfigurable RF devices as they can enable compact systems with spatial adaptation capability. Specifically, a 5 element linear 28 GHz mm-wave antenna array design that can achieve beam-steering via phase shifters and spatial adaptation via microfluidics is detailed. Simulated realized gain patterns at various array positions and phase shifter states are subsequently utilized in link and system level simulations to demonstrate the advantages of the proposed concept. It is shown that a wireless communications system can achieve 51% improvement in the mean signal-to-interference ratio due to the spatial adaptation capability.

CHAPTER 2

RANDOM SUBCARRIER ALLOCATION IN COGNITIVE HETEROGENEOUS NETWORKS WITH SUPERMODULAR GAME[1]

Increasing demand on higher data rates and the scarcity on spectrum to which this demand leads shift providers to establish the new types of networks, namely cognitive HetNets. In such networks includes the deployment of networks with small foot print called femtocells within large footprints networks called macrocells. The femtocell networks serves the purpose of providing reliable communication links to the indoor users. While this solution resolves high data rate demand, these networks suffer from interference among femto and macro users since they share the spectrum. Studies were carried out to solve this interference problem by coordination or mitigation methods. A brief study about interference coordination can be attained from [39].

Femtocell, also called as enhanced Home Node B (HeNB), is an emerging technology with a low power usage that can provide the high data rate for the end user that cannot be covered by the closest PBS due to bad channel conditions. In terms of access mode, it can either be open, close or hybrid [2]. In open access mode, FBS can be used by FUE and MUE while it is used only FUE in close access mode. On the other hand, in hybrid access mode, it is used by both FUE and MUE, however, most of the resources are typically allocated to the FUE due to its higher priority in accessing the FBS[2].

Since femtocells are user deployed, there is no central unit controlled by the macrocell for allocating the resources among the SU and PU. Such feature can result in interference problems on the PU and among the SU. Therefore, there is a need for a decentralized resource allocation techniques where the SU can dynamically select the spectrum that can share with the PUE while

[1]This chapter was published in IEEE Military Communications Conference (MILCOM) held in Baltimore, Maryland, in 6-8 Oct., 2014. Permission is included in Appendix A.

[2]FUE and MUE will be used as secondary and primary user,respectively, throughout this chapter.

providing the desired data rate to the SU and maintaining the interference level to the PU at a desired level. The potential solution to this significant problem is to use the game theoretical approach. Game theory deals with an interaction between, at least, two nodes/users where there exists two types of games; cooperative and non-cooperative games. While cooperative games construct a game with the coalitions which refer to a subgroup of a group of users, non-cooperative games construct a game with independently acting users. An important difference between these two games is the availability of the payoffs of the other players at each player. In cooperative games, users in a subgroup know what the others do, but in non-cooperative games, such information is not available. In this chapter, we also use a non-cooperative game type solve the problem of subcarrier allocation among SUs to be shared with the PUs.

Game theoretical methods are used in different fields in wireless communication. One such field is resource allocation which has been studied using different types of games. In [5, 35, 40], authors utilize the supermodular games to solve this problem, while authors use potential games in [17, 18, 41, 42]. Supermodular games has some advantageous on top of the potential games. It is not necessary to prove the concavity of utility functions or dealing with interior solutions in supermodular games [34].

In this chapter, our main objective is to solve the problem of subcarrier allocation for the SU using supermodular games. Under certain conditions, the supermodular games guarantee at least one NE. In previous studies mentioned above, subcarriers are selected based on the payoff of each subcarrier via utilizing supermodular games [3]. Each SU sweeps through the all subcarriers to determine the ones which have the highest payoff. If the payoff of the best selected subcarriers is larger than the ones which are selected in previous iteration, SU changes its subcarriers. While this approach has an advantage in terms of fast convergence rate, i.e. to reach the NE faster, it requires high feedback load. On the other hand, in random subcarrier allocation technique [36], each SU picks certain number of random subcarriers based on its need and only considers these subcarriers when making a decision. This has the advantage of limited feedback since only the number of subcarriers considered in each iteration is much less than considering all subcarriers. Our objective

[3] In Section 2.3, this previous algorithm is called as best selection algorithm.

is to use this technique with supermodular games. This should provide lower feedback load against higher convergence rate. We will present analysis and simulation to show this trade-off among convergence and feedback load, and our results indicate that we can have significant reduction in feedback on the expense of convergence, which makes our algorithm beneficial in slowly varying channels.

The remainder of this chapter is organized as follows. In Section 2.1, the system model is introduced. Then, game theoretical model is performed in Section 2.2. Section 2.3 comprises numerical results of the proposed approach, and finally, conclusions are drawn in Chapter 7.

2.1 System Model

In this chapter, we consider an uplink scenario with one PBS. In this PBS, there are random number of PUs denoted as $\mathcal{M} = \{1,2,\ldots,M\}$. Random number of SBSs are distributed within the area of PBS. Each SBS has a number of SUs denoted as $\mathcal{F} = \{1,2,\ldots,F\}$. This structure can be seen in Figure2.1.

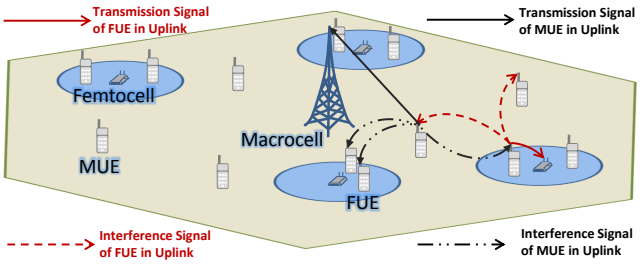

Figure 2.1 System view. There are FUEs, FBSs and MUEs under one macrocell.

The random resource allocation is performed among SUs since PUs are assigned to resources by PBS with the consideration of interference in between them. As mentioned above, because SUs are not controlled by PBS, they can cause interference on PUs. On the contrary, PUs can also interfere with SUs. Therefore, by looking at the SU perspective, PUs can be seen as interfering source. Thus, the power of received signal on SU can be expressed as

$$\mathcal{P}_{RX} = P_{\mathcal{F}} - P_{\mathcal{F},int} - P_{\mathcal{M},int}, \tag{2.1}$$

where $P_{\mathcal{F}}, P_{\mathcal{F},int}, P_{\mathcal{M},int}$ are the received signal strength (RSS) of SU, other interfering SUs and interfering PUs, respectively. RSS of SU can be defined as

$$P_{\mathcal{F}}(dBm) = P_{(tx)} + G - PL$$

where $P_{(tx)}$ is the power of transmitted signal, G is the transmitter antenna gain, and PL is the path loss.

2.2 Game Theoretical Model

In this section, we provide supermodular game formulation followed by the general game theoretical model. Random subcarrier allocation scheme is mentioned in detailed at the end of the section.

Game theory is a tool which provides a mathematical solution method to the problems which can be solved via strategic thinking. In non-cooperative games, the mathematical structure is made of three components; *a set of players, a set of strategies and utility function.* These components can be defined as

- The set of players as a set of SUs denoted with $\mathcal{I} = \{1,2,\ldots,I\}$,
- The set of strategies as a least interfered subcarrier selection denoted with $S_i = \{s_1, s_2, \ldots, s_k\}$,
- Utility function as the RSS difference between player i and other players, j denoted with $U_i(s_i, s_{-i})$. The sum of RSSs of the other players is defined as the total interference power.

The whole game, $\mathcal{G}$, with these three components can be written as

$$\mathcal{G} = \langle \mathcal{I}, S_{i,i\epsilon\mathcal{I}}, U_{i,i\epsilon\mathcal{I}} \rangle \tag{2.2}$$

As seen in (2.2), each player chooses a strategy to achieve the best utility, i.e. each SU picks the subcarriers which has the highest RSS difference level. If the game is played iteratively, either

sequentially or simultaneously, each SU checks the subcarriers which have been picked in previous round, and compares them with the others in each iteration. If there is/are subcarrier(s) with the higher utility, then it changes its subcarrier locations. When all players reach the NE, then they stop looking for the new subcarriers. This NE is a point where there is no need to deviate profitably for players. It can be defined mathematically as

$$U_i(s_i^*, s_j^*) \geq U_i(s_i, s_j^*), \forall i \in \mathcal{I}, \forall s_i \in S_i \tag{2.3}$$

where s_j shows the strategies for all players except i.

In the literature, selection of the highest utility is expressed with the best response correspondence. The aim is to maximize the utility by playing with the most profitable strategy for each player. This approach of playing game is reached the players to the NE. The best response correspondence is defined as

$$\mathcal{B}_i(s_{-i}) \in \arg\max_{s_i \in S_i} U_i(s_i, s_{-i}) \tag{2.4}$$

In this chapter, we express the utility (or payoff) function as the RSS difference between player i and other players j on each subcarrier. Each player picks the number of subcarriers depending on its needs. Then, it changes its subcarriers by looking at the RSS difference of them, accordingly. The utility function can be defined mathematically as

$$U_i(s_i, s_{-i}) = \sum_{k=1}^{K} \left(P_i^k s_i^k - \sum_{j=1, j\neq i}^{\mathcal{I}} P_j^k s_j^r \right). \tag{2.5}$$

where k = {1,2,. . . ,K} is the subcarrier index, P_i^k is the RSS on k^{th} subcarrier of i^{th} player, s_i shows the least interfered selected subcarriers. $s_i^k = 1$ means that the k^{th} subcarrier is selected by the player i.

2.2.1 Supermodular Game Formulation

Supermodular game is a type of non-cooperative game. The characterization of supermodular game is defined with strategic complementarities. In other words, when one player changes his strategy towards his benefit, other players also have an incentive to do the same towards their benefit, e.g. better/higher SINR under the constant transmission power.

Definition 3 *A game $\mathcal{G}$ is considered as supermodular game if, $\forall i \in \mathcal{I}$,*

- *S_i is a compact set of $\mathbb{R}$,*
- *U_i is semi-continuous in (s_i, s_j),*
- *U_i has increasing differences in (s_i, s_j).*

To obtain pure Nash equilibria with supermodular games, these features need to be satisfied. According to our strategy, a player look for resources which have the least interference power (P_j). Since P_j is bounded with the minimum ($P_{\min}$) and maximum ($P_{\max}$) levels, i.e. [$P_{\min}$=0,$P_{\max}$], which is a compact set of $\mathbb{R}$, this satisfies the compactness feature of supermodular game. On the other hand, let $\mathcal{P}_k$ be the RSS difference on subcarrier r, and let's assume the first player calculates the RSS difference on its side. If all players use the same subcarrier with the first player, since $P_j = P_{\max}$, the minimum RSS difference on this subcarrier would be achieved, $\mathcal{P}_{\min}$. When only the first player uses the same subcarrier, since $P_j = P_{\min}$, we would reach the maximum RSS level, $\mathcal{P}_{\max}$. Because $\mathcal{P}_r$ oscillates between $\mathcal{P}_{\min}$ and $\mathcal{P}_{\max}$, this satisfies the semi-continuity feature. To satisfy last feature, we need to prove that $U_i(s_i, s_{-i})$ is twice continuously differentiable, i.e.

$$\frac{\partial^2 U_i(s_i, s_{-i})}{\partial s_i \partial s_j} \geq 0 \tag{2.6}$$

We apply the utility function given in (2.5) to (2.6) to prove that U_i has increasing differences. First order partial differentiation of (2.5) can be written as

$$\frac{\partial U_i(s_i, s_{-i})}{\partial s_i} = \frac{\partial}{\partial s_i} \sum_{k=1}^{K} \left(P_i^k s_i^k - \sum_{j=1, j\neq i}^{\mathcal{I}} P_j^k s_j^k \right), \tag{2.7}$$

$$= KP_i.$$

Second order partial differentiation of (7) can be written as

$$\frac{\partial^2 U_i(s_i, s_{-i})}{\partial s_i \partial s_j} = \frac{\partial^2}{\partial s_i \partial s_j} (KP_i) = 0 \geq 0 \tag{2.8}$$

This results that the utility function in (2.5) satisfies the conditions for supermodular game. Supermodular games have two important features [5]:

- There is at least one pure NE
- It has monotonically increasing property in its best responses.

2.2.2 Random Subcarrier Allocation Scheme

This scheme is based on the selection of random subcarriers. The key thing is that when SU picks random subcarriers, it looks at only the payoffs of those selected subcarriers. But, in previous studies, SU looks for the subcarriers which have the best payoff via sweeping through the all subcarriers. This causes tremendous amount of feedback sent by SU.

We provide detailed explanation of our algorithm in Table 2.1. As seen from the algorithm, random subcarriers are allocated to each user in the system. Based on its needs, each SU picks certain number of random subcarriers in each iteration. These selected subcarriers are compared with its own subcarriers in terms of their utilities. If there is subcarrier(s) whose utility is higher than its own subcarrier's utility, SU takes these newly selected subcarriers by removing its own subcarriers. As these removed subcarriers could equal to the number of total subcarriers which an SU uses, it can also be only one subcarrier. This continues until each SU reaches the NE. By doing

Table 2.1 Random subcarrier allocation algorithm

#	Simultaneous Game Algorithm
1	PUs = randomly distribute PUs to PBS
2	SUs = randomly distribute SUs to SBSs
3	RS = assign random subcarriers to PUs and SUs
4	RSS = calculate the RSS difference in each subcarrier
5	*for* iterations(1,2,...)
6	*for* SUs(1,2,...)
7	pick certain number of random subcarriers
8	compare them with the ones previously selected
9	*if* new subcarriers have higher payoff, change your subcarriers with those new subcarriers *if* not, keep your previous subcarriers
10	*end*
11	*if* any SU changes its subcarrier profitably
12	do the next iteration to allow others to change their subcarriers profitably, too
13	*end*
14	*end*

this, the number of feedback is decreased to very small amounts as seen in performance evaluations section.

2.3 Performance Evaluation

In this section, we derive the simulation results. We compare our random subcarrier allocation algorithm with previous algorithm which is based on the selection of subcarriers which have the highest payoff [5, 35, 40]. First, we look at the utility of both algorithms. Then, we compare the capacity and the throughput of the SUs.

In this chapter, we are playing the game simultaneously. No recording from previous SU is held unless an iteration is completed. We consider one OFDM symbol with the FFT size of 1024, i.e. the bandwidth is 10MHz. All SUs, PUs, SBSs, and PBSs are allocated randomly. We assume there are ten SBSs with two SUs, twelve PUs and one PBS. We consider users as static, i.e. there is no mobility, and duplexing as time division duplexing (TDD) in between transceiver. This provides the channel reciprocity. Other system simulation parameters can be seen on Table 2.2.

We use two path loss models taken from 3GPP 36.814 standards. Path loss model from PU to SBS is defined as,

$$PL_{PU,SBS} = \max(15.3 + 37.6log_{10}R, 38.46 + 20log_{10}R) + 0.7d_{2D,indoor} + L_{ow}, \quad (2.9)$$

where R is distance in m which is random, L_{ow} is the penetration loss of an outdoor wall which is equal to 20dB, and $d_{2D,indoor}$ shows the distance inside the house. This is for 2GHz central frequency.

Similarly, path loss model from SU to SBS is defined as,

$$PL_{SU,SBS} = 38.46 + 20log_{10}R + 0.7d_{2D,indoor}, \quad (2.10)$$

Table 2.2 Simulation parameters

Simulation Parameters	Parameter Value
Power of UE	23dBm
UE Antenna Gain	5dBi
Noise Figure	5dB
Bandwidth	10MHz
Bandwidth of subcarrier	15KHz
Number of subcarriers/SU	40
Number of subcarriers/PU	75
Number of SUs/SBS	2
Number of SBSs	10
Number of PUs	12
Carrier Frequency	2GHz
Modulation Order	QPSK
Femtocell radius	15m
Macrocell radius	500m
Shadowing standard deviation	8dB (MU) - 4dB (FU)
FFT size	1024
Penetration Loss	20dB

Figure2.2 shows the payoffs of the two algorithms. In this analysis, for the sake of clarity, we plot only one randomly selected SU's results instead of all SUs. Our algorithm reaches the NE in the seventh iteration while the best selection algorithm reaches it in the third iteration. An important thing is that when both algorithms reaches the NE, their payoff turns out to be the

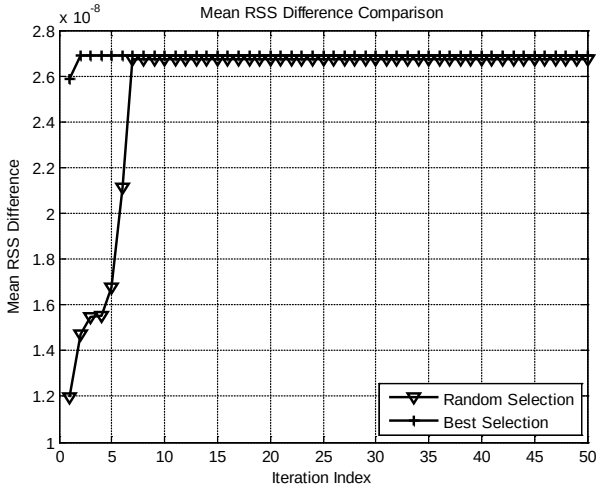

Figure 2.2 Mean utility values in each iteration. Random selection algorithm raises convergence rate while it decreases the feedback load tremendously in terms of utility function.

same level. By achieving this after a few more iterations, we indicate that our algorithm saves SU to perform a significant amount of sweeping for the subcarriers which have the highest payoff. It only needs to look at the number of subcarriers it needs. By doing this, feedback load which is the number of subcarriers sent from the SU to SBS is reduced tremendously. While the feedback load is equal to 7*40=280 subcarriers in our algorithm, it equals to 3*1024=3072 subcarriers in the best selection algorithm.

2.3.1 Capacity Level Analysis

At this part, we perform the capacity analysis in terms of cumulative distribution function (CDF) and the mean value of the capacities of the SUs on both algorithms. Capacity is defined as

$$\begin{aligned} C_i &= \log(1 + SINR_i), \\ &= \log\left(1 + \frac{P_{\mathcal{F}}}{P_{\mathcal{F},int} + P_{\mathcal{M},int} + w_0}\right). \end{aligned} \tag{2.11}$$

where w_0 shows the additive white Gaussian noise (AWGN).

In Figure2.3, we compare both algorithms with the initial condition of the system. At the beginning of the game, we allocate the users to the random subcarriers. Initial condition refers to

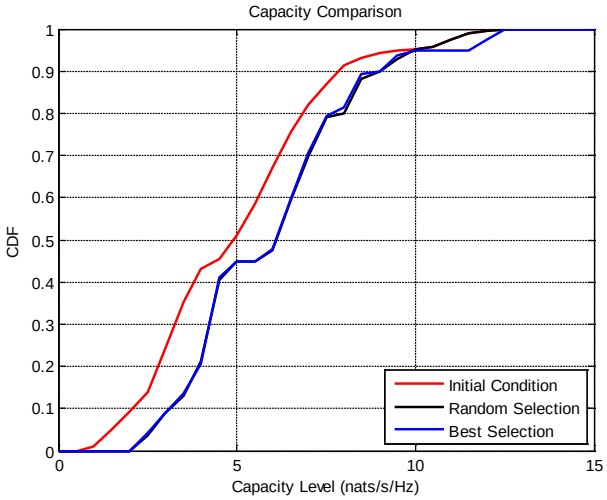

Figure 2.3 Capacity level vs. CDF for the whole system. At the NE point, both algorithms give similar result in terms of capacity level.

that moment. These CDF curves show the capacity values when the players reach the NE. Both algorithms improve the capacity of the system by 10% compared to initial condition in majority of the capacity values. On the other hand, the capacity values obtained by our algorithm are the same as the capacity values obtained by the previous algorithm in general. This result indicates that our algorithm is a strong candidate for the future networks.

Similarly, Figure2.4 shows the mean capacity level of all SUs for both algorithms. This figure also proves that for all users, our algorithm can reach the same NE attained from the previous algorithm. In terms of the mean feedback loads, our algorithm has 2040 feedbacks while the best selection algorithm has 5120 feedbacks. On the other hand, significant increment on mean capacity is obtained in both algorithms. This provides more spectral efficient system as well.

2.3.2 Throughput Analysis

It is also noted that in each analysis, we pick different SU's result to show the effect of game theoretical approach on different players.

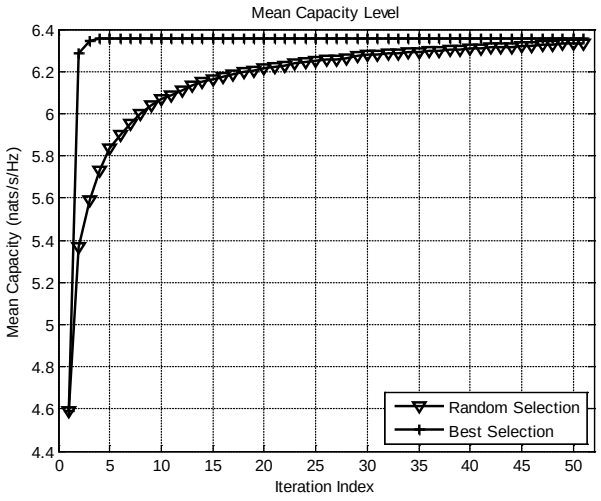

Figure 2.4 Mean capacity level becomes the same in the NE. Capacity increases with decreasing feedback load in random selection model.

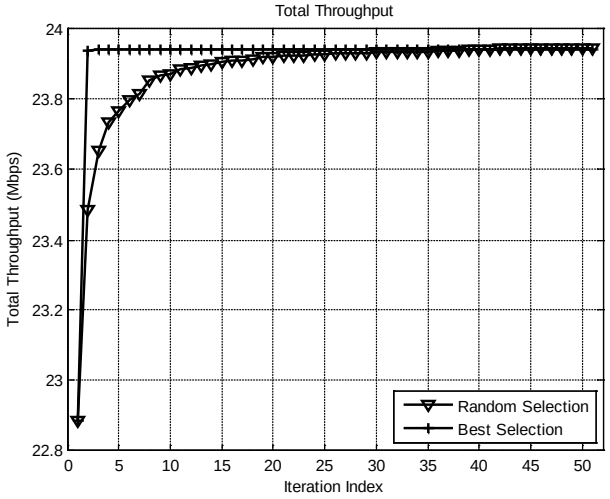

Figure 2.5 Total throughput increases 1.05Mbps in both algorithms when they reach the NE.

In this section, we analyze the performance improvement on an SU's total throughput. The throughput is calculated similar to [41] as

$$T_i^k(\mathrm{SINR}_i^k) = \max_{d_i^k} d_i^k(1 - P_e(\mathrm{SINR}_i^k, d_i^k)). \tag{2.12}$$

where d_i^k is the raw data rate on k^{th} subcarrier of user i, T_i^k is the throughput on k^{th} subcarrier of user i, P_e is the probability of error as a function of SINR value.

After achieving T_i^k, the total throughput can be defined as the sum of the throughput of all used subcarriers by the SUs. Mathematically,

$$T_{SU} = \sum_{k=1}^{K} (T_i^k). \tag{2.13}$$

Figure2.4 shows the total throughput of SUs. The increment on throughput is 1.05Mbps. While the convergence rate is increasing in our algorithm compared to the best selection algorithm, feedback load decreases remarkably when both algorithms are on the same NE.

CHAPTER 3

JOINT SUBCARRIER AND ANTENNA STATE SELECTION FOR COGNITIVE HETEROGENEOUS NETWORKS WITH RECONFIGURABLE ANTENNAS[1]

Cognitive HetNets have been recently presented as a promising solution for spectrum scarcity that holds back the high demand in wireless usage. This scarcity problem can be solved with various cognitive approaches which are named as interweave, underlay and overlay approaches. Among those approaches, we adopt the underlay approach where the SUs are allowed to share the spectrum with the PUs under limited interference constraint. In this constraint, the power transmitted by the SUs must guarantee that the interference at the PUs is below a predetermined threshold. However, in most practical cases, this interference constraint is limited to very small values that can lead to a reduction in the transmitted power by the SU resulting in an unacceptable performance. Moreover, since the PUs should operate with no coordination with the SUs, the interference levels from the PUs transmissions at the SUs receivers may be extremely high, and thus, degrading performance. One way to solve this issue is to use MIMO system by creating independent spatial dimensions through different antennas, and hence, the best antenna can be found to provide best performance for the SU. Although MIMO has many advantages over single-input single-output (SISO), the requirement of multiple antenna usage, which has some limitations such as distance in between two antennas [29], renders impractical the implementation of more than two antennas on mobile devices such as cell phone.

In this chapter, we adopt an emerging technology called RA. Compared to MIMO system, the importance of RAs comes from their physical sizes which make them to be feasibly employed at the SUs and their ability to provide different antenna radiation patterns for every antenna element

[1]This chapter was published in IEEE Transactions on Communications, vol. 63, no. 11, pp. 4015-4025, Nov. 2015. Permission is included in Appendix A.

using hardware techniques. Reconfigurability of antenna adds a degree of freedom[2] in terms of system capability to tackle the random nature of the wireless channel. This degree of freedom of reconfigurability depends on antenna structure and reconfigurability method. The choice of a reconfiguration mechanism is based on the design space and performance level required. Antenna reconfigurability can be categorized into four different reconfigurability functions, namely, a) reconfiguring resonance frequency, b) reconfiguring radiation pattern, c) reconfiguring polarization state, and d) a combination thereof [23]. By reconfiguring its frequency, RA can carry out spectrum allocation and frequency hopping to enhance the system capacity and can also reduce in-band frequency interference by reconfiguring its radiation pattern and polarization [24].

These reconfigurable features of the RA have attracted the interest of the research community to improve the performance of wireless communication systems in different applications. For example, SU can select the best state of the RA that maximizes SINR or capacity [25]. RAs can also be utilized to detect intruders to enhance security in communication systems [26]. For MIMO multiuser OFDM system, RAs are utilized to increase the performance in terms of capacity of MIMO systems for slowly fading environments and in different multipath environment including rich and sparse [27–30]. In [31], the authors use RAs to achieve blind interference alignment by introducing channel fluctuations resulting in independent signal-to-noise ratio values at predetermined time instants via blind antenna switching.

We consider a multiuser OFDM multicell cognitive HetNets where each SU is equipped with an RA. Our aim is to maximize the system capacity by jointly selecting the subcarrier and antenna state for each SU, and hence, reduce the interference in the system. This problem has been well-studied for the omni-directional antenna case within the OFDMA, where various resource allocation techniques have been proposed. Among these several techniques, game theoretical resource allocation has gained the interest of the research community because game theory provides the tools necessary to manage the interactions between players (users)[3] in order to improve the performance of the network while maintaining the interference coordination between users. Differ-

[2]Theoretically, the number of degree of freedom depends on the number of states that an RA provides. For instance, if an RA has three radiation patterns of different point directions and be able to operate in two different frequency bands, it can be said that this RA has six degree of freedoms.

[3]Throughout this chapter, 'player' and 'user' are used interchangeably.

ent game theoretical methods, which can be categorized as cooperative and non-cooperative games, are used in the resource allocation literatures on HetNets. For example, in [9], cooperative games are utilized to achieve resource allocation where the players establish coalitions. It is assumed that the group of players in the same coalition know what the others are doing. However, because of the uncoordinated nature of HetNets, cooperative games are not suitable for studies focused on the uplink scenarios. Therefore, more attention has been given to non-cooperative games by researchers. Stackelberg games as a non-cooperative framework are utilized in resource and power allocation studies in [10–14]. In Stackelberg games, there are leaders as the entities from primary networks and the followers as the entities from secondary networks, i.e., a two-stage game has to be introduced. However, since SUs are the interference sources and the unlicensed users, playing the game among PUs is not necessary because of having one central controller under one primary network scenario. In [15], Bayesian auction games are introduced within the resource allocation literature. This type of game is based on a bidder (user) and an auctioneer (access point). While each user bids for the available bandwidth based on its need, the access point distributes the bandwidth considering the proportional fairness criterion. Since this approach requires a central unit for decision-making, it is not appropriate for uncoordinated networks. In [16–18], authors propose resource allocation techniques by utilizing potential games because these games have a very significant property, namely, the FIP property which leads to NE convergence [6]. Therefore, potential games are used in this study to solve the problem of jointly finding the antenna state and subcarriers for each SU and the convergence to NE is shown. To the best of our knowledge, no prior study considers the exploitation of the spatial dimension, which can be achieved via utilizing RAs, in subcarrier allocation concept under a game theoretical framework.

In this chapter, we develop resource allocation technique for cognitive HetNets by exploiting RAs. Our objective is to use the capabilities of RAs to generate independent channel gains with different parameters to improve the capacity of cognitive HetNets. We use game theory to solve this problem and, in particular, we model the problem as potential games to solve the problem of jointly finding the antenna state and subcarriers for each SU as these games can be shown to achieve NE for our utility function. Since the number of antenna states in RA can be large, this might increase

the computational complexity in the system. To reduce the complexity, we divided our solution into two steps. In the first step, before playing the game, the players select the candidate antenna states set based on either of two different approaches. In the FPSS approach, all players have the same predetermined states (or radiation patterns). On the other hand, in the APSS approach, players select the states based on the locations of BSs and the SINR measurements in each state. In the second step, after selecting a candidate set, the game starts to be played. We focus on two different algorithms in terms of RA state selection, namely RS and BeS. Both techniques are based on the best subcarriers selection in terms of their capacity measurements among all available subcarriers achieved by the SU. In the BeS algorithm, this process is performed for each state, while SBS sends capacity reports of the subcarriers for only one randomly selected state with the aim of reducing the FL in the RS algorithm. Our results show that, while RS gives lower FL than BeS for RAs with two states, it becomes higher when we consider more than three states in an RA. This is due to the fact that the RS scheme requires more iterations to converge to NE compared to the BeS scheme as the number of states increases. On the other hand, we are showing that as the number of antenna states in RAs increases, the capacity enhances further.

As such, the contributions can be summarized as follows:

1. We formulate a model for cognitive HetNets where SUs are equipped with RAs. Different numbers of antenna states in RAs are analyzed with various beam widths and pointing directions.

2. Before playing the game, the APSS approach is introduced to increase the convergence rate. After the game has started, the RS and BeS algorithms are utilized to achieve joint subcarrier and antenna state selection.

3. SUs with RAs and conventional omni-directional antenna are compared to show the performance gain of the proposed algorithms in terms of overall capacity. On the other hand, the trade-offs are also presented in terms of convergence rates and FLs. Total capacity improvements are investigated for increasing numbers of SUs as well. Our results show

that an RA equipped with a 60° beam width provides the highest increase in the capacity gains compared to conventional antennas.

The remainder of this chapter is organized as follows. In Section 3.1, the system model with power control mechanism and RA structure is presented. The problem and potential game formulations are given in Section 3.2. In Section 3.3, detailed explanation of two different algorithms are given. The first algorithm is the candidate antenna state selection, which is performed before the game is played and the second algorithm is the subcarrier allocation and antenna state selection algorithm, which is performed during the game. Also, a proof of NE existence and convergence is provided. Section 3.4 offers numerical results for the proposed approach and, finally, conclusions are drawn in Chapter 7.

3.1 System Model

We consider a network composed of one PBS and multiple SBSs in which M PUs and $\mathcal{I}$ SUs are located randomly as seen in Figure 3.1. It is assumed that SUs are equipped with RAs that have the capability of choosing an antenna state among N possible states. The PUs, PBS and SBSs all use omni-directional antennas. It is worth mentioning that the purpose of assuming omni-directional antennas at the other users is to focus on quantifying the gains of exploiting RAs at the SUs within the game structure. We also assume that the users are using orthogonal frequency-division multiple access technique, where each SU is assigned a number of subcarriers among a total number of subcarriers K. The capacity of user i can be expressed as follows,

$$C_i = \sum_{k=1}^{K} \log_2 \left(1 + \frac{P_i^{\nu_i} g_{ik}^{\nu_i} a_{ik}}{\sum_{\substack{j=1, \\ j \neq i}}^{\mathcal{I}} Q_{jk}^{\nu_j} + \sum_{m=1}^{M} \tilde{Q}_{mk} + w_0} \right) \tag{3.1}$$

where $k = 1, 2, \ldots, K$ is the subcarrier index, ν_i indicates the antenna state index for user i, and $P_i^{\nu_i}$ denotes the transmit power for user i assuming antenna state ν_i is selected. Parameter a_{ik} is the indicator function of the kth subcarrier, where a_{ik} can take value 0 or 1 depending on whether the kth subcarrier is selected for user i or not. Variable $g_{ik}^{\nu_i}$ is the channel gain on the kth subcarrier

and antenna state ν_i, respectively; $Q_{jk}^{\nu_j}$ indicates the interference due to the received signal from the jth SU on the kth subcarrier, and is given by $Q_{jk}^{\nu_j} = P_j^{\nu_j} g_{jk}^{\nu_j} a_{jk}$, where $P_j^{\nu_j}$ shows the transmit power; $g_{jk}^{\nu_j}$ is the channel gain of the kth subcarrier and a_{jk} is the indicator function of the kth subcarrier for the jth PU. On the other hand, $\tilde{Q}_{mk}$ denotes the interference due to the received signal from the mth PU on the kth subcarrier, and is given by $\tilde{Q}_{mk} = \tilde{P}_m \tilde{g}_{mk} \tilde{a}_{mk}$, where $\tilde{P}_m$ shows the transmit power, $\tilde{g}_{mk}$ is the channel gain of the kth subcarrier and $\tilde{a}_{mk}$ is the indicator function of the kth subcarrier for the mth PU. The term w_0 represents the additive white Gaussian noise.

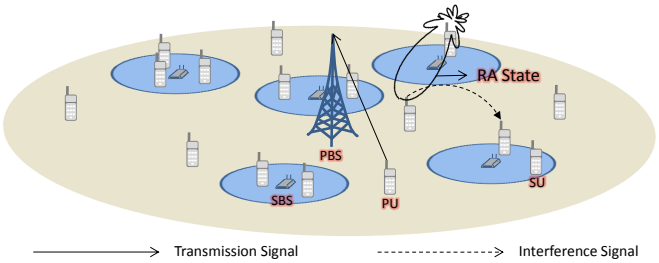

Figure 3.1 Cognitive heterogeneous network structure. SUs use the reconfigurable antennas with the ability of selecting different states than others.

3.1.1 Power Control

In cognitive networks, the SUs should make sure that the interference level at the primary receiver should be less than a predetermined value. Hence, we consider the following two constraints when the SU transmits a signal with a transmit power of $P_i^{\nu_i}$,

$$\begin{aligned} \bar{Q}_i^{\nu_i} &\leqslant \frac{\bar{Q}_{\max}}{\mathcal{I}} \\ P_i^{\nu_i} &\leqslant P_{\max} \end{aligned} \tag{3.2}$$

where $\frac{\bar{Q}_{\max}}{\mathcal{I}}$ indicates maximum allowable interference power in PBS caused by SU on antenna state ν_i whereas $P_{\max}$ indicates maximum transmit power constraint of SU on the νth antenna state. Interference power from the νth antenna state induced on PBS, $\bar{Q}_i^{\nu_i}$, can be defined as

$$\bar{Q}_i^{\nu_i} = P_i^{\nu_i} \bar{g}^{\nu_i}, \tag{3.3}$$

where $\bar{g}^{\nu_i}$ is the channel gain between the SU and the PBS. By combining the two constraints, the adjusted transmit power of SU i, $P_i^{\nu_i}$ can be rewritten as

$$P_i^{\nu_i} = \min\left(\frac{\bar{Q}_{\max}}{\mathcal{I}\bar{g}^{\nu_i}}, P_{\max}\right). \tag{3.4}$$

The above constraint requires full knowledge of the channel state information between the SU and PBS. Such condition may not be practical, therefore, in this chapter, we adopt a more realistic constraint. The probability that the interference exceeds the threshold should be below threshold ϵ, *i.e.*,

$$\Pr\left(\bar{Q}_i^{\nu_i} > \frac{\bar{Q}_{\max}}{\mathcal{I}}\right) \leqslant \epsilon. \tag{3.5}$$

Under the assumption that the channel between SU and PBS is Rayleigh with variance $\lambda_i^{\nu_i}$, $P_i^{\nu_i}$ can be written as follows [43],

$$P_i^{\nu_i} = \min\left(\frac{\bar{Q}_{\max}}{\mathcal{I}\lambda_i^{\nu_i}\ln(\frac{1}{\epsilon})}, P_{\max}\right). \tag{3.6}$$

In this scenario, the transmit power of the SU requires only knowledge of the channel variance $\lambda_i^{\nu_i}$, which can be obtained easily[4]. Therefore, using (3.6), each SU can determine its transmission power so as to guarantee the condition shown in (3.5).

3.1.2 Reconfigurable Antenna Structure

We study the impact of an RA system in terms of its pointing direction of maximum antenna gain, and its beam width. The adopted antenna characteristic is based on the well known 3GPP antenna model [44], which can be written as

$$A(\theta) = -\min\left[12\left(\frac{\theta-\theta_{pd}}{\theta_{3\text{dB}}}\right)^2, A_m\right] \tag{3.7}$$

[4]Since the channel variance is utilized in this power control algorithm, subcarrier index is omitted.

where θ_{pd} is the pointing direction (i.e., bore-sight of the antenna), $-180^\circ \leqslant \theta \leqslant 180^\circ$, $\theta_{3\text{dB}}$ is the 3dB beam width of the antenna in degrees, A_m is the maximum attenuation. We extend the application of this model to RA research work. The RA parameters for multiple antenna states are θ_{pd} for every value of the other reconfigurable parameter $\theta_{3\text{dB}}$. Pointing directions of every antenna states are reconfigured to a selected number of antenna states (N) starting from boresight direction of 0° and in steps of $\frac{360^\circ}{N}$. For instance, for RA of 8 radiation states, their pointing directions are 0°, 45°, 90°, 135°, 180°, 225°, 270°, and 315° and for a specified value for the reconfigurable parameter θ_{3dB}.

3.2 Problem Formulation

We consider the problem of finding the best antenna state and subcarrier for each user i so as to maximize the sum capacity of all players or equivalently,

$$C_{\max} = \max_{a_{ik}^{\nu_i}} \sum_{i \in \mathcal{I}} U_i(a_i, \nu_i) \tag{3.8}$$

subject to:

$$\sum_i a_{ik} = 1$$

where this constraint ensures that each subcarrier is employed by a single user and $U_i(a_i, \nu_i)$ is the utility function which is defined as the sum capacity of the selected subcarriers that is, equivalently $U_i(a_i, \nu_i) = C_i$ as defined in (3.1). At this point, it is worth mentioning the reason why we pick this utility function. In [18] and [16], authors utilize the total interference as utility function. While this utility function provides the total interference power in the whole network for player i, it doesn't provide any information about the player i's channel with its own BS. Therefore, there is a possibility that the player i might have a bad channel response in some of the selected subcarriers which can degrade the player i's communication in some selected subcarrier. On the other hand, since player i's RSS is not computed by its own BS, the calculation of the interference that the player i generates may not reflect the enough information about the antenna states and hence, the

player i may select the wrong state. To solve this issue, we expressed the utility function as the capacity.

This problem is a multidimensional optimization problem for which finding the optimal solution can become complex. To circumvent this issue, we use game theory to develop a solution for this problem that achieves convergence and to show the benefits of using RAs at the SUs.

Game theory provides a mathematical framework for an environment where there are non-cooperative players interacting with one another. In our framework, the players are defined as the SUs and denoted with i, $i \in \mathcal{I}$. On the other hand, strategies take the form of subcarrier and antenna state selection, which we denote by $s_i = \{a_i, \nu_i\}$ for player i, $s_i \in S_i$ where S_i is the strategy set of player i. With the utility function $U_i(a_i, \nu_i)$, the game $\mathcal{G}$ can be written with the three-tuple $\mathcal{G} = \langle \mathcal{I}, S_i, U_i \rangle$. With a given utility function and strategies, NE, which is an equilibrium point where the players have no incentive to change their strategies, can be formulated as

$$\begin{aligned} U_i(s_i^*, s_{-i}^*) &\geq U_i(s_i, s_{-i}^*) \\ \forall i \in \mathcal{I}, \forall s_i, s_{-i} &\in S \end{aligned} \tag{3.9}$$

where S indicates the set of strategy profiles for player i and every other player $-i$ and '*' indicates the equilibrium point.

3.2.1 Potential Game Formulation

A game is said to be a potential game defined with a potential function. When a player changes its strategy, the change in its utility function is reflected in the potential function. The following definition can be found in [6].

Definition 4 *A game $\mathcal{G}$ is said to be an ordinal potential game if it admits an ordinal potential. A function V is an ordinal potential for $\mathcal{G}$ if for every $i \in \mathcal{I}$ and for every $s_{-i} \in S_{-i}$*

$$U_i(s_i', s_{-i}) - U_i(s_i, s_{-i}) > 0 \text{ iff}$$
$$V(s_i', s_{-i}) \ - V(s_i, s_{-i}) > 0$$
$$\forall s_i, s_i' \in S_i. \tag{3.10}$$

It is guaranteed that there is at least one pure NE in ordinal potential games. In this chapter, we define the potential function similar to [45–47] as

$$V(S) = \sum_{k=1}^{K} \log_2 \left(\sum_{n \in \mathcal{I}} P_n^{\nu_n} g_{nk}^{\nu_n} a_{nk} + \sum_{m=1}^{M} \tilde{Q}_{mk} + w_0 \right) \tag{3.11}$$

Since $S = (\{a_i, \nu_i\}, \{a_{-i}, \nu_{-i}\})$, the potential function $V(\{a_i, \nu_i\}, \{a_{-i}, \nu_{-i}\})$ can be expressed as

$$V(\{a_i, \nu_i\}, \{a_{-i}, \nu_{-i}\}) = \sum_{k=1}^{K} \log_2 \left(\sum_{\substack{n \in \mathcal{I}, \\ n \neq i}} P_n^{\nu_n} g_{nk}^{\nu_n} a_{nk} + P_i^{\nu_i} g_{ik}^{\nu_i} a_{ik} + \sum_{m \in M} \tilde{Q}_{mk} + w_0 \right). \tag{3.12}$$

If the ith player changes its strategy from $\{a_i, \nu_i\}$ to $\{a_i', \nu_i'\}$, then the potential function $V(\{a_i', \nu_i'\}, \{a_{-i}, \nu_{-i}\})$ becomes

$$V(\{a_i', \nu_i'\}, \{a_{-i}, \nu_{-i}\}) = \sum_{k=1}^{K} \log_2 \left(\sum_{\substack{n \in \mathcal{I}, \\ n \neq i}} P_n^{\nu_n} g_{nk}^{\nu_n} a_{nk} + (P_i^{\nu_i} g_{ik}^{\nu_i} a_{ik})' + \sum_{m \in M} \tilde{Q}_{mk} + w_0 \right). \tag{3.13}$$

The subtraction of (3.12) from (3.13) can be performed as follows.

$$\begin{aligned} &V(\{a_i', \nu_i'\}, \{a_{-i}, \nu_{-i}\}) - V(\{a_i, \nu_i\}, \{a_{-i}, \nu_{-i}\}) \\ &= \sum_{k=1}^{K} \left[\log_2 \left(\sum_{\substack{n \in \mathcal{I}, \\ n \neq i}} P_n^{\nu_n} g_{nk}^{\nu_n} a_{nk} + (P_i^{\nu_i} g_{ik}^{\nu_i} a_{ik})' + \sum_{m \in M} \tilde{Q}_{mk} + w_0 \right) \right. \\ &\quad \left. - \log_2 \left(\sum_{\substack{n \in \mathcal{I}, \\ n \neq i}} P_n^{\nu_n} g_{nk}^{\nu_n} a_{nk} + P_i^{\nu_i} g_{ik}^{\nu_i} a_{ik} + \sum_{m \in M} \tilde{Q}_{mk} + w_0 \right) \right]. \end{aligned} \tag{3.14}$$

Since all players' strategies except player i are fixed, the difference obtained from the subtraction in (3.14) will only depend on the difference between $(P_i^{\nu_i} g_{ik}^{\nu_i} a_{ik})'$ and $P_i^{\nu_i} g_{ik}^{\nu_i} a_{ik}$. In this chapter, the players play with the best or better response correspondence in BeS or RS algorithm, respectively. Therefore, the change on the ith player's strategy will lead to following result.

$$V(\{a_i', \nu_i'\}, \{a_{-i}, \nu_{-i}\}) - V(\{a_i, \nu_i\}, \{a_{-i}, \nu_{-i}\}) > 0 \tag{3.15}$$

This indicates that the condition which is defined in (3.10) for the ordinal potential game is satisfied with our scheme.

3.2.2 Nash Equilibrium Convergence

The NE convergence with potential games can be shown over the FIP [6], because this property guarantees NE convergence and indicates the increment of the utility function in each path. Suppose that ξ_i is the path of player i in strategy set of S_i and the game is played sequentially. The sequence of strategies through iterations is $\xi_i = (s_i^0, s_i^1, s_i^2, \cdots)$. In BeS scheme, the players play with their best responses. If it is assumed that the new strategy s_i^l provides the best response for player i in its utility with respect to the previous strategy s_i^{l-1}, i.e., $s_i^l = \arg\max U_i(s_i^l, s_{-i}^{l-1})$, $s_i^l \in S_i$, then, the new utility function becomes $U_i(s_i^l, s_{-i}^{l-1}) > U_i(s_i^{l-1}, s_{-i}^{l-1})$. For this case, the potential function $V(s_i^l)$ in each path should satisfy the sequence of $V(s_i^0) < V(s_i^1) < V(s_i^2) < \cdots$ according the FIP property. In ordinal potential games, when players begin with random strategy profiles, if each player sequentially changes its strategy towards its unique best response, the game reaches NE within finite steps [48]. Since, in this chapter, the players play with the best responses in their strategies, then this proves convergence to NE.

Best responses require the search among all antenna states, which increase the FL. To alleviate this problem, in the RS algorithm, a random state selection algorithm is proposed. Instead of playing with best responses, players select the antenna states based on the better responses, i.e., the player changes its strategy if the utility of the randomly selected antenna state offers a higher payoff. So, if $U_i(s_i^l, s_{-i}) > U_i(s_i^{l-1}, s_{-i})$, s_i^l is said to be the better response correspondence in the ith player strategies. Thus, as indicated in [16], when better responses are satisfied, NE convergence

can be achieved. At this point, it is worth mentioning that the main difference between the BeS and RS algorithms is the convergence rate. Since RS algorithm is based on better responses, it has slower convergence rate. This statement can also be supported by simulations as seen in Figure 3.5.

3.3 Solution Framework and Nash Equilibrium Convergence

In this section, we develop a framework for jointly selecting the antenna state and subcarrier for each user. The framework is divided into two step. In the first step, namely candidate antenna state set, SUs only define a subset of the available antenna states from which the antenna state is selected. The objective of this step to limit the search space for the antenna states and hence improve the computational complexity of the proposed solution. In the second step, a joint subcarrier and antenna state selection game is played among the antenna states that only belong to the candidate antenna state set determined in the first step. It is important to note that candidate antenna state set selection is performed before playing the game. After the candidate set is selected, the users start to play the game according to the RS and BeS algorithms. At the end of the section, we show that NE convergence can be achieved.

3.3.1 Step 1: Candidate Antenna State Set

Two approaches are introduced to select candidate antenna states. In APSS approach, the SUs selects the set of antenna states based on location information before the game starts. Alternatively in FPSS approach, state selection is fixed and assumed to be the same for all SUs.

As described earlier, the RA at the SU can have multiple antenna state pointing directions depending on the beam width. For instance, if the adaptive beam width is 45°, the total number of states would be eight, i.e., $N = 360°/45°$=8. Naturally, the complexity of the subcarrier allocation problem in (3.2) increases as the number of states increases. To reduce complexity, each SU selects a candidate antenna state set among those fixed directions from which the SU selects the antenna state while running the joint antenna state and subcarrier allocation game. In particular, we consider selecting these candidate states based on the geographical location of the PBS and the SINR measurements performed for the states in the direction between both the SBS and PBS.

Specifically, we sort the antenna states according to the ratio of signal strength received from the SBS and signal strength received from the PBS; the first state would be the one with the highest ratio. This candidate set selection approach is called the APSS approach. To explain this selection technique further, let us assume that the RA can provide eight states, as seen in Figure 3.2, and only three states can be selected for the candidate antenna state set. By applying this technique, the candidate antenna state selection set is composed of state 1, state 3, and state 8. We note that state 2 is not selected even if it provides higher signal strength from the SBS. This is due to that fact the state 2 experiences a very high interference level from PBS and hence the ratio of signal strengths from SBS and PBS will be lower than that experienced from state 3. In the APSS approach, the candidate set will be different for the SU depending on its location with respect to the SBS and PBS.

Another way of selecting the candidate set states is called the FPSS approach. This method does not require the location information of the SBS and PBS, or performing any SINR measurement. In this later case, we assume that the candidate set is fixed for all SUs, i.e., the same for all SUs where the candidate set should be selected to maximize the coverage of the antenna. For instance, if SUs have two states, the best antenna states to maximize the coverage would be those pointing to 0° and 180° since the location information is not required in this stage.

3.3.2 Step 2: Joint Subcarrier Allocation and Antenna State Selection

In this game, subcarrier allocation is performed based on best responses. If the players have omni-directional antennas, they select the subcarriers whose capacity values are the highest. The number of subcarriers assigned to a player depends on their needs. When a player obtains the capacity reports for each subcarriers, it sweeps through them, and looks for the ones that have the highest capacity values. If the players have RAs, i.e., multiple antenna states, they obtain the reports for all subcarriers from each antenna states. When the player selects the best subcarriers that correspond to every antenna states, it computes the sum capacity of the selected subcarriers for each antenna state. After computing the utility of each states, the player selects the one that has the highest payoff. This is referred to as the BeS algorithm.

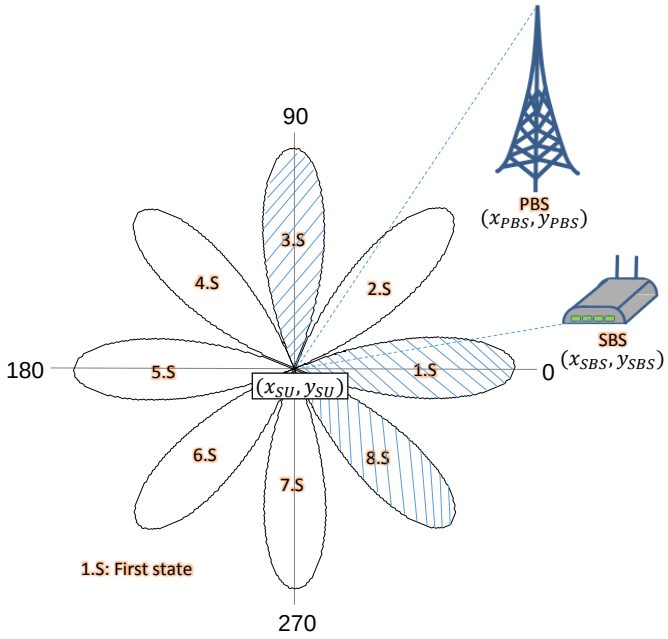

Figure 3.2 Based on the geographic location of PBS and SBS, SU selects the states which would cause the least interference onto PBS and provide the highest possible signal strength onto SBS. In this example, SU picks first, third and eighth states when it is in (0,0) coordinates.

Obtaining the reports for each subcarrier in each state may cause higher FL, which is defined as the number of reports sent by the transmitter to the receiver to be able to select the best subcarriers and state. It can mathematically be expressed as

$$FL_{BeS} = \sum_{t \in T} \sum_{i \in \mathcal{I}} B_{t,i} N. \tag{3.16}$$

where T is the number of iterations needed for BeS algorithm, N is the number of states and $B_{t,i}$ is the number of measurements needed for the ith user at tth iteration, which depends on the number of subcarriers. To decrease the FL, instead of taking the reports in every state, the player can select the state randomly in each iteration, and take the reports for the subcarriers in this state only. When it selects the best subcarriers, it compares the sum capacity result, $U_i(s_i', s_{-i})$, with the one that was achieved in the previous iteration, $U_i(s_i, s_{-i})$. If the utility $U_i(s_i', s_{-i})$ is higher than the utility $U_i(s_i, s_{-i})$, then the player picks these newly selected subcarriers and their associated state. This completes the description of the RS algorithm, which is summarized in Table 3.1. So,

the FL for the RS algorithm can be expressed as follows.

$$FL_{RS} = \sum_{t \in T1} \sum_{i \in \mathcal{I}} B_{t,i}. \tag{3.17}$$

where $T1$ is the number of iterations needed for RS algorithm. In Section 3.4, the FLs are compared for both algorithms.

In Figure 3.3, the BeS and RS algorithms are compared with an exhaustive search algorithm under the two secondary network scenarios. As seen in the figure, since BeS and exhaustive search algorithm search for the resources and the state which have the highest capacity results, both schemes provide similar performance.

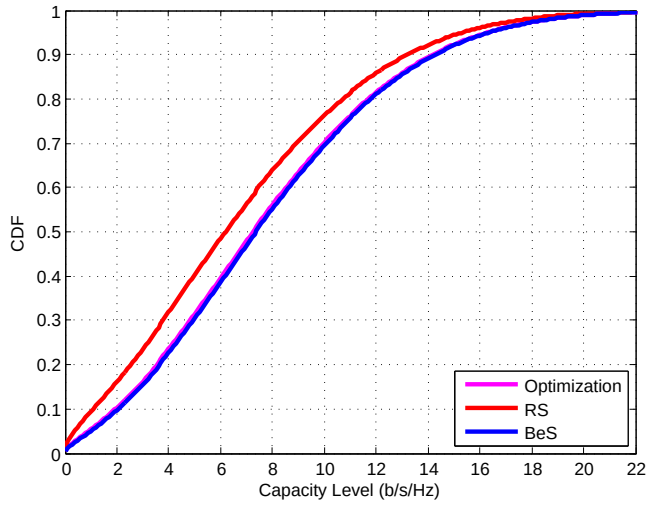

Figure 3.3 The BeS algorithm outperforms the RS algorithm and it can provides a level of performance close to the exhaustive search algorithm.

3.4 Performance Evaluations

In this section, we provide performance results for the algorithms proposed in Section 3.3. We assume a network with one PBS, 20 PUs, and 20 SBSs, which can be viewed as a femtocell. Each SBS has two SUs. The radius of coverage circle for SBS is 40m. The minimum distance between the PUs and SUs to the PBS and SBS, respectively, is 3m. The SBSs are randomly distributed within a PBS coverage area. Similarly, the SUs are also randomly distributed within

Table 3.1 Subcarrier allocation algorithm with random state selection

#	The Game algorithm
1	Allocate random subcarriers to each player with a random state
2	*for* t = 1:T (iterations)
3	*for* i = 1:$\mathcal{I}$
4	Randomly select one antenna state, ν
5	*for* k = 1:K
6	Calculate $U_i(a_i, \nu_i)$
7	*end*
8	if $U_i(s_i', s_{-i}) > U_i(s_i, s_{-i})$
9	Select antenna state with $U_i(s_i', s_{-i})$
10	*end*
11	*end*
12	*end*

a SBS coverage area. The tolerance ϵ in (3.5) is assumed to be 0.05, and the maximum allowable interference power $\bar{Q}_{\max}$ is set to -77dBm. All other simulation parameters are compiled in Table 3.2.

Table 3.2 Simulation parameters

Simulation Parameters	Parameter Value
Cell type	Hexagonal
Power of UE	23dBm
UE Antenna Gain	5dBi
Noise Figure	5dB
Bandwidth	10MHz
FFT size	1024
Number of subcarriers/SU	50
Number of subcarriers/PU	50
Number of SUs/SBS	2
Number of SBSs	10,15,20,25,30
Number of PUs	20
Modulation Order	QPSK
PBS radius	500m
SBS radius	40m
Number of states	6
Shadowing standard deviation	8dB (PU) - 4dB (SU)

The adopted channel model is the clustered delay line model taken from WINNER II D1.1.2 V1.1 [49]. The path loss models defined in Table 3.3 are obtained from the 3GPP 36.814 standard [50].

Table 3.3 Path loss models

Case	Model
PU to SBS	$PL = \max(15.3 + 37.6\log_{10} R, 38.46 + 20\log_{10} R) + 0.7d_{2D,indoor} + qL_{iw} + L_{ow}$
SU to SBS	$PL = 38.46 + 20\log_{10} R + 0.7d_{2D,indoor}$
SU to PBS	$PL = 15.3 + 37.6l\log_{10} R + L_{ow}$
R is distance in m, L_{ow} is the penetration loss of an outdoor wall which is equal to 20dB, L_{iw} is the penetration loss of the wall separating apartments which is equal to 5dB, q is the number of walls separating apartments between UE and SBS which is equal to 1, and $d_{2D,indoor}$ shows the distance inside the house central frequency is 2 GHz.	

In Figure 3.4, the BeS and RS algorithms are shown using the FPSS approach. The beam width is assumed to be equal to 60°. Figure 3.4 indicates that, when the number of states increases, the capacity values also increase. This can be explained by the fact that increasing the number of states increases the number of channels with independent channel impulse responses. This gives a higher chance to find an antenna state that has better channel condition for every user. As explained above, in FPSS, all users play the game among the predetermined candidate antenna states. For instance, for the two-state case, all users select between two states with the beam directions of 0° and 180°. If the SBS is located in the direction of 90° and, hence, the beam cannot be directed towards that direction, a low capacity value is achieved with high probability. But, for the six-state case, for which the antenna can direct the beam to more pointing directions, it can select the one that is more directed towards the SBS.

This figure also shows the difference between the BeS and RS algorithms. The BeS algorithm gives better results for any number of antenna states. The comparison between these two algorithms can be seen in Table 3.4. This table shows the difference in terms of percentage from the omni-directional case in the 50th percentile.

Table 3.4 Percentage difference in RS & BeS algorithms

	2 States	3 States	4 States	5 States	6 States
RS	9.3%	27.9%	36%	40.7%	46.5%
BeS	20.9%	37.2%	44.2%	50%	54.7%

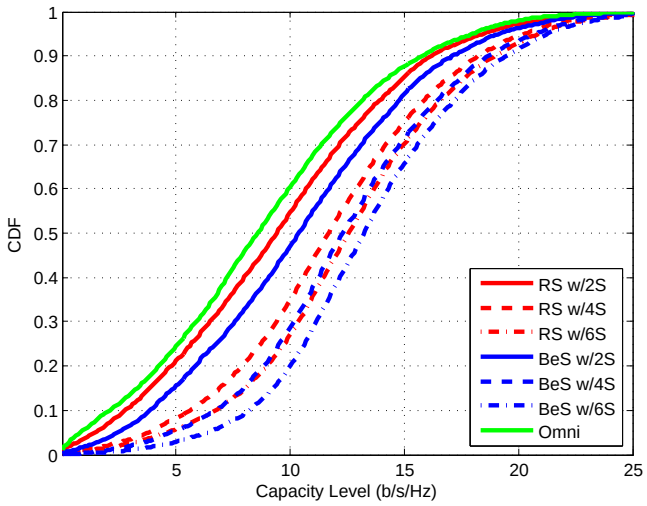

Figure 3.4 When the antenna state selection is not adaptive, i.e., it is fixed for all users, the capacity difference in terms of percentage from 2S case to 6S case in 50% level is 37.2% and 33.8% in RS and BeS algorithms, respectively.

As mentioned in Section 3.3.1, before the players play the game, antenna state selection is performed. Figure 3.5 shows the mean capacity results achieved with the APSS approach in each iteration. While this figure gives information about the difference between the number of cases for both RS and BeS algorithms, it also shows in which iteration NE is reached, i.e., the convergence rate can be obtained. While NE is reached in the 4th, 15th, 24th, 29th and 42nd iteration in RS, it is reached in the 4th iteration in BeS algorithm with two-to-six states, respectively. Also, it is attained in the 5th iteration in the omni-directional antenna case. Based on iteration information attained above, FLs can be seen in Table 3.5 for both algorithms.

Table 3.5 Feedback loads for RS & BeS

	Feedback Loads					
	Omni	2 States	3 State	4 State	5 State	6 State
RS	5120	4096	15360	24576	29696	43008
BeS	5120	8192	12288	16384	20480	24576

Table 3.5 presents the FL for the RS and BeS algorithms for different values of the antenna states. As it is evident from the values, RS does not necessarily provide the lowest FL since the RS algorithm requires more iterations to achieve the NE. For instance, for a number of states above

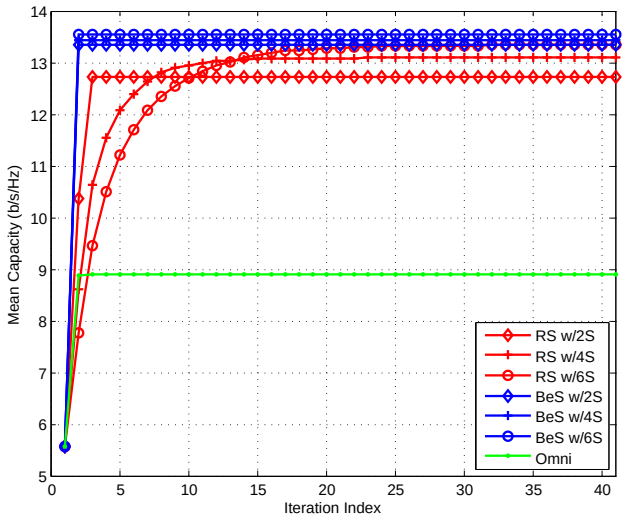

Figure 3.5 Users reach the NE in each case. In RS algorithm, when the number states increases, convergence to NE is taken longer duration because of the randomly selection of the state information.

two, BeS provides lower FL and higher capacity. This shows that there exists a tradeoff between the FL and the amount of capacity required.

In Figure 3.6, the capacity levels of different states are compared under the APSS approach for both the RS and BeS algorithms. As shown in previous results, BeS gives higher capacity gains. The important point in this figure is that the RAs with various number of states offer similar performance. For instance, the difference between the two and six-state cases is negligible. Since the user can select the antenna pointing direction based on the location and SINR measurements before playing the game, this leads to playing the game among the best states which have the least interference and highest received transmission power. If PBS and SBS are in the same direction, then through power control, interference is kept under a certain threshold. In terms of FLs, the two-state case provides the lowest level, as seen in Table 3.5. This APSS approach saves users from tremendous amount of FLs. Thus the energy consumption is decreased significantly.

Table 3.6 compares the gain in mean and median capacity level from omni-directional antenna case to other state cases in terms of percentage values.

Figure 3.7 compares the results for FPSS and APSS in terms of the number of antenna states used during the game. As seen from the figure, the FPSS approach with six states provides a

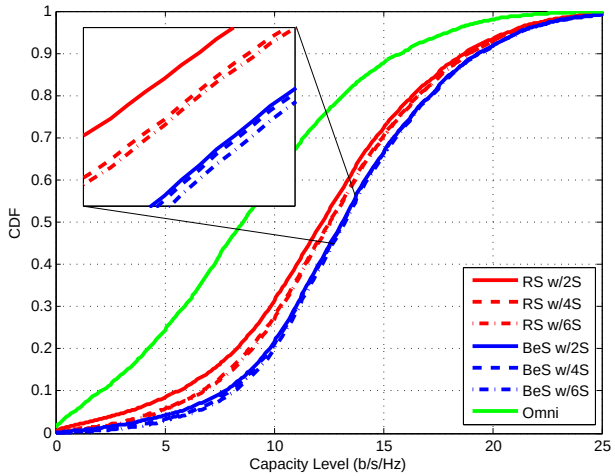

Figure 3.6 When state selection is adaptive for all users, the mean capacity difference from 2S case to 6S case is %3.2 and %2.2 in the RS and BeS algorithms, respectively.

Table 3.6 Capacity gains in terms of mean&meadian level for RS & BeS

	Algorithm	2 States	3 State	4 State	5 State	6 State
Mean	RS	%42.4	%43.8	%44.8	%45	%45.6
	BeS	%50	%50.8	%51	%52.2	%52.2
Median	RS	%46.6	%46.5	%47.7	%47.7	%48.5
	BeS	%53	%53.4	%53.5	%54.2	%54.2

capacity gain similar to the APSS approach with two states. Thus, the FL is reduced by playing the game among only two states instead of six states. Moreover, as mentioned above, it also decreases the complexity.

In Figure 3.8, the total capacity change, which is obtained by summing the capacity results of all the users in the network, is shown with different numbers of SUs. When the number of users increases, the total capacity also increases. Since this figure is obtained with APSS, both the RS and BeS algorithms attain almost the same capacity values for the users with different number of states. This figure also supports our previous results in terms of the closeness in the capacity values with APSS approach. When the users employ omni-directional antenna, they perform the worst. As shown in this figure, usage of RAs in all devices provides better results even when the number of users increases. To find in what number of SUs the system would provide the highest capacity, one can observe from the curves in Figure 3.8 that there is a trend toward a maximum value. The data presented in Figure 3.8 are used to model the trend via fitting a second order equation as a

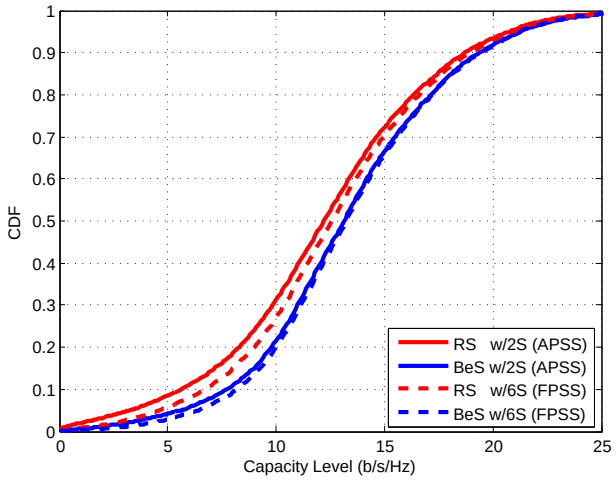

Figure 3.7 Capacity values in APSS approach with two states are very close to ones in FPSS approach with six states.

function of number of users x. The second order polynomial equation $y = ax^2+bx+c$ is utilized. By equating the first order derivative of this equation to zero, i.e., $0 = 2ax + b$, the maximum number of SUs can be identified. Table 3.7 shows the number of SUs that yields the highest capacity in the network for each antenna state case. It can be seen that RS serves slightly more users, and both RS and BeS serve much higher number of users.

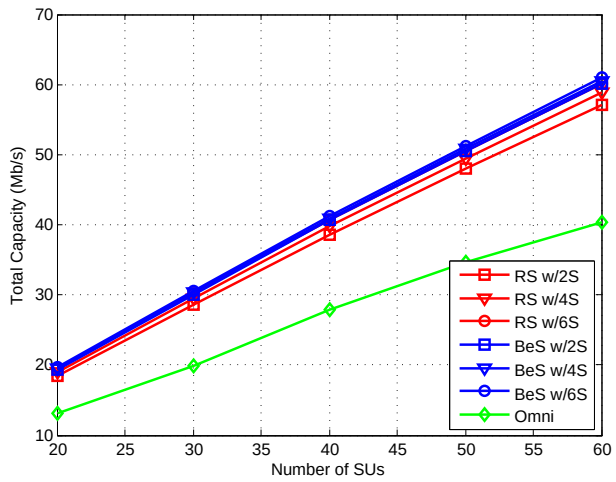

Figure 3.8 When the number of SUs increases, the total capacity also increases. The capacity values of the users who have different number of states are very close to one another.

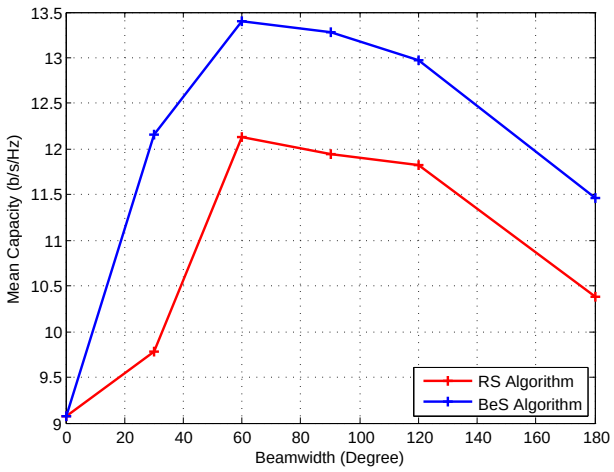

Figure 3.9 When the beam width is 60°, the maximum mean capacity level is obtained.

Table 3.7 The maximum number of SUs who would perform the highest capacity in the network for RS & BeS

	Omni	w/2S	w/3S	w/4S	w/5S	w/6S
RS	117	283	280	266	294	294
BeS	117	277	278	287	280	289

Figure 3.9 shows the mean capacity change for different beam widths. To achieve that, we compare the beam widths of 30°, 60°, 90°, 120° and 180°. The number of states is constant in each case, i.e., each user has two states with APSS. As seen on the figure, the highest mean capacity value is obtained when the beam width is 60° in both the RS and BeS algorithms. This is a very significant result for RA studies. When the beam width is 30°, although users experience less interference due to the narrow beam width, the received transmission power also becomes negatively affected. On the other hand, increasing the beam width will reduce the chance of attenuation of the signal of interest, but it increases the level of interference. Therefore, when the beam width is 180°, the capacity gain of the system decreases. Figure 3.9 indicates that the mean capacity results attained from the antenna states with the beam width of 30° and 180° are close to each other. For future system designs with RAs, 60°, 90° and 120° beam widths can be utilized.

CHAPTER 4

PARTIALLY OVERLAPPING FILTERED MULTITONE WITH RECONFIGURABLE ANTENNAS IN HETEROGENEOUS NETWORKS

Due to the unprecedented increase in the wireless usage demand, researchers have primarily focused on spectrally efficient solutions. As one of the most efficient solutions, OFDM has been proposed to satisfy this demand. On the other hand, its robustness against fading caused by multipath propagation and inter-symbol interference make OFDM widely used technique in today's systems. In coordinated networks such as homogeneous networks, OFDM provides high spectral efficiency. However, OFDM is highly vulnerable to interference coming from other users in uncoordinated networks such as cognitive HetNets or self-organizing networks. In cognitive HetNets, SUs are unlicensed users that need to utilize the licensed bands. Therefore, SUs produce destructive interference over licensed PUs due to their presence in the primary network area. While SUs cause high interference on PUs, they may also create interference on other SUs.

Various solutions have been proposed in the literature to handle/decrease the interference in cognitive HetNets. One group of studies focuses on the game theoretical resource allocation techniques. Since GT investigates the interactions between two or more nodes and can provide a solution among uncoordinated players (users), it has been utilized extensively in the resource allocation studies. S-modular games are used in [51] to carry out the subcarrier allocation. [10, 11, 13, 14] utilized the Stackelberg game which is based on the leader and followers scenario. When there are multiple primary and secondary networks, this game can be utilized to perform resource allocation. While a cooperative game approach is used in [9], potential games are proposed with resource and power allocation literature in [16, 17, 52].

Another group of studies focuses on the POCs [33,53] to reduce the interference in cognitive HetNets. In WiFi networks, there are three non-overlapping channels among the eleven available channels. POCs is utilized when there are more than three users in a WiFi network. For example, for four users case, instead of using non-overlapping channels of 1, 6 and 11, channels 1, 4, 7 and 11 are proposed to be used in a partially overlapping manner. Also, in [54–56], POCs concept is utilized to increase throughput. In [57], a game theoretical POCs is proposed where players are trying to find the least aggregated interference channel. Cooperative games are used among access points in [58] to increase throughput, and hence, to decrease the interference.

Recently, POTs concept has been introduced in [32] to reduce the interference coming from other users in uncoordinated networks. Rather than utilizing the overlapping channels as in POCs techniques, intentional CFS is performed in the POTs concept. The allocated resources to two uncoordinated users i and j are illustrated in Figure 4.1a and Figure 4.1b (solid curve) where i and j are assigned at the same time. Before j is provided with a frequency shift, both users fully overlap each other, i.e., they fully interfere with each other. To decrease the interference, j introduces some CFS (dashed curve) as shown in Figure 4.1b. Partially overlapping scheme can therefore be achieved at the subcarrier level to reduce the cross interference as depicted in Figure 4.1c.

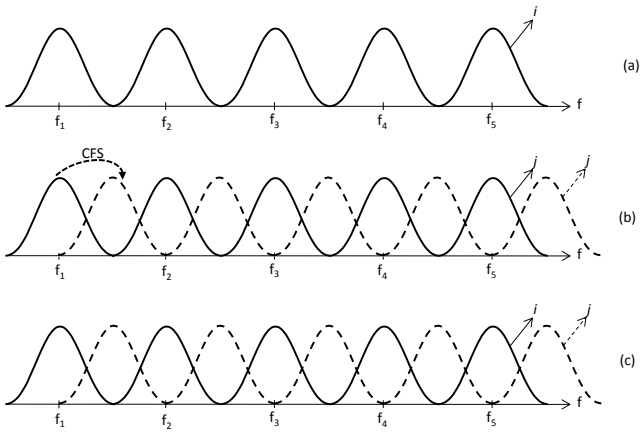

Figure 4.1 Users i and j fully overlap in (a). j performs CFS to decrease the interference in (b). i and j partially overlap in (c).

The POTs concept in the frequency domain at the link level has recently been proposed in [32]. In this chapter, system level analysis of this concept is performed with both orthogonal

and non-orthogonal waveforms where the results are compared with OFDM. As a scheme, FMT is utilized due to certain advantages over OFDM such as providing flexibility in resource allocation, not requiring synchronization between transmissions in both ends of a link, and not necessitating the cyclic prefix usage [38]. When partially overlapping scheme is performed among multiple users, two questions arise:

1. Which user should perform partially overlapping in the cognitive HetNets system structure?

2. How much overlapping should a user carry out, i.e. what percentage[1] of the frequency shift should a user adopt?

If all users introduce the same amount of CFS at the same time, partially overlapping would not be achieved since the users would still fully overlap each other. In this case, all users will capture the same interference. To overcome this issue, we propose game theoretical POFMT technique. While GT is utilized to determine the FSR in the frequency domain, it may also be used to select the antenna state (radiation pattern) of RA to achieve partially overlapping in the space domain. In RAs, the antenna characteristics can be reconfigured electrically or mechanically. In the fixed directions, different radiation patterns can be generated with RAs. Also, they have the capability to work in different operating frequencies [23] which can provide additional degree of freedom in the user equipment. The main motivation to use these antennas in this chapter is their physical sizes and capability of generating multiple states. MIMO technology can also be used to form multiple states. Due to the challenges such as minimum distance requirement between two antennas, MIMO technology is currently not feasible in mobile devices. RA therefore becomes a possible future solution for small devices. In the literature, RAs have been utilized in various studies. In [27, 29, 30], RAs are used with MIMO to increase the system performance in different environments. RAs are utilized in [26] to perform the intrusion detection. These antennas are used in [25] to perform sub-channel allocation and a blind interference alignment with RAs is proposed

[1]It is considered that 50% equals $f_0/2$, where f_0 is a subcarrier spacing.

in [31]. To the best of our knowledge, however, RAs have not been utilized with POTs in the literature.

In this chapter, POFMT with RAs is proposed within a game theoretical framework. In our previous study [37], we investigated the POFMT concept with only orthogonal waveforms in the system level without utilizing the RAs. In this chapter, non-orthogonal waveforms are introduced. Additionally, RAs are also utilized to introduce the space domain partially overlapping and to further improve the system performance. A joint FSR and antenna state selection game is proposed. While SUs search for the FSR to reduce the interference from other SUs in the environment, they also determine the antenna state where the highest utility can be achieved for the relevant FSR. The existence of NE in this game is proved theoretically with potential games and simulations. As demonstrated with simulation results, POFMT scheme with RAs outperforms OFDM in terms of capacity with the expense of slightly lower spectral efficiency in the system.

The contributions can be summarized as follows:

1. System level implementation and analysis of POTs are introduced in the cognitive HetNets with homogeneous 2-D Poisson point process (PPP) realization.

2. Orthogonal and non-orthogonal waveforms are investigated under POTs concept with various subcarrier spacing and filter roll-off and dispersion parameter values. The results are compared with OFDM. When the different subcarrier spacing values are examined, the filter roll-off value is fixed. Similarly, when the different roll-off values are investigated, the filter subcarrier spacing value is fixed.

3. RA is utilized to achieve the partially overlapping in space domain. Joint FSR and antenna state selection is introduced. The results are compared with omni-directional antenna usage.

4. Play&Wait (P'nW) algorithm is introduced. In this algorithm, players randomly play for some time and then wait for some random time. As a result, players may reach NE.

The remainder of this chapter is organized as follows. In Section 4.1, the system model is introduced where the transmission, channel, and reception models are given within the system

model. The problem formulation with potential games and the game algorithm is explained in Section 4.2. Section 4.3 entails numerical results of the proposed approach. Conclusions are drawn in Chapter 7.

4.1 System Model

We consider an uplink scenario which has multiple SBSs and SUs within a coverage area of primary cell. We also consider that the SBSs are distributed in an area as a realization of homogeneous 2-D PPP of ϕ with the intensity λ as seen in Figure 4.2. It is assumed that each SBS serves to a single SU and there is only one SBS-SU pair in each Voronoi cell. We also consider that SUs are equipped with RAs while SBSs use omni-directional antenna. SUs are assumed to be able to introduce an intentional frequency shift compared to the other links.

4.1.1 Transmission Model

The transmitted signal of ith SU, $i \in \mathcal{I}$, where $\mathcal{I}$ is the set of SUs, is given by

$$x_i(t;\varphi_i) = \sum_{m=-\infty}^{\infty} \sum_{k=0}^{K-1} X_{kmi} g(t - mT) e^{\mathrm{j}2\pi k(f_0+\varphi_i)t}, \tag{4.1}$$

where K is the total number of subcarriers, X_{kmi} is the modulated symbols on the kth subcarrier of mth symbol, f_0 is the subcarrier spacing, T is the symbol duration, $g(t)$ is the prototype filter, and $\varphi \in [0, f_0]$ is the frequency shift introduced by ith user, which aims to reduce the interference coming from other users with the concept of POTs.

4.1.2 Channel Model

We consider utilizing an antenna model given in 3GPP standards [50] as an RA. This model captures different large scale attenuations with respect to the νth RA state, $\nu \in \Lambda$ where Λ is the state set of antenna, and is given by

$$A_\nu(\theta) = -\min\left[12\left(\frac{\theta}{\theta_{3\mathrm{dB}}}\right)^2, A_{\max}\right]. \tag{4.2}$$

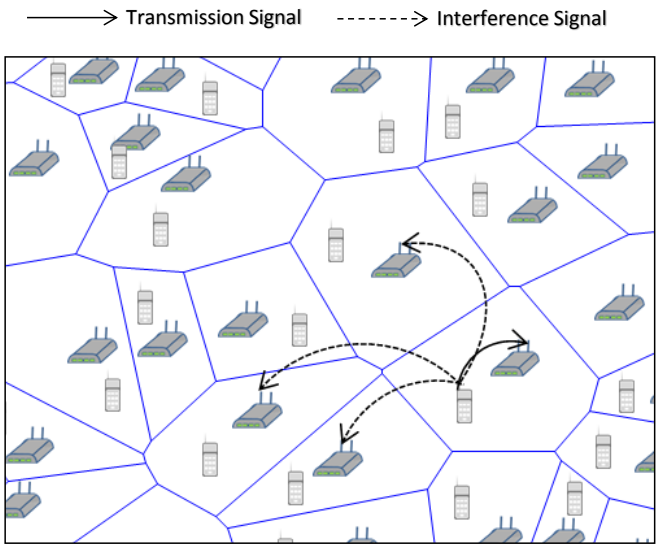

Figure 4.2 System view. In Poisson point process approach, the system has multiple SBSs with a single SU and each voronoi cell has one SBS-SU pair. Also, each user has RA which can form a state in one direction.

where θ is the angle between the direction of relevant BS and the boresight direction, $-180° \leqslant \theta \leqslant 180°$, $\theta_{3\text{dB}}$ is the 3 dB beamwidth of the antenna, and $A_{\max}$ is the maximum attenuation. In this chapter, we consider fixed boresight directions towards where the antenna can generate the radiation pattern. For instance, when an RA generates six beams, and the angle between beams is 60°, then, the boresight directions become 0°, 60°, 120°, 180°, 240° and 300° by starting from 0°. With the consideration of small scale Rayleigh fading, channel impulse response for the νth antenna state is given as $h(t,\tau;\nu) = \sum_{\ell=0}^{L-1} \varrho_\ell(t;\nu)\delta(t-\tau_\ell)$ where ℓ is the path index, L is the total number of paths, τ_ℓ is the delay of the ℓth tap, and $\varrho_\ell(t)$ is the path gains. The channels of ith intended user and jth interfering user are denoted with $h_i(t,\tau;\nu_i)$ and $h_j(t,\tau;\nu_j)$.

The received signal strength (RSS) of the user is calculated as $RSS = P_{\text{tx}} + G - PL$ where P_{tx} is the transmit power, G is the transmit antenna gain, and PL is the path loss. The transmit antenna gain can be calculated as $G = G_{\text{tx}} + A_\nu(\theta)$ where G_{tx} is the constant antenna gain given in [50] and $A_\nu(\theta)$ is the attenuation.

4.1.3 Reception Model

The received signal of SBS of the ith SU is expressed as

$$y_i(t;\varphi_i,\nu_i) = \int_\tau \int_\varphi H_i(t,\tau;\nu_i)x_i(t-\tau;\varphi_i)\mathrm{d}\varphi\mathrm{d}\tau + \sum_{j\in\mathcal{I},j\neq i} \int_\tau \int_\varphi H_j(t,\tau;\nu_j)x_j(t-\tau;\varphi_j)\mathrm{d}\varphi\mathrm{d}\tau + w(t), \tag{4.3}$$

where j is the interfering users index, $w(t)$ is the additive white Gaussian noise, $H_i(t,\tau;\nu_i)$ and $H_j(t,\tau;\nu_j)$ are the Fourier transformations of $h_i(t,\tau;\nu_i)$ and $h_j(t,\tau;\nu_j)$, respectively.

The location of the users with respect to their corresponding SBS is critical in terms of RA state. If the direction of the interfering users' antenna state ν_j is not towards the ith SBS, lower interference power is captured when compared to the case where all users are equipped with the omni-directional antenna. Thus, in order to obtain the received symbol, the received signal is projected onto the corresponding received filter as

$$\begin{aligned}\tilde{X}_{lni}(\varphi_i,\nu_i) &= \left\langle y_i(t;\varphi_i,\nu_i), g(t-nT)e^{\mathrm{j}2\pi l(f_0+\varphi_i)t}\right\rangle \\ &= \int_t r_i(t,\tau;\varphi_i,\nu_i)g(t-nT)e^{-\mathrm{j}2\pi l(f_0+\varphi_i)t}\mathrm{d}t \\ &+ \sum_{\substack{j\in\mathcal{I},\\ j\neq i}} \sum_{n=-\infty}^{\infty} \sum_{l=0}^{K-1} \int_t r_j(t,\tau;\varphi_i,\nu_j)g(t-nT) \\ &\times e^{-\mathrm{j}2\pi l(f_0+\varphi_i)t}\mathrm{d}t + w(t),\end{aligned} \tag{4.4}$$

where $r_i(t,\tau;\varphi_i,\nu_i) = \int_\tau \int_\varphi H_i(t,\tau;\nu_i)x_i(t-\tau;\varphi_i)\mathrm{d}\varphi\mathrm{d}\tau$. As it can be seen in (4.4), SBS employs the same frequency shift of ith user in order to receive the symbol properly. Otherwise, the transmit pulse shape will be captured partially, which can degrade the performance tremendously in terms of capacity. Alternatively, the same situation provides significant advantage against the interfering users that introduce different amount of frequency shift φ_j. Since the interfering signal is captured based on φ_j, the SINR of the ith user is increased significantly. Therefore, SINR of SBS of the ith

SU can be expressed as

$$SINR_i = \frac{P_i(\varphi_i, \nu_i)}{P_j(\varphi_i, \nu_j) + w_0}. \tag{4.5}$$

In (4.5),

$$P_i(\varphi_i, \nu_i) = \mathbb{E}\left[\left| \int_t r_i(t, \tau; \varphi_i, \nu_i) g(t - nT) \times e^{-\mathrm{j}2\pi l(f_0+\varphi_i)t} \mathrm{d}t \right|^2\right],$$

and

$$P_j(\varphi_i, \nu_j) = \sum_{\substack{j\in\mathcal{I},\\ j\neq i}} \sum_{n=-\infty}^{\infty} \sum_{l=0}^{K-1} \mathbb{E}\left[\left| \int_t r_j(t, \tau; \varphi_i, \nu_j) \times g(t - nT) e^{-\mathrm{j}2\pi l(f_0+\varphi_i)t} \mathrm{d}t \right|^2\right]$$

4.2 Problem Formulation

We consider joint FSR and antenna state selection among SUs in cognitive HetNets within the game theoretical framework. GT is a mathematical tool which provides a solution method in an uncoordinated environment. It investigates the interactions between two or more agents. Since it relies on the strategic thinking, for uncoordinated networks, GT can be exploited by the SUs which are defined as players and denoted with i. The strategies are given as the FSR and antenna state selection and can be denoted with $s_i = \{\varphi_i, \nu_i\}$, $s_i \in S_i$ where Si is the strategy set of player i. Finally, the utility function is defined as the capacity of the player i and expressed as

$$U_i(\varphi_i, \nu_i) = \log_2(1 + SINR_i). \tag{4.6}$$

Thus, the game $\mathcal{G}$ can be described with three components as $\mathcal{G} = \langle \mathcal{I}, S_i, U_i \rangle$. So, the NE can be formulated as

$$U_i(s_i^*, s_{-i}^*) \geq U_i(s_i, s_{-i}^*) \qquad \forall i \in \mathcal{I}, \forall s_i, s_{-i} \in S \tag{4.7}$$

where s_{-i} represents the strategies for all players except i, '*' shows the equilibrium point, and S is the strategy profile of all players.

4.2.1 Potential Game Formulation

A game is considered as potential game when a function called potential function exists. This function reflects the change of one player's utility function with respect to its unilateral deviation. [6] defines a game as an ordinal potential game as in the following.

Definition 5 *A game $\mathcal{G}$ is said to be an ordinal potential game if it admits an ordinal potential. A function V is an ordinal potential for $\mathcal{G}$ if, for all, $i \in \mathcal{I}$*

$$\begin{aligned} U_i(s_i', s_{-i}) - U_i(s_i, s_{-i}) > 0 \text{ iff} \\ V(s_i', s_{-i}) \ - V(s_i, s_{-i}) > 0 \\ \forall s_i, s_i' \in S_i. \end{aligned} \tag{4.8}$$

where s_i' indicate the change in the strategy of player i.

Ordinal potential games guarantee that there is at least one pure NE. In this chapter, the potential function is defined as follows [45]

$$V(S) = \log_2 \left(\sum_{b \in \mathcal{I}} P_b(\varphi_b, \nu_b) + w_0 \right) \tag{4.9}$$

where $S = (\{\varphi_i, \nu_i\}, \{\varphi_{-i}, \nu_{-i}\})$. So, the potential function $V(\{\varphi_i, \nu_i\}, \{\varphi_{-i}, \nu_{-i}\})$ can be expressed as

$$\begin{aligned} & V(\{\varphi_i, \nu_i\}, \{\varphi_{-i}, \nu_{-i}\}) \\ & = \log_2 \left(\sum_{\substack{b \in \mathcal{I}, \\ b \neq i}} P_b(\varphi_b, \nu_b) + P_i(\varphi_i, \nu_i) + w_0 \right) \end{aligned} \tag{4.10}$$

When player i changes its strategy from $\{\varphi_i, \nu_i\}$ to $\{\varphi_i', \nu_i'\}$, the potential function $V(\{\varphi_i', \nu_i'\}, \{\varphi_{-i}, \nu_{-i}\})$ would be

$$\begin{aligned} & V(\{\varphi_i', \nu_i'\}, \{\varphi_{-i}, \nu_{-i}\}) \\ & = \log_2 \left(\sum_{\substack{b \in \mathcal{I}, \\ b \neq i}} P_b(\varphi_b, \nu_b) + P_i(\varphi_i, \nu_i)' + w_0 \right), \end{aligned} \tag{4.11}$$

Since the strategies of all users except i remain unchanged, the difference between potential functions would become

$$V(\{a_i', \nu_i'\}, \{a_{-i}, \nu_{-i}\}) - V(\{a_i, \nu_i\}, \{a_{-i}, \nu_{-i}\}) > 0 \tag{4.12}$$

Equation (4.12) shows that our scheme is an ordinal potential game. So, the NE existence is proved.

4.2.2 Convergence to Nash Equilibrium

Every finite potential game has a FIP [59]. A path in strategy set S is defined as a sequence of $\gamma = \{s_0, s_1, s_2, \dots\}$. For a finite path, there are initial and terminal points of γ as s_0 and the last element. γ is considered as having an improvement path if $U_i(s_z) > U_i(s_{z-1})$, so the potential function $V(s_0) < V(s_1) < V(s_2) < \dots$. Since, in our scheme, we play with the best response correspondences, no player would select the strategy which will provide smaller utility and smaller potential function. This indicates that our scheme has the FIP, and, as shown in Figure 4.6b and Figure 4.7b, converges to NE.

4.2.3 FSR and Antenna State Selection Scheme

In this scheme, the players first choose the FSR from the set of $\varphi = \{0\%, 50\%\}$. By introducing the shift with the interval of 50%, a player looks for a position where it captures the least interference. At the same time, a player selects the antenna state which provides the highest SINR result among the all available states. To reach NE, "P'nW" algorithm is introduced. In this

algorithm, each player plays the game for random time and waits for random time. For instance, for two players case, player i plays the game for 3 seconds and waits for 4 seconds. At the same time, player j plays for 2 seconds and waits for 1 second. Then, after waiting for 4 seconds, player i plays again for 5 seconds and waits for 3 seconds. In each time, players are playing and waiting for random time. After some iterations, NE can be reached with this algorithm. The detailed explanation of this game can be seen in Table 4.1.

Table 4.1 FSR and antenna state selection scheme

#	Sequential Game Algorithm
1	Assign the same FSR and antenna state to each player
2	*for* iterations = {1,2,...}
3	*for* $i = \{1,2,\dots\}$
4	*for* $\varphi = \{\varphi_{i,1}, \varphi_{i,2}, \dots\}$
5	introduce an FSR
6	*for* $\Lambda = \{\nu_{i,1}, \nu_{i,2}, \dots\}$
7	select an antenna state of player i
8	calculate $\mathbb{E}\left[\left| \int_t r_i(t,\tau;\varphi_i,\nu_i) g(t-nT) \times e^{-\mathrm{j}2\pi l(f_0+\varphi_i)t} \mathrm{d}t \right|^2\right]$ (player i's received signal power)
9	calculate $\sum_{j\in\mathcal{I},j\neq i} \sum_{n=-\infty}^{\infty} \sum_{l=0}^{K-1} \mathbb{E}\left[\left| \int_t r_j(t,\tau;\varphi_i,\nu_j) \times g(t-nT) e^{-\mathrm{j}2\pi l(f_0+\varphi_i)t} \mathrm{d}t \right|^2\right]$ (interfering players' received signal power)
10	calculate $U_i(\varphi,\Lambda)$
11	*end*
12	*end*
13	pick the highest payoff from the set of $U_i(\varphi,\Lambda)$ **if** the payoff selected in previous iteration is the highest one, don't change the strategy
14	update the antenna state and FSR indexes for player i
15	*end*
16	*end*

4.3 Performance Evaluation

In this section, performance results are provided to show the performance of the system with the POFMT in cognitive HetNets. The results can be categorized into two groups: 1) To demonstrate the advantages of POTs concept in frequency domain over OFDM, each SU is equipped with omni-directional antenna. The performance results with omni-directional antenna is shown in Figures 4.3a-4.5. 2) Joint partially overlapping in frequency and space domain performance results are depicted in Figure 4.6-4.7. Here, we do not consider mobility for SUs. All of the simulation parameters are listed in Table 4.2 where the parameter values for RA and the path loss model are taken from [60] and [50], respectively. The path loss model employed in this chapter is $PL(\text{dB}) = max(15.3 + 37.6\log_{10} R, 38.46 + 20\log_{10} R) + 0.7d_{2D} + qL_{iw} + L_{ow}$, where R is the distance between transmitter and receiver, d_{2D} is the total distance inside the houses, q is the number of walls separating houses between transmitter and receiver, L_{iw} is the penetration loss of wall separating houses, and L_{ow} is the penetration loss of outdoor walls of houses. As a filter, we use a band limited root raised cosine filter (RRCF) with a roll-off factor β to obtain orthogonal waveform. The response of the filter is

$$h_{RRCF}(t) = \begin{cases} \left(1 - \beta + 4\frac{\beta}{\pi}\right), & t = 0 \\ \frac{\beta}{\sqrt{2}}\left[\left(1 + \frac{2}{\pi}\right)\sin\left(\frac{\pi}{4\beta}\right) + \left(1 - \frac{2}{\pi}\right)\cos\left(\frac{\pi}{4\beta}\right)\right], & t = \pm\frac{T}{4\beta} \\ \frac{\sin\left[\pi\frac{t}{T}(1-\beta)\right] + 4\beta\frac{t}{T}\cos\left[\pi\frac{t}{T}(1+\beta)\right]}{\pi\frac{t}{T}\left[1-\left(4\beta\frac{t}{T}\right)^2\right]}. \end{cases} \tag{4.13}$$

To attain non-orthogonal signal, we utilize the Gaussian filter (GF), which is distributed in both time and frequency domain in an optimum way and defined as [32]

$$h_{GF}(t) = (2\rho)^{1/4} e^{-\pi\rho t^2} \tag{4.14}$$

where ρ is the dispersion adjustment parameter of the pulse in time and frequency. We consider that all transceiver pairs use the same filter for a given scenario.

Table 4.2 Simulation parameters

Simulation Parameters	Parameter Value
Power of UE	23dBm
Number of subcarriers	16
Maximum antenna attenuation	20dBm
Maximum antenna gain	12dBi
Antenna beamwidth	120
Modulation Order	QPSK
d_{2D}	20m
q	1
L_{iw}	5dB
L_{ow}	20dB

4.3.1 POFMT for Various Filter Roll-off and Dispersion Parameter Values

SINR distributions of the orthogonal waveform with various filter roll-off values and OFDM signal are shown in Figure 4.3a. Orthogonal waveform is labeled as RRCF in the legend. As seen from Figure 4.3a, when β value increases, the SINR values of RRCF decrease. This is basically because the higher β values spread over the frequency more. Although there is a considerable amount of the subcarrier spacing (i.e., 1.5), the gap in between two consecutive subcarriers diminishes. The intended users therefore can capture more interference from other users. As compared to OFDM, POFMT with RRCF provides higher SINR gain.

In Figure 4.3b, the comparison of the SINR distributions of the non-orthogonal waveform and OFDM is shown. Non-orthogonal waveform is labeled as GF in the legend. As indicated in Figure 4.3b, when the value of ρ decreases, the system can achieve higher SINR gain. The aim in this analysis is to show the effect of partially overlapping with various ρ values when the subcarrier spacing is equal to 1, i.e., when there is no gap between subcarriers. If $\rho = 1$, the SINR distribution of GF would be very close to the SINR distribution of OFDM. The difference between these two distributions is negligible. On the other hand, when $\rho = 0.2$, a high amount of gain can be achieved. As indicated in [32], when the value of ρ decreases, the subcarriers shrink in frequency, which leads to increasing gap in between subcarriers. While lower ρ values provide less interference on other players, they increase the self-interference. This causes higher inter-symbol interference on each player. So, this trade-off needs to be taken into account in the system design.

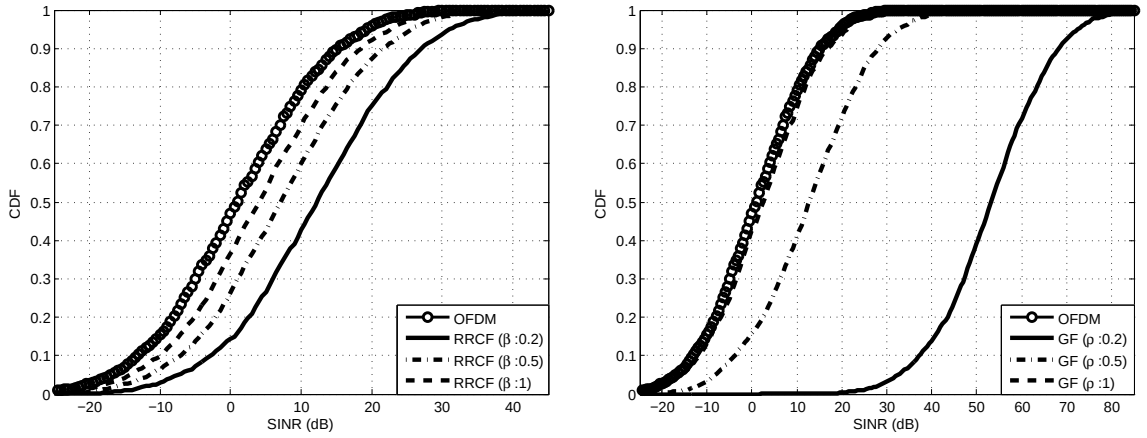

(a) (b)

Figure 4.3 (a)When subcarrier spacing is constant, increasing the filter roll-off decreases the SINR gain in orthogonal waveforms. (b) When subcarrier spacing is constant, increasing the filter control parameter decreases the SINR gain in non-orthogonal waveforms.

4.3.2 POFMT for Various Subcarrier Spacing

Orthogonal waveforms have an important feature, which is to keep the signal energy same before and after passing through the receiver filter [32]. This is advantageous for the signal transmitted from the legitimate transmitter. However, if the signal is coming from the interfering source, it becomes disadvantageous. Therefore, to reduce the energy of the signal taken from the interfering SU, subcarrier spacing is utilized with partially overlapping technique. Figure 4.4a shows the effect of POFMT in terms of the interference mitigation in orthogonal waveforms for various subcarrier spacing values. As seen in this figure, when the subcarrier spacing increases, the system gives higher performance gain in terms of SINR if the filter roll-off value is constant. It is basically because the higher subcarrier spacing leaves more gap between subcarriers, and hence, the intended SU captures less interference from the other SUs who are not fully overlapped. Alternatively, since there is no spacing between subcarriers in OFDM scheme, it gives the least SINR gain.

When a system is designed, it would be desirable to use high subcarrier spacing with the expense of higher bandwidth occupation since increasing subcarrier spacing decreases the interference. Figure 4.4b shows the bandwidth usage in terms of mean SINR level for orthogonal waveforms. As seen in the figure, x-axis is labeled as subcarrier spacing which is multiplied with the bandwidth

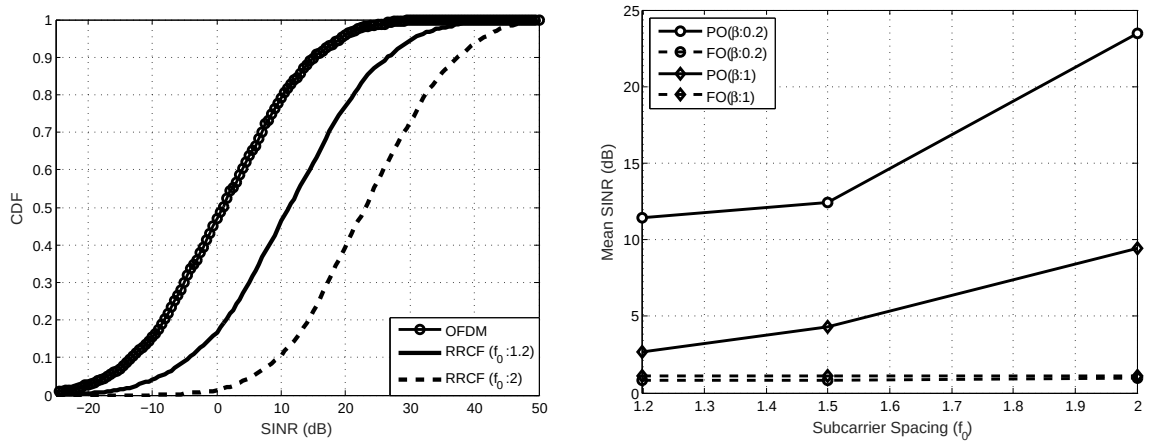

(a) (b)

Figure 4.4 (a)When filter roll-off is constant, increasing the subcarrier spacing increases the SINR gain in orthogonal waveforms. (b)When the subcarrier spacing increases, i.e., in other words, when the bandwidth usage rises, mean SINR level also increases in orthogonal waveforms.

of individual subcarrier to find how much bandwidth is used. For instance, if a bandwidth of a subcarrier is 15KHz as being in 3GPP standards and there are 16 subcarriers, total bandwidth usage is said to be 240KHz and 360KHz for subcarrier spacings of 1 and 1.5, respectively, without considering the guard bands. As seen in Figure 4.4b, when more bandwidth is allocated in POTs case, mean SINR gain increases in both schemes. If the same bandwidth as occupied with OFDM scheme is desired to be used, some subcarriers need to be turned off. In this case, there would be a slight loss in spectral efficiency. This introduces the tradeoff within POFMT technique. One will either use a complex interference reduction method in receiver without losing from the spectral efficiency [32] or select the significant interference mitigation with less spectral efficiency.

Similarly, in Figure 4.5a, the SINR distributions of OFDM and non-orthogonal schemes with various subcarrier spacing values are given while the filter control parameter is constant. Similar to orthogonal scheme, SINR gains increase with the higher subcarrier spacing values. Significant gain can be achieved when f_0=2. Figure 4.5b depicts the mean SINR variation for different subcarrier spacing values. This figure also proves the higher performance gain achievement depending on the higher f_0 values.

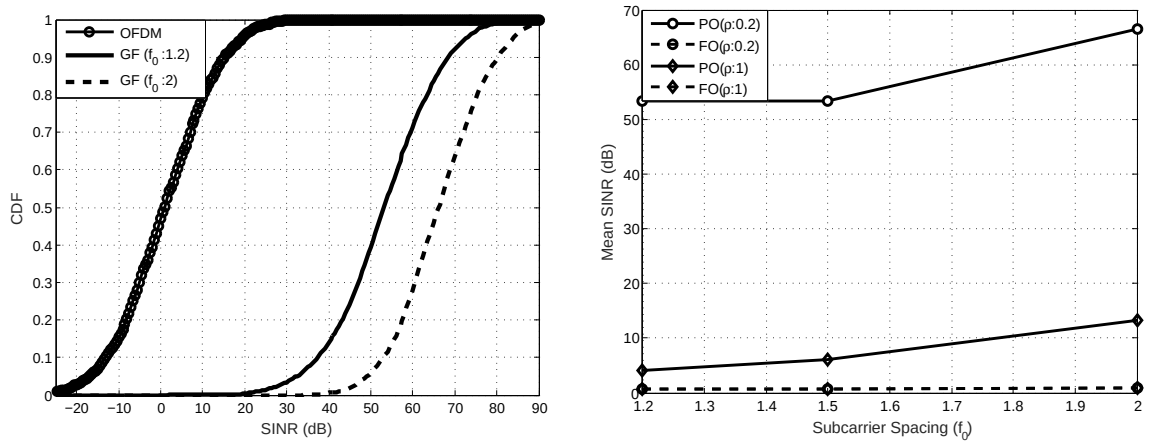

(a) (b)

Figure 4.5 (a)When filter control parameter is constant, increasing the subcarrier spacing increases the SINR gain in non-orthogonal waveforms. (b)When the subcarrier spacing increases, i.e., in other words, when the bandwidth usage rises, mean SINR level also increases in non-orthogonal waveforms.

For fully overlapping (FO) case, bandwidth increment does not make any difference in system gain because the gaps are not utilized by the players. Moreover, more bandwidth is occupied unnecessarily. These figures also indicate the benefit of POFMT technique over conventional FO case. For the same amount of bandwidth usage, proposed technique outperforms in terms of SINR.

4.3.3 POFMT with Reconfigurable Antenna

In this chapter, POFMT is investigated in both frequency and space domains. To exploit the space domain, RAs are utilized within the partially overlapping concept. In Figure 4.6 and Figure 4.7, the advantages of RA over conventional omni-directional antenna are shown when POFMT in frequency domain is performed with both antennas. Figures 4.6a and 4.7a show the distribution of the capacity values of orthogonal and non-orthogonal schemes, respectively. Since RAs can form a state in fixed and different directions, it can help to decrease the interference induced on intended players. At the same time, if the serving BS is in the boresight direction, RA can provide higher antenna gains. Therefore, when joint partially overlapping in frequency and space domains is performed, the system performance can be improved further in terms of capacity. Finally, Figure 4.6b and Figure 4.7b show the mean capacity values in each iteration of

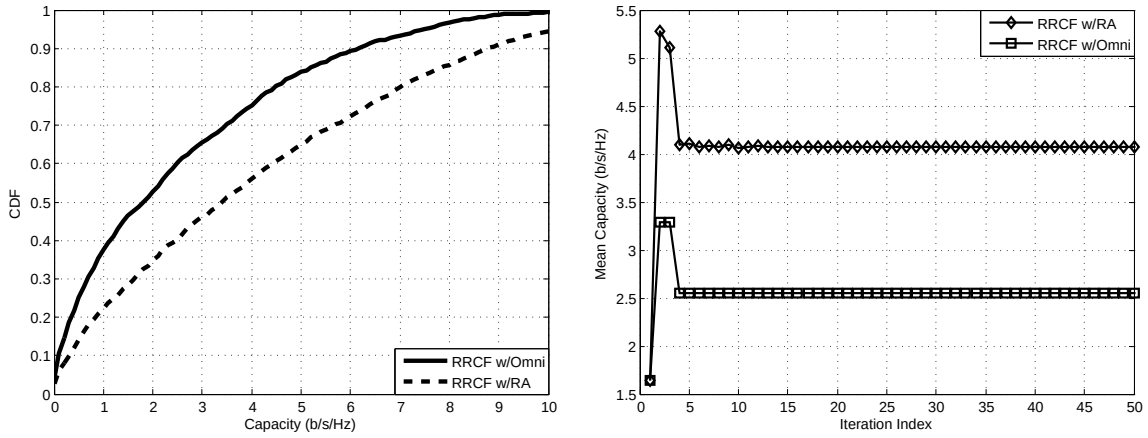

(a) (b)

Figure 4.6 (a)When RAs are used within POT concept, the system gain can be increased further in orthogonal schemes. (b) The system with orthogonal scheme and RA can reach the NE.

the algorithm in orthogonal and non-orthogonal schemes, respectively. NE existence can be proved with these figures. The increment from FO case to partially overlapping can be clearly seen in these figures. When the RAs are used with partially overlapping concept, the system capacity can be increased further. These results show that the POFMT with RAs is the candidate solution against the significant interference problem in the cognitive HetNets.

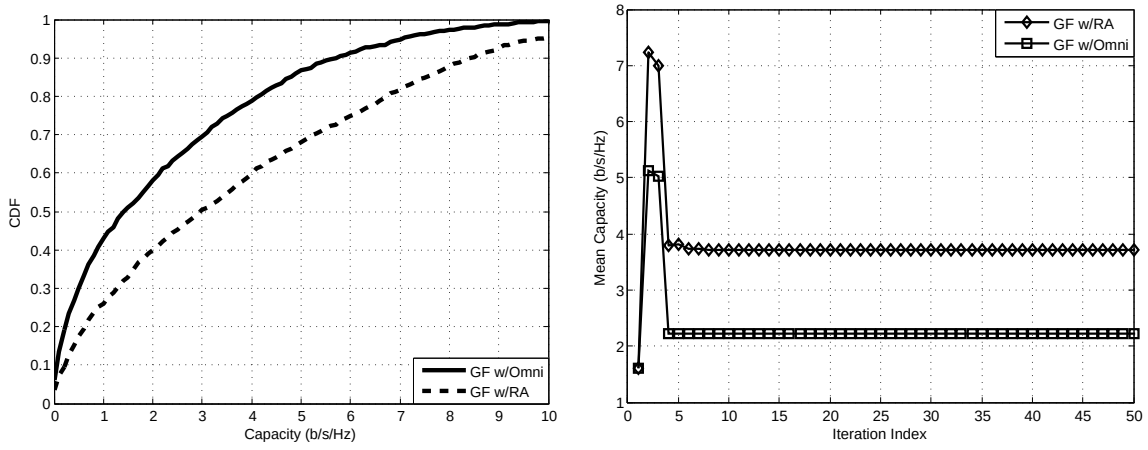

(a) (b)

Figure 4.7 (a)When RAs are used within POT concept, the system gain can be increased further in non-orthogonal schemes. (b)The system with non-orthogonal scheme and RA can reach the NE.

CHAPTER 5

RESOURCE ALLOCATION WITH PARTIALLY OVERLAPPING FILTERED MULTITONE IN HETEROGENEOUS NETWORKS[1]

POTs have recently gained interests due to the capability of solving the interference problem in cognitive HetNets by introducing the intentional CFS. By virtue of high spectral efficiency, OFDM is extensively utilized in today's systems. However, OFDM is vulnerable against the other user interference due to the selfish behavior of the SUs in cognitive HetNets. At this point, POTs has been proposed as a promising solution for cognitive HetNets against this interference problem [32]. In POTs concept, the gaps between subcarriers are utilized by the SUs. For the case of two SUs, if one SU allocates all available subcarriers, the other SU also uses the same subcarriers by intentionally shifting the carrier frequency as seen in Figure 5.1. By performing partial overlapping among SUs, other user interference can significantly be reduced [37].

In the literature, the other user interference has been proposed to be mitigated via utilizing the partially overlapping channels and various game theoretical resource allocation techniques. In [57] and [58], authors exploit the gaps between channels in a partial overlapping manner in WiFi networks to increase the throughput, and hence, reduce the interference. In terms of resource allocation, while in [13], Stackelberg games are utilized in cognitive HetNets, authors in [51] use the supermodular games to perform resource allocation. In [61], potential games are utilized to allocate subcarriers in uncoordinated networks. However, no study considers the resource allocation with POTs.

While one advantageous of POTs is to decrease the other user interference, another advantageous over OFDM can be given as allowing asynchronous transmission, which is also a significant

[1]This chapter was published in IEEE Communications Letters, vol. 20, no. 5, pp. 962-965, May 2016. Permission is included in Appendix A.

issue in cognitive HetNets, by employing the FMT [38]. It is noted that the usage of FMT provides flexibility on adjusting the gap (stemming from the guard-band) between subcarriers by alternating the filter parameters such as roll-off factor. Since this gap is negligible in OFDM scheme, this makes FMT more suitable for POTs concept. In this study, we develop a resource allocation technique for POFMT within a game theoretical framework in cognitive HetNets. In downlink, SBSs as players perform the resource allocation by searching for the best subcarriers which are constrained to be in consecutive order. To perform subcarrier selection, SBS picks a certain number of subcarriers based on the total need of SU by starting from the first available subcarrier and computes the utility of the selected subcarriers. Then, it shifts the subcarriers intentionally to introduce the CFS and calculates the utility in this position, too. The SBS performs this operation throughout the all available subcarriers. After obtaining the capacity results for every position and subcarriers, SBS selects the one which provides the highest utility. With this scheme, the existence of NE is proved theoretically and by simulations. As indicated in simulation results, the proposed scheme outperforms OFDM with a slightly slower convergence rate.

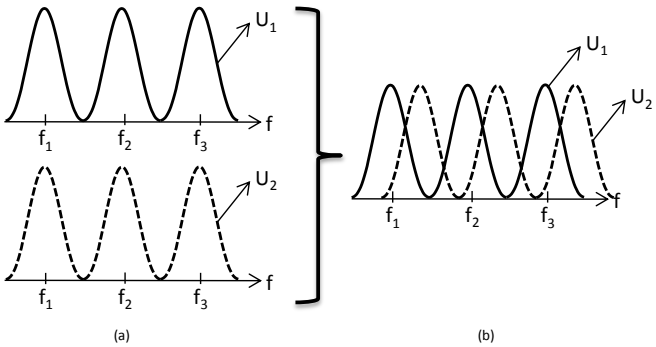

Figure 5.1 (a) Both users allocate the same resources at the same time. This leads to fully overlapping case where the highest interference is achieved. (b) U_2 is shifting the carrier frequency. Therefore, users are partially overlapped to each other. This reduces the other user interference.

The remainder of this paper is organized as follows. In Section 5.1, the system model is introduced with the transmission and reception models. The problem formulation and potential game formulation with the proof of NE convergence are explained in Section 5.2 in which the

subcarrier and FSR selection scheme is also introduced. Section 5.3 entails numerical results of the proposed approach. Conclusion is drawn in Chapter 7.

5.1 System Model

We consider a downlink scenario with multiple SBSs, where each SBS serves multiple SU in a given area. Each SU allocates the certain number of subcarriers under the assumption that the total number of available resources is higher than the total number of resources that SUs served by a single SBS need. It is assumed that the intentional CFS is performed by the SBS with the orthogonal waveforms.

The transmitted signal of the SBS i , $i \in \mathcal{I}$ which is the total number of SBSs, is defined as

$$x_i(t;\varphi_i,a_i) = \sum_{m=-\infty}^{\infty}\sum_{k=0}^{K-1} X_{kmi}\, g(t-mT)\, e^{\mathrm{j}2\pi k(f_0+\varphi_i)t} a_{ki}, \tag{5.1}$$

where K is the total number of subcarriers, f_0 is the subcarrier spacing, $g(t)$ is the prototype filter, T is the symbol duration, X_{kmi} is the modulated symbols on the kth subcarrier of mth symbol, a_{ki} is the indicator function, where if the kth subcarrier is used by the SBS i, then $a_{ki} = 1$, if not, then $a_{ki} = 0$, and $\varphi \in [0, f_0]$ is the frequency shift introduced by the SBS i. The aim in CFS is to decrease the other SBS interference.

With a Rayleigh fading channel consideration, the received signal of the SU of the SBS i is given by

$$y_i(t;\varphi_i,a_i) = \int_\tau\int_\varphi H_i(t,\tau)x_i(t-\tau;\varphi_i,a_i)\mathrm{d}\varphi\mathrm{d}\tau + \sum_{j\in\mathcal{I},j\neq i}\int_\tau\int_\varphi H_j(t,\tau)x_j(t-\tau;\varphi_j,a_j)\mathrm{d}\varphi\mathrm{d}\tau + w(t), \tag{5.2}$$

where j is the interfering SBSs index, $H_i(t,\tau)$ and $H_j(t,\tau)$ are the Fourier transformations of $h_i(t,\tau)$ and $h_j(t,\tau)$, respectively and $w(t)$ is the additive white Gaussian noise. The received symbol can

be obtained by projecting the corresponding received filter onto the received signal as

$$\begin{aligned}\tilde{X}_{lni}(\varphi_i, a_i) &= \left\langle y_i(t;\varphi_i,\nu_i), g(t-nT)e^{\mathrm{j}2\pi l(f_0+\varphi_i)t} \right\rangle \\ &= \int_t r_i(t,\tau;\varphi_i,a_i)g(t-nT)e^{-\mathrm{j}2\pi l(f_0+\varphi_i)t}\mathrm{d}t \\ &\quad + \sum_{\substack{j\in\mathcal{I},\\ j\neq i}} \sum_{n=-\infty}^{\infty} \sum_{l=0}^{K-1} \int_t r_j(t,\tau;\varphi_i,a_j)g(t-nT)e^{-\mathrm{j}2\pi l(f_0+\varphi_i)t}\mathrm{d}t + w(t), \end{aligned} \tag{5.3}$$

where $r_i(t,\tau;\varphi_i,a_i) = \int_\tau \int_\varphi H_i(t,\tau)x_i(t-\tau;\varphi_i,a_i)\mathrm{d}\varphi\mathrm{d}\tau$.

It is important to mention that for SU to obtain the symbols properly, it needs to employ the same amount of FSR with the SBS. Otherwise, the signal will be taken partially. On the other hand, it becomes advantages when the interference coming from other SBSs is captured. Finally, the SINR of the SU can be expressed as

$$SINR_i = \frac{P_i(\varphi_i, a_i)}{P_j(\varphi_i, a_j) + w_0} \tag{5.4}$$

where

$$P_i(\varphi_i, a_i) = \mathbb{E}\left[\left| \int_t r_i(t,\tau;\varphi_i,a_i)g(t-nT)e^{-\mathrm{j}2\pi l(f_0+\varphi_i)t}\mathrm{d}t \right|^2\right],$$

and

$$P_j(\varphi_i, a_j) = \sum_{\substack{j\in\mathcal{I},\\ j\neq i}} \sum_{n=-\infty}^{\infty} \sum_{l=0}^{K-1} \mathbb{E}\left[\left| \int_t r_j(t,\tau;\varphi_i,a_j)g(t-nT)e^{-\mathrm{j}2\pi l(f_0+\varphi_i)t}\mathrm{d}t \right|^2\right].$$

5.2 Problem Formulation

In this study, we consider joint subcarrier and FSR selection to perform the resource allocation with the POFMT. This is a multidimensional optimization problem. However, since finding the optimum solution increases the overhead and the complexity of the system [18], we formulate

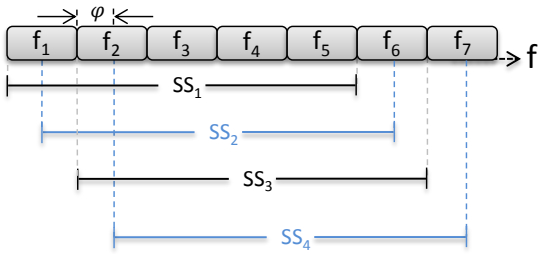

Figure 5.2 A player searches for the consecutive subcarriers which give the highest utility by sliding the subcarrier set (SS) through all the available ones.

our problem within the game theoretical structure. GT provides a solution among selfishly behaved players (users) who are interacted with each other. In GT, each player changes its strategy to increase its utility towards its benefits. In this paper, we define the players as the SBSs, strategies as the selection of subcarriers and FSR which are denoted with $s_i = \{\varphi_i, a_i\}$, $s_i \in S_i$ where S_i is the strategy set of player i. Finally, the utility function is defined as the capacity of the ith player and given as

$$U_i(\varphi_i, a_i) = \log_2(1 + SINR_i). \tag{5.5}$$

When the players play with their best responses, they aim at reaching the NE in GT. So, the NE can be defined as

$$\begin{aligned} U_i(s_i^*, s_{-i}^*) &\geq U_i(s_i, s_{-i}^*) \\ \forall i \in \mathcal{I}, \forall s_i, s_{-i} &\in S \end{aligned} \tag{5.6}$$

where s_{-i} indicates the strategies for all players except i, S is the strategy profile of all players and '*' represents the equilibrium point.

5.2.1 Subcarrier and Frequency Shift Ratio Selection Scheme

The selection of subcarrier and FSR is performed with P'nW algorithm given in [37]. In this algorithm, players play and wait for random time. For instance, for two players case, player-1 plays for 3ms and waits for 5ms while player-2 plays for 4ms and waits for 2ms.

In OFDMA structure, the players can pick any subcarriers among the available ones, i.e., the selected subcarriers don't have to be consecutive. However, when the players perform the subcarrier selection with POFMT, they need to select the ones which are in consecutive order. Otherwise, an intra-cell interference problem may occur. On the other hand, it is a challenging task to manage the frequency shift in randomly allocated subcarriers among multiple users. Another problem with this randomized scheme is to increase the loss in the spectral efficiency. Because of these drawbacks, we introduce the constraint on the selection of subcarriers in terms of performing it in a consecutive order.

With this constraint, a player searches for the consecutive subcarriers which give the highest utility by sliding the subcarriers through all the available ones as seen in Figure 5.2 which is shown for the selection of five subcarriers as an example. The player first picks the subcarriers of f_1 to f_5 and computes the utility for these subcarriers. Then, it introduces the CFS and again, computes the utility for the shifted consecutive subcarriers, i.e., for $(f_1+\varphi)$ to $(f_5+\varphi)$. After calculating the utility for all subcarriers with their corresponding CFS, the player selects the ones which provide the highest capacity result. If the same SBS serves to more than one SU, SBS assigns the first SU to its best responses and then, follow the same step for other SUs in a round-robin manner. The game steps can be seen in Table 5.1, too.

5.2.2 Potential Game Formulation

Potential games are defined with a potential function which shows the unilateral deviation of a player with respect to other players. As given in [6], there are various potential games. Among those, the ordinal potential games are defined as follows.

Definition 6 *A game $\mathcal{G}$ is said to be an ordinal potential game if it admits an ordinal potential. A function V is an ordinal potential for $\mathcal{G}$ if, for all, $i \in \mathcal{I}$ and $\forall s_i, s_i' \in S_i$*

$$U_i(s_i', s_{-i}) - U_i(s_i, s_{-i}) > 0 \text{ iff } V(s_i', s_{-i}) \ - V(s_i, s_{-i}) > 0 \tag{5.7}$$

where s_i' indicate the deviation of the strategy of the ith player.

NE existence is guaranteed with ordinal potential games [6]. In this study, we define the potential function similar to [45] as

$$V(S) = \log_2 \left(\sum_{b \in \mathcal{I}} P_b(\varphi_b, a_b) + w_0 \right), \tag{5.8}$$

where $S = (s_i, s_{-i})$. When the potential function $V(s_i, s_{-i})$ is rewritten, ith player's potential can be separated as follows.

$$V(s_i, s_{-i}) = \log_2 \left(\sum_{\substack{b \in \mathcal{I}, \\ b \neq i}} P_b(\varphi_b, a_b) + P_i(\varphi_i, a_i) + w_0 \right), \tag{5.9}$$

If only the ith player alters its strategy from s_i to s_i', the potential function $V(s_i', s_{-i})$ can be expressed as

$$V(s_i', s_{-i}) = \log_2 \left(\sum_{\substack{b \in \mathcal{I}, \\ b \neq i}} P_b(\varphi_b, a_b) + P_i(\varphi_i, a_i)' + w_0 \right), \tag{5.10}$$

When (5.9) is subtracted from (5.10), and since the only the ith player changes its strategy, i.e., other players strategies remain the same, the following result is observed.

$$V(s_i', s_{-i}) - V(s_i, s_{-i}) > 0. \tag{5.11}$$

Thus, the condition in (5.7) would be satisfied with (3.15). This proves the NE existence.

Table 5.1 Subcarrier and FSR selection scheme

#	Game Algorithm
1	Assign the same subcarriers and carrier frequency shift ratio to each player
2	*for* iterations = {1,2,...}
3	*for* i = {1,2,...}
4	*for* $\varphi_i = [0, \ldots, f_0]$
5	select an FSR
6	*for* Subcarrier set = $\{SS_1, SS_2, \ldots\}$
7	compute $U_i(\varphi_i, a_i)$
8	*end*
9	*end*
10	pick/allocate the best resources and FSR to i
11	*end*
12	*end*

5.2.3 Convergence to Nash Equilibrium

As mentioned in Section 5.2.2, ordinal potential games has at least one pure NE. To show the NE convergence in potential games, FIP which is a significant feature of the potential games is being utilized. In FIP, $\xi_i = (s_i^0, s_i^1, s_i^2, \cdots)$ is defined as a sequence of path of the strategy set of S_i for player i. It is assumed that the new and previous strategies of player i are s_i^l and s_i^{l-1}, respectively. Based on the improvement path of ξ_i, the potential function $V(s_i^l)$ should satisfy $V(s_i^0) < V(s_i^1) < V(s_i^2) < \cdots$. Since the players play with their best responses in this paper, the potential function with the new strategy will become $V(s_i^l) > V(s_i^{l-1})$. Therefore, the improvement path of the potential functions would be satisfied. This proves the convergence to unique NE with our algorithm for a given scenario.

5.3 Performance Evaluation

We consider there are 20 SBSs which are randomly distributed in a given area, and each SBS serves to 2 SUs. We assume that there are 64 available subcarriers and each SU needs 16 subcarrier. To perform orthogonal transmission with FMTs, we utilize the band limited RRCF with a roll-off factor β taken as 0.35. We adopt a path loss model which is defined as $PL(\text{dB}) = 43.3log10(R) + 11.5 + 20 * log10(f_c)$, where R is the distance between transceivers and f_c is the

center frequency, which is 2GHz [50]. Finally, the subcarrier spacing is taken as 1.2, i.e., $f_0 = 1+0.2$ which introduces slight loss in spectral efficiency.

Figure 5.3a shows the cumulative distribution function curves of the proposed and existing schemes. As an existing scheme, OFDM is utilized. As seen in figure, the proposed scheme provides higher performance gain in terms of the capacity. While the introducing only CFS decreases the other user interference as shown in [37], CFS with subcarrier allocation provides further reduction in interference. It is basically because each user may select the different subcarriers and/or only some of the subcarriers might be allocated by other user(s). In the mean capacity level, the proposed scheme gives 94% higher capacity gain. In Fig. 5.3b, the mean capacity of the system in each iteration is depicted for both schemes. This figure proves that the proposed scheme reaches the NE with slightly slower convergence rate which is basically due to the consecutiveness constraint we introduced in our scheme. That is, while some resources might have high capacity gain in the selected subcarriers, some other resources might have lower gain. Therefore, finding the more resources with the highest gain takes longer duration for each user, and hence, equilibrium is achieved more slowly.

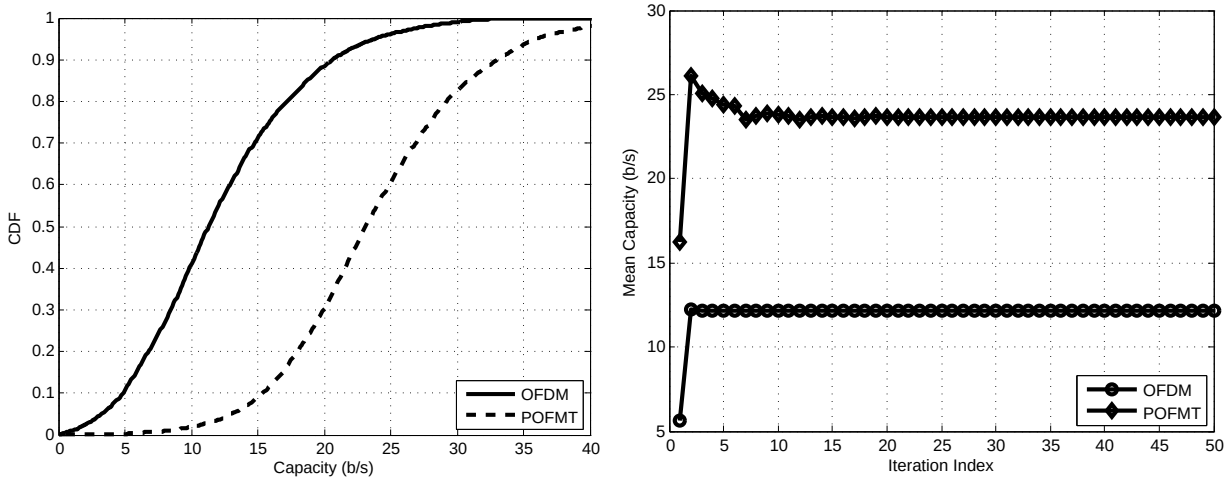

(a) (b)

Figure 5.3 (a)The resource allocation with POFMT outperforms the resource allocation with OFDM. (b)POFMT algorithm reaches the NE. However, the convergence rate is slow.

CHAPTER 6

MILLIMETER-WAVE WIRELESS CHANNEL CONTROL USING SPATIALLY ADAPTIVE ANTENNA ARRAYS[1]

Wireless channel formation is conventionally accepted as an uncontrollable phenomenon since the physical environment and propagation scenario that determine the fading and time-varying response are assumed to be random. Wireless communication techniques treat the channel response as a given parameter and try to compensate the fading and distortion via equalization [62] and/or benefit from multitudes of independent channels by employing multiple antennas [63]. This causes overall performance of the state-of-the-art techniques to depend on the randomness level of the wireless channel.

In contrast to the traditional wireless spectrum below 6 GHz, small wavelengths of mm-wave bands make physical displacements on the order of several wavelengths practically achievable within compact devices. Based on this observation, a wireless channel control concept utilizing spatially, i.e., position adaptive antenna arrays is proposed. The main principle relies on the fact that the phase of each multipath component is affected by the position of the antenna array. The system level objective is therefore to find the best array position that will provide a constructive combination of the individual components for maximizing the received signal power and reduce fading, especially in narrowband systems. For the broadband systems, controlling the channel will reduce the burden on the scheduler by finding the better channel for the same resource(s) allocated to a user. On the other hand, this concept also provides additional degree of freedom for the system and increases the reliability with spatial diversity via displacing the antenna array spatially.

[1]This chapter was published in IEEE Communications Letters, vol.pp, no.99, pp.1-1. Permission is included in Appendix A.

To carry out this control concept, the microfluidically reconfigurable RF devices are employed in this study. References [64–66] have recently utilized repositionable selectively metallized plates inside microfluidic channels bonded to printed circuit board (PCB) substrates to realize wideband frequency tunable antennas, filters, and mm-wave beam-steering focal plane arrays. As compared to a mechanical assembly, a microfluidic based approach requires movement of a lower mass, i.e., a selectively metallized plate defining the antennas by allowing to keep the feed network stationary [66]. This is expected to result in low-cost, compact, and efficient devices.

To demonstrate the advantages of the proposed channel control concept, the following section considers a wireless communication system model at 28 GHz in which a BS and a UE employ spatially adaptive antenna arrays and omni-directional antennas, respectively. Section 6.2 summarizes the design, layout, and simulated performance of the antenna array. Section 6.3 presents the evaluation of the system performance. It is shown that the wireless communications system observe 51% gain in the mean SINR due to the inclusion of spatial adaptation capability.

6.1 System Model

Figure 6.1 depicts the downlink scenario in which a BS and a UE are equipped with a spatially adaptive linear antenna array and an omni-directional antenna, respectively. The considered antenna array is capable of changing its position along the y-axis using microfluidics and perform beam-steering in the orthogonal x-z plane using phase shifters.

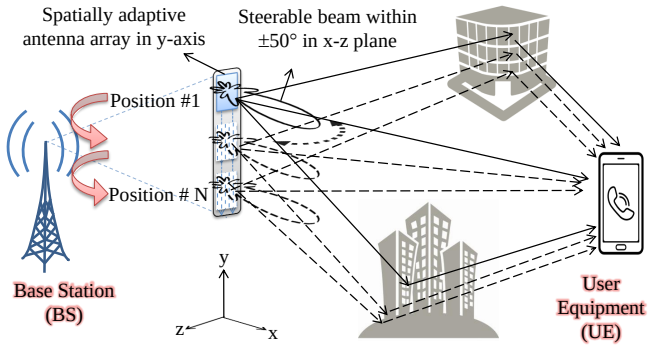

Figure 6.1 Base station (BS) changes position of the antenna array to maximize signal power and reduce fading.

.

After passing through the wireless multipath channel, the transmitted signal $x(t)$ is received as

$$y(t;) = x(t) * h(t, \tau;) + w(t), \tag{6.1}$$

where $h(t, \tau;)$ is the channel response between the transmitter and the receiver including the radiation pattern and the multipath reflections, is the spatial offset of the transmitter antenna array and $w(t)$ is the additive white Gaussian noise. In a directional transmit (tx) or receive (rx) scenario, resulting channel response is determined by the weighted sum of the taps as

$$h(t, \tau;) = \sum_{k=1}^{K} \sum_{l=1}^{L} g_{kl}(t, \tau;) u_{\text{tx}}(\theta_k^{\text{tx}}()) u_{\text{rx}}(\theta_k^{\text{rx}}()) \delta(\tau - \tau_{kl}), \tag{6.2}$$

where l is the path index, L is the total number of paths, τ is the delay of the lth path, $g_{kl}(t, \tau;)$ is the complex channel gain of lth path of kth cluster, and $u(\theta_k())$ is the antenna gain factor as a function of the departure/arrival angle of the tx/rx signal path. In this scenario, the multipath environment itself is considered to be time invariant. Thus, the only source of change in the multipath response is the spatial offset of the transmitter antenna array. Therefore, the time variable can be substituted into the offset value, i.e., (t). In addition, the bandwidth of the signal is considered not to be sufficiently large enough for resolving each path in a cluster. Thus, the paths in each cluster are combined to constitute one tap per cluster as would be valid in indoor environments. Consequently, by dropping the path dependency in multipath delays via $\tau_{kl} \approx \tau_k$, the channel response can be further simplified as

$$h(\tau;) = \sum_{k=1}^{K} g_k(\tau;) u_{\text{tx}}(\theta_k^{\text{tx}}()) u_{\text{rx}}(\theta_k^{\text{rx}}()) \delta(\tau - \tau_k). \tag{6.3}$$

Mm-wave channels are known to be sparse [67]. Therefore, small alterations in the antenna location in the range of few wavelengths is expected to vary the phase of each tap coefficient due to change in total propagation distance. This sparse nature of the mm-wave multipath channel is the

key enabling factor that makes the control of the overall channel response via spatial adaptation possible.

6.2 Spatially Adaptive Antenna Array

Fig. 6.2 depicts the structure and substrate stack-up of the 5 element linear 28 GHz patch antenna array that is considered for the performance evaluation of the proposed wireless channel control concept. A 254 μm thick 54×30 mm^2 RT5880LZ PCB ($\epsilon_r = 1.96$, $\tan\delta = 0.0027$) acts as a selectively metallized plate placed inside a microfluidic channel that is prepared within 1 mm thick polydimethylsiloxane layer (PDMS, $\epsilon_r = 2.7$, $\tan\delta = 0.04$). The remaining volume of the microfluidic channel is filled with a low-loss dielectric solution (FC-40, $\epsilon_r = 1.9$, $\tan\delta = 0.0005$). The top and bottom surfaces of the RT5880LZ PCB carry the patch antenna and the 50 Ω microstrip feed line (M2) metallization patterns, respectively. The feed lines are electrically connected to the antennas with vias. The microfluidic channel is bonded to a 127 μm thick 105×40 mm^2 RT5880 PCB ($\epsilon_r = 2.2$, $\tan\delta = 0.0009$) using a 6 μm thick benzocyclobutene (BCB, $\epsilon_r = 2.65$, $\tan\delta = 0.0008$) layer. The top surface of the RT5880 PCB carries the stationary microstrip feed lines (M1), the grounding pads (M1), and the vias. Its bottom surface is the ground plane of the antenna system. This substrate stack-up is similar to the recent microfluidically reconfigurable antenna [64] and filter [65] realizations with the exception of utilizing thinner layers and lower permittivity PCBs for enhanced radiation performance at 28 GHz. Piezoelectric micropumps drive a closed loop fluid system and generate the flow to reposition the PCB inside the microfluidic channel [64–66]. Distances d= 0 mm and d= 45 mm denote that the PCB located inside the microfluidic channel is at its farthest and closest position to the input/output RF ports of the stationary feed network, respectively. Fig. 6.2 also illustrates the state of the PCB inside the microfluidic channel at d= 10 mm, d= 22.5 mm, and d= 45 mm positions.

Fig. 6.3 shows the layout details of the antenna and the feed lines. In a physical device implementation, the input/output RF port of the stationary feed network (M1 trace) is expected to be interconnected with other PCB layers that will be hosted under the ground plane of the antenna system and interface with the digital phase shifters. The thin BCB insulator between the M1 trace

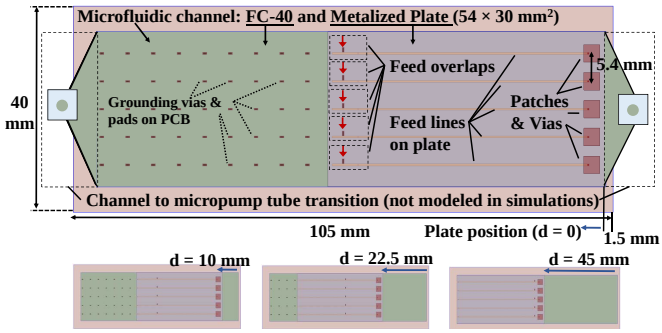

(a)

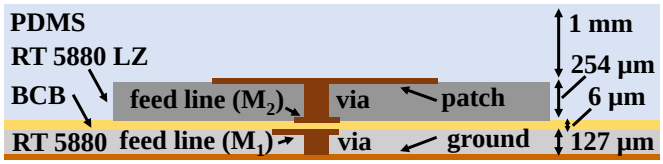

(b)

Figure 6.2 (a) 5 element linear patch antenna array that can perform spatial, i.e., position adaptation using microfluidics; (b) Substrate stack-up in which an RT5880LZ PCB is located inside a microfluidic channel (formed by bonding PDMS mold onto RT5880 PCB with 6 μm thick BCB layer).

and the feed line inside the microfluidic channel (M2 trace) allows for strong capacitive coupling in overlapping regions. This is utilized for allowing the RF signal to pass between the two traces without making physical electrical contact.

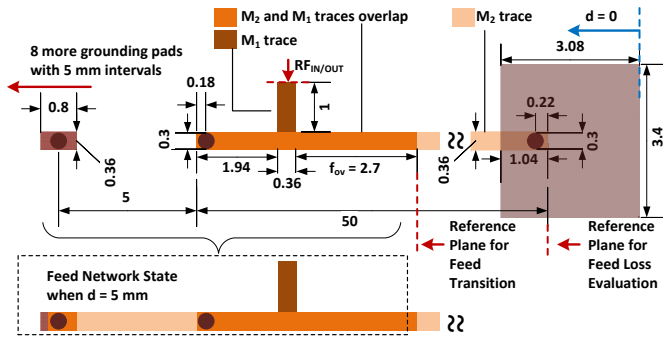

Figure 6.3 Layout details of the antenna, feed network, and grounding vias (units: mm).

.

The feed line design is carried out using Momentum Suite of the Keysight's Advanced Design System (ADS) software due to its accuracy and effectiveness in handling planar layered geometries. The 50Ω microstrip lines are designed for the selected substrate stack-up using the

procedure outlined in [66]. As shown in Fig. 6.3, the feed lines maintain a constant overlap length (f_{ov}) of 2.7 mm at any (d) position of the moving PCB. A 1.94 mm long ($\approx \lambda_g/4$, where λ_g is the guided wavelength of 10.71 mm at 28 GHz) short-ended stub is placed to create an open circuit condition at one end of the T-junction to fully direct the signal from the RF port to the antenna, and vice versa. As depicted in Fig. 6.4(a), f_{ov} affects the bandwidth of the feed network and it is selected to get the largest $S_{21} > -0.5$ dB bandwidth around 28 GHz. As the PCB inside the microfluidic channel moves to greater d positions, the open-ended M2 trace that remains outside of the overlap area exhibits resonances that hinder the functionality of the feed network (see Fig. 6.4(b)). This issue is alleviated by grounding the M2 trace in 5 mm periods using grounding pads and vias over the PCB of the stationary feed network (see Fig. 6.4(c)). Fig. 6.4(d) demonstrates the S_{21} performance of the feed network at 28 GHz as the PCB inside the microfluidic channel is positioned from d= 0 mm to d= 45 mm. As seen, the loss is linearly proportional to the feed line length and 0.15 dB loss at d= 0 mm implies the effectiveness of the designed feed transition.

Antenna array design is carried out with Ansys HFSS v16.2 to account for the finite substrate and ground plane effects. The patch antenna element of the array has a footprint of 3.4×3.08 mm^2 and resonates at 28 GHz with a 3.2 GHz of $S_{11} < -10$ dB bandwidth. The element separation within the array is 5.4 mm and corresponds to $\lambda/2$, where λ is the free space wavelength. The radiation efficiency is 80% when the array is located at its closest position, i.e., d= 45mm to the RF ports and is primarily affected by the dielectric loss of the PDMS mold that forms the microfluidic channel. In this position, the uniformly excited array exhibits 11.1 dB realized broadside gain with 20° half-power-beamwidth (HPBW) in the x-z plane. As expected, a lower radiation efficiency is attained when the array moves to different positions due to the increased feed line loss. The realized gain of the array drops by ~ 5 dB as the beam is scanned to $\theta = \pm 50°$ from the broadside using a progressive phase shift of $\beta = \mp 7\pi/8$. This 100° range is taken as the FoV of the array. To represent the beam-steering performance accurately, 15 different realized gain patterns are extracted by varying β in $\pi/8$ increments which is also possible to accomplish with commercially available discrete phase shifters. The array position is varied with d= 2.5mm, i.e., $\sim \lambda/4$ increments to sample both correlated and uncorrelated wireless channel gains. Consequently, the total dataset

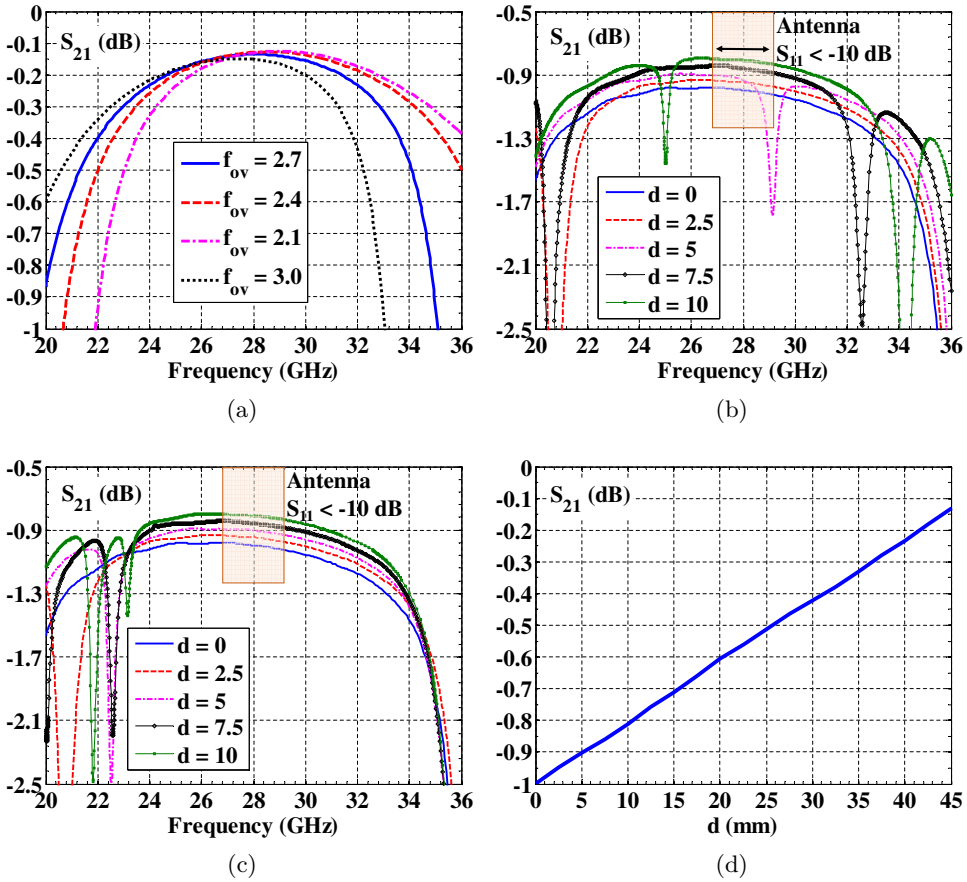

Figure 6.4 (a) S_{21} performance of the feed network for: (a) various overlap length f_{ov} values (reference plane is taken for feed transition); (b) no grounding pads and vias (c) with grounding pads and vias (d) different array positions d (reference plane is taken for feed loss evaluation).

obtained from full-wave electromagnetics simulations consists of 285 realized gain patterns. Fig. 6.5 depicts representative patterns for various β and d combinations. It is observed that the main lobe characteristic of the radiation pattern is mostly independent of the array position. Therefore, the feed network loss is the major parameter that affects the performance of the array as it is spatially adapted.

6.3 Performance Evaluation

To demonstrate the advantage of the proposed concept in the link level, an environment is considered where $800\lambda \times 800\lambda$ multipath reflection region with scatterers is placed in between a BS

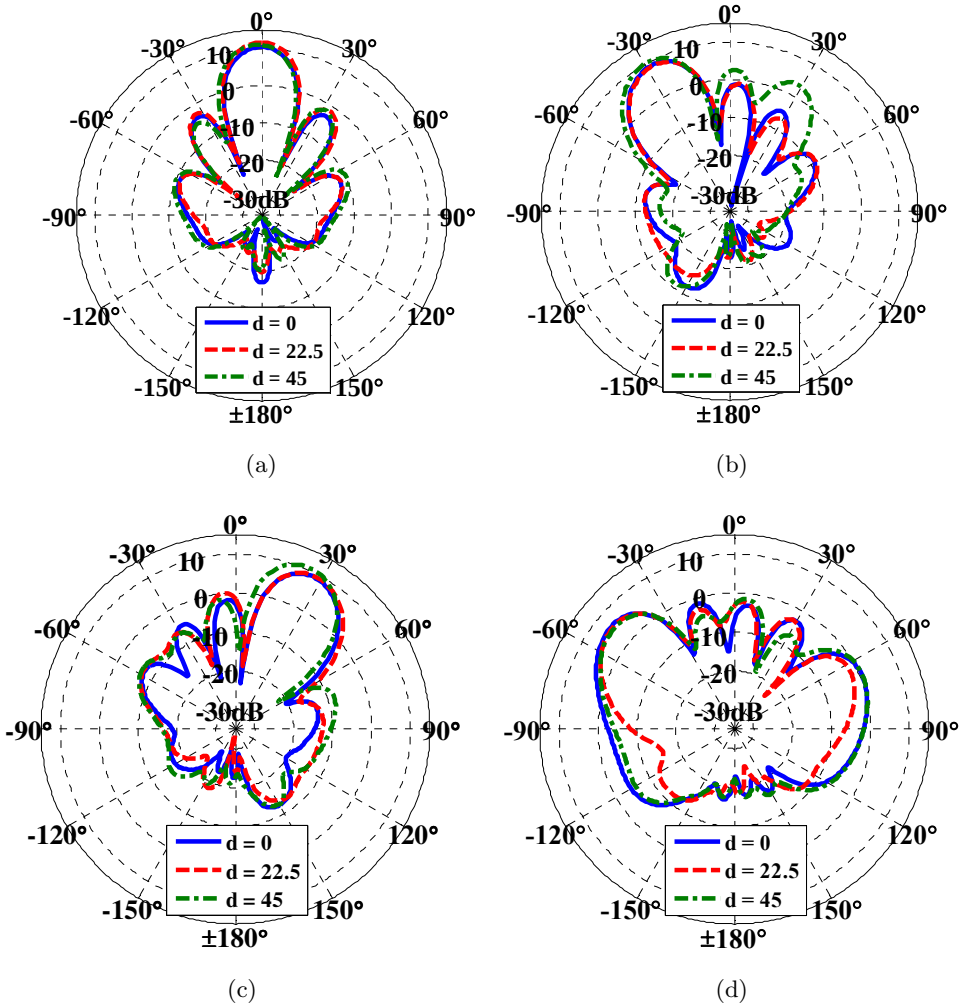

(a) (b) (c) (d)

Figure 6.5 Simulated x-z plane realized gain patterns of the antenna array at various d positions for progressive phase shifts of (a) $\beta = 0$, (b) $\beta = \pi/4$, (c) $\beta = -\pi/4$, and (d) $\beta = 7\pi/8$.

and a UE separated 2000λ apart. The number of scatterers are randomly selected from the Poisson distribution in each realization of the link level simulation (between 2-4) and a single ray reflected from a scatterer is considered. A path loss model and the scenario parameters are adopted from [67] and is given as $PL(dB) = \alpha + \beta 10\log_{10} r_0$ where r_0 is the distance, α is the best fit floating point ($\alpha = 72$) and β is the slope of best fit ($\beta = 2.92$). Different channels are achieved for a BS by spatially displacing the antenna array position as given in equation (6.3). Fig. 6.6(a) depicts the link capacity in terms of spectral efficiency as the spatial adaptation range of the antenna array in the BS is increased from 0λ, i.e., no adaptation to 4.5λ. While antenna gain is considered as

5dBi for the omni-directional antenna, the "beam-steering only" scenario uses the realized gain performance of the antenna array positioned at d= 45 mm, i.e., best radiation efficiency and performs beam angle adaptations based on the observed channel gain. On the other hand, the "spatial & beam-steering" scenario harnesses beam angle and position adaptations simultaneously to maximize channel gain. As depicted in Fig. 6.6(a), the link capacity increases up to 2 bit/s/Hz with the 4.5λ spatial adaptation range of the antenna array over beam-steering only array. When the range increases, the link capacity gain increases due to providing more uncorrelated channel responses on the receiver.

The system level advantage of the proposed concept is demonstrated by considering a scenario in which 50 small cells are randomly distributed within a 200×200 m^2 area with each BS serving a single user and has randomly distributed scatterers [67]. The transmit power of each BS is considered as 30 dBm which is taken from [50]. Each BS is assumed to be a selfish, i.e., there is no coordination between small BSs. In narrowband systems, it is also assumed that all BSs allocate the same resource at the same time. A game theoretical framework is established as in [68]. However, in this framework, BSs are modeled to perform simultaneous array position and beam angle selection affecting the received signal strength (RSS) evaluation. This joint behavior also provides interference management in the system. In addition, equation (6.3) is adapted for modeling wireless channels. The same framework is also modeled with a beam-steering only array for comparison. Every BS searches for the best antenna position and state in terms of SINR. The results are drawn when the system reaches the equilibrium. Similar to link level results, the distribution of spatially adaptive array provides better performance than beam-steering only arrays under the interference coming from the other users in the environment. Fig. 6.6(b) shows the CDF of the SINR results. In the mean SINR value, spatially adaptive antenna arrays achieve 51% improvement with respect to beam-steering only arrays. Fig. 6.6(c) indicates the mean SINR difference in each user separately and presents the advantage of the spatially adaptive arrays per user case. As seen from the figure, the SINR of each user is increased with the spatially adaptive arrays up to 5.4 dB as compared to the beam-steering only arrays.

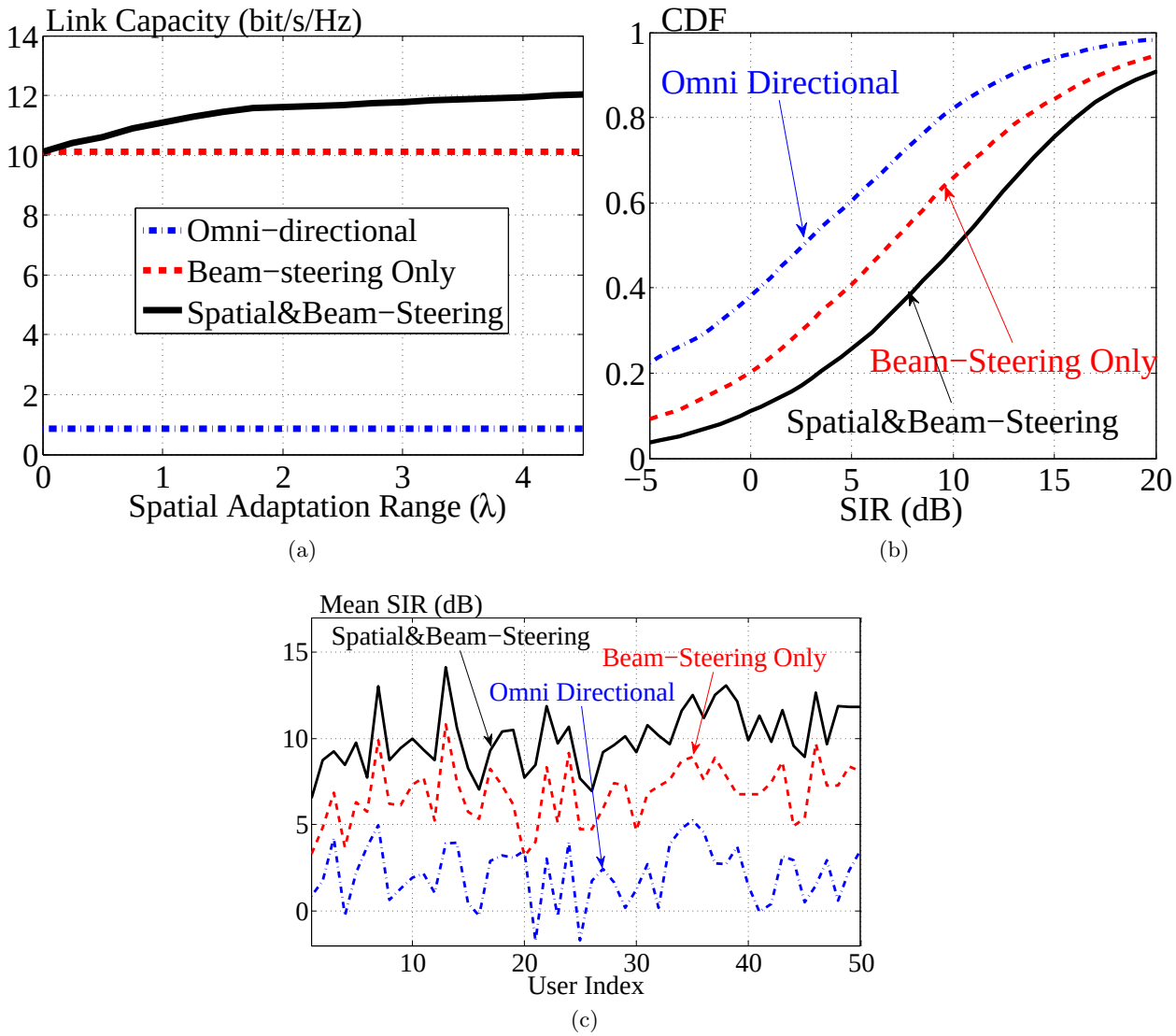

Figure 6.6 (a) Link capacity vs. spatial adaptation range; (b) SIR gains of wireless systems utilizing different types of antennas at BSs; (c) Mean SIR gains of each individual user within the wireless systems. "Spatial and Beam-Steering" arrays of the system exhibit 4.5λ spatial adaptation capability.

CHAPTER 7

CONCLUSION AND OPEN ISSUES

Cognitive HetNets have been proposed as a promising solution to increase the per user data rate which is achieved by shrinking the cell sizes, i.e., by forming the small cells such as femtocells, picocells. While shrinking the cell increases the spectrum efficiency, it also increases the other user interference due to having uncoordinated structure. Therefore, interference mitigation in cognitive HetNets becomes a significant subject in wireless communication systems. In this dissertation, we focus on the interference mitigation techniques in the system level.

In the second chapter, we proposed the random subcarrier allocation algorithm in cognitive HetNets within a game theoretical approach to handle the interference. As a game type, we used supermodular games which have at least one pure NE and monotonically increasing property in their best responses. Apart from the previous studies which is based on sweeping all subcarriers to find the ones which have the highest utility, we picked random subcarriers as many as user needs and look at the payoffs of only those subcarriers. Our simulation results showed that we achieved similar results with the previous studies in terms of increasing utility, capacity and throughput levels. This remarkably decreases the the feedback loads on the SUs on the expense of slow convergence rate. At the same time, this saves the battery power in the mobile devices.

In the third chapter, we presented the resource allocation techniques with the usage of RAs in UEs. Since RAs have different radiation states that may lead to different channel conditions, they provide different gains for each state. By utilizing this feature of RAs, we showed that RA can improve the total system capacity. We used two different algorithms, namely RS and BeS. While a player selects the best resources with the best state in each iteration in the BeS algorithm, it chooses again the best resources but with one randomly selected state in the RS algorithm. The aim in the RS algorithm is to decrease the FL. According to our results, if an RA has two

states, the resulting FL obtained is lower in RS. If there are more than three states, then the BeS algorithm provides lower FL. Our results also show that when the number of states increases, the total system capacity increases as well. By comparing the beam width dependable capacity results, we obtained that the highest mean capacity is achieved with 60° beam width. Also, by performing APSS before the game starts, we showed that, instead of dealing with many states such as four or five states, the two-state selection case gives similar performance results to six states selection case.

In the fourth chapter, we proposed POFMT within game theoretical framework. In orthogonal frequency-division multiple accessing technique, resources are allocated accordingly to manage the interference between users when the whole network is controlled by a central unit. However, in uncoordinated networks, it is impossible to establish coordination among users, which leads to increasing interference in the shared environment. To decrease the interference in uncoordinated networks, POFMT was proposed within game theoretical framework in this chapter. As players, users introduced joint partially overlapping in frequency and space domains. While frequency domain partially overlapping was fulfilled by giving intentional CFS, RAs were utilized to introduce space domain partially overlapping. The system was evaluated with various subcarrier spacing and filter control parameter values to show the advantages of partially overlapping in only frequency domain. It is found that increasing subcarrier spacing decreases the interference in the system. Also, when the filter control parameter decreases, the system gain increases. With the utilization of RAs, the system performance is shown to increase further.

In the fifth chapter, we presented the game theoretical resource allocation with POFMT in cognitive HetNets. In cognitive HetNets, the users are affected by the high interference coming from the other users in the environment. To mitigate this interference, in this chapter, we proposed the game theoretical resource allocation with POFMT in cognitive HetNets. While SBSs look for the consecutive subcarriers which have the highest utility, they also perform the CFS. By jointly selecting the subcarriers and FSR, the system performance was significantly increased in terms of the capacity gain with the expense of slight loss in spectral efficiency. It is noted that the POFMT concept is offered for cognitive HetNets where significant other user interference is possessed. On the other hand, asynchronous transmission is also allowed with POFMT. Due to the constraint

we introduced, the convergence rate to NE becomes slower when compared to OFDM. While this concept can be implemented in 4G cognitive HetNets, this can also be considered for the future generations' cognitive HetNets.

In the sixth chapter, we presented a wireless channel control concept based on spatial adaptation of antenna arrays. Small wavelengths at mm-wave bands make it possible to apply this concept within compact devices. Recently introduced microfluidically reconfigurable RF devices can achieve these spatial adaptations efficiently and in a simple way by keeping the feed networks and control devices (such as phase shifters) stationary. Specifically, a 5 element 28 GHz antenna array design that achieve spatial adaptation over a 4.5λ distance via microfluidics was discussed. Subsequently, its performance was utilized in example wireless link and system level scenarios. This spatially adaptive antenna array provided 2 bit/s/Hz capacity gain over its traditional counterpart. In addition, 51% increment in the mean SINR can be obtained in the wireless communications system when the array acquired the spatial adaptation capability.

In this dissertation, possible extensions can be listed as follows:

1. For the studies where we utilized the RAs, it is assumed that only the SUs are equipped with RAs. The scenario where PUs, SBSs and PBS are all equipped with RAs or any combination of them in the network needs further investigation.

2. For resource allocation studies, learning algorithm can be applied. If the SU learns from previous actions, it can utilize this information to decrease the FL further.

3. For POFMT study, it is assumed that the time domain synchronization is perfectly obtained. For the scenario where there are multiple SUs served by one SBS, i.e., there will be multiple SBSs with multiple SUs, SUs have to satisfy the time synchronization with their single BS. So, this needs further investigation.

4. For POFMT study, another extension can be considered as finding the optimum subcarrier spacing.

5. For channel control study, future work can focus on experimental verification of the presented antenna array and investigation of the wireless link/system level performances under different scenarios such as for broadband systems.

REFERENCES

[1] [Online]. Available: http://apps.fcc.gov/ecfs/document/view?id=7020396128

[2] V. Chandrasekhar, J. Andrews, and A. Gatherer, "Femtocell networks: a survey," *IEEE Communications Magazine*, vol. 46, no. 9, pp. 59–67, 2008.

[3] J. V. Neumann and O. Morgenstern, *Theory of games and economic behavior*. Princeton University Press, 1944.

[4] J. Nash, "Non-cooperative games," *The Annals of Mathematics*, vol. 54, no. 2, pp. 286–295, 1951.

[5] E. J. Hong, S. Y. Yun, and D.-H. Cho, "Decentralized power control scheme in femtocell networks: A game theoretic approach," in *IEEE 20th International Symp. on Personal, Indoor and Mobile Radio Communications*, Sept 2009, pp. 415–419.

[6] D. Monderer and L. S. Shapley, "Potential games," *Games and Economic Behavior*, vol. 14, no. 1, pp. 124 – 143, 1996.

[7] *Physical Channels and Modulation (Release 11)*, 3GPP TS 36.211 V11.0.0 Std., September 2012.

[8] I. Sesia, Stefania; Toufik and M. Baker, *LTE The UMTS Long Term Evolution From Theory to Practice*. A John Wiley and Sons, 2009.

[9] O. Gharehshiran, A. Attar, and V. Krishnamurthy, "Collaborative sub-channel allocation in cognitive LTE femto-cells: A cooperative game-theoretic approach," *IEEE Trans. Commun.*, vol. 61, pp. 325–334, January 2013.

[10] S. Guruacharya, D. Niyato, D. I. Kim, and E. Hossain, "Hierarchical competition for downlink power allocation in OFDMA femtocell networks," *IEEE Trans. Wireless Commun.*, vol. 12, pp. 1543–1553, April 2013.

[11] S. Parsaeefard, M. van der Schaar, and A. Sharafat, "Robust power control for heterogeneous users in shared unlicensed bands," *IEEE Trans. Wireless Commun.*, vol. 13, pp. 3167–3182, June 2014.

[12] R. Xie, F. Yu, H. Ji, and Y. Li, "Energy-efficient resource allocation for heterogeneous cognitive radio networks with femtocells," *IEEE Trans. Wireless Commun.*, vol. 11, pp. 3910–3920, November 2012.

[13] S. Bu, F. Yu, and H. Yanikomeroglu, "Interference-aware energy-efficient resource allocation for OFDMA-based heterogeneous networks with incomplete channel state information," *IEEE Trans. Veh. Technol.*, vol. 64, no. 3, pp. 1036–1050, 2015.

[14] Y. Xiao, G. Bi, D. Niyato, and L. DaSilva, "A hierarchical game theoretic framework for cognitive radio networks," *IEEE J. Sel. Areas Commun.*, vol. 30, pp. 2053–2069, November 2012.

[15] K. Akkarajitsakul, "Distributed resource allocation in wireless networks under uncertainty and application of Bayesian game," *IEEE Commun. Mag.*, vol. 49, pp. 120–127, 2011.

[16] Q. D. La, Y. H. Chew, and B. H. Soong, "Performance analysis of downlink multi-cell OFDMA systems based on potential game," *IEEE Trans. Wireless Commun.*, vol. 11, pp. 3358–3367, September 2012.

[17] S. Buzzi, G. Colavolpe, D. Saturnino, and A. Zappone, "Potential games for energy-efficient power control and subcarrier allocation in uplink multicell OFDMA systems," *IEEE J. Sel. Topics Signal Process.*, vol. 6, pp. 89–103, April 2012.

[18] L. Liang and G. Feng, "A game-theoretic framework for interference coordination in OFDMA relay networks," *IEEE Trans. Veh. Technol.*, vol. 61, pp. 321–332, Jan. 2012.

[19] B. Danobeitia, G. Femenias, and F. Riera-Palou, "An optimization framework for scheduling and resource allocation in multi-stream heterogeneous mimo-ofdma wireless networks," in *IFIP Wireless Days (WD)*, 2012, pp. 1–3.

[20] J. Smith, E. Chong, A. Maciejewski, and H. Siegel, "Decentralized market-based resource allocation in a heterogeneous computing system," in *IEEE International Symposium on Parallel and Distributed Processing (IPDPS)*, 2008, pp. 1–12.

[21] S. Sardellitti and S. Barbarossa, "Joint optimization of collaborative sensing and radio resource allocation in small-cell networks," *IEEE Transactions on Signal Processing*, vol. 61, no. 18, pp. 4506–4520, 2013.

[22] P. Xue, P. Gong, J. H. Park, D. Park, and D. K. Kim, "Max-min fairness based radio resource management in fourth generation heterogeneous networks," in *9th International Symposium on Communications and Information Technology (ISCIT)*, 2009, pp. 208–213.

[23] J. T. Bernhard, *Reconfigurable Antennas*. Morgan & Claypool Publishers, 2007.

[24] D. Rodrigo, B. Cetiner, and L. Jofre, "Frequency, radiation pattern and polarization reconfigurable antenna using a parasitic pixel layer," *IEEE Trans. Antennas and Propag.*, vol. 62, no. 6, pp. 3422–3427, June 2014.

[25] A.-H. Tsai, L.-C. Wang, J.-H. Huang, and R.-B. Hwang, "Stable subchannel allocation for OFDMA femtocells with switched multi-beam directional antennas," in *IEEE Global Telecommunications Conf. (GLOBECOM 2011)*, Dec 2011, pp. 1–6.

[26] P. Mookiah and K. Dandekar, "Enhancing wireless security through reconfigurable antennas," in *IEEE Radio and Wireless Symp. (RWS)*, 2010, pp. 593–596.

[27] P. Martin, P. Smith, and R. Murch, "Improving space-time code performance in slow fading channels using reconfigurable antennas," *IEEE Communications Letters*, vol. 16, no. 4, pp. 494–497, 2012.

[28] A. Sayeed and V. Raghavan, "Maximizing MIMO capacity in sparse multipath with reconfigurable antenna arrays," *IEEE J. Sel. Topics Signal Process.*, vol. 1, pp. 156–166, 2007.

[29] J. Boerman and J. Bernhard, "Performance study of pattern reconfigurable antennas in MIMO communication systems," *IEEE Trans. Antennas Propag.*, vol. 56, pp. 231–236, 2008.

[30] F. Fazel, A. Grau, H. Jafarkhani, and F. Flaviis, "Space-time-state block coded MIMO communication systems using reconfigurable antennas," *IEEE Trans. Wireless Commun.*, vol. 8, no. 12, pp. 6019–6029, 2009.

[31] T. Gou, C. Wang, and S. Jafar, "Aiming perfectly in the dark-blind interference alignment through staggered antenna switching," *IEEE Trans. Signal Process.*, vol. 59, pp. 2734–2744, June 2011.

[32] A. Sahin, E. Bala, I. Guvenc, R. Yang, and H. Arslan, "Partially overlapping tones for uncoordinated networks," *IEEE Trans.Commun.*, vol. 62, pp. 3363–3375, Sept 2014.

[33] R. E. B. S. Mishra, A. and W. Arbaugh, "Exploiting partially overlapping channels in wireless networks: Turning a peril into an advantage," in *5th ACM SIGCOMM Conf. on Internet Measurement*, 2005.

[34] C. Saraydar, N. B. Mandayam, and D. Goodman, "Efficient power control via pricing in wireless data networks," *IEEE Trans. Commun.*, vol. 50, pp. 291–303, 2002.

[35] S. Hamouda, Z. Bennour, S. Tabbane, and A. Morell, "A game theoretic power control scheme for femtocells under macro-user QoS constraint," in *IEEE 23rd International Symp. on Personal Indoor and Mobile Radio Communications (PIMRC)*, Sept 2012, pp. 243–247.

[36] S. Ekin, M. Abdallah, K. Qaraqe, and E. Serpedin, "Random subcarrier allocation in OFDM-based cognitive radio networks," *IEEE Trans. Signal Process.*, vol. 60, pp. 4758–4774, 2012.

[37] M. Yilmaz and H. Arslan, "Game theoretical partially overlapping filtered multi-tones in cognitive heterogeneous networks," in *IEEE Military Communications Conf. (MILCOM)*, Oct 2014, pp. 411–415.

[38] G. Cherubini, E. Eleftheriou, and S. Olcer, "Filtered multitone modulation for very high-speed digital subscriber lines," *IEEE J. Sel. Areas Commun.*, vol. 20, pp. 1016–1028, Jun 2002.

[39] D. Lopez-Perez, I. Guvenc, G. De la Roche, M. Kountouris, T. Quek, and J. Zhang, "Enhanced intercell interference coordination challenges in heterogeneous networks," *IEEE Wireless Commun.*, vol. 18, no. 3, pp. 22–30, 2011.

[40] S. Lu, Y. Sun, Y. Ge, E. Dutkiewicz, and J. Zhou, "Joint power and rate control in ad hoc networks using a supermodular game approach," in *IEEE Wireless Communications and Networking Conference (WCNC)*, 2010, pp. 1–6.

[41] Z. Lu, Y. Yang, X. Wen, Y. Ju, and W. Zheng, "A cross-layer resource allocation scheme for icic in lte-advanced," *Journal of Network and Computer Applications*, vol. 34, no. 6, pp. 1861 – 1868, 2011. [Online]. Available: http://www.sciencedirect.com/science/article/pii/S1084804511000063

[42] J. Zheng, Y. Cai, and D. Wu, "Subcarrier allocation based on correlated equilibrium in multi-cell ofdma systems," *EURASIP Journal on Wireless Communications and Networking*, vol. 2012, no. 1, p. 233, 2012. [Online]. Available: http://jwcn.eurasipjournals.com/content/2012/1/233

[43] K. Tourki, K. Qaraqe, and M.-S. Alouini, "Outage analysis for underlay cognitive networks using incremental regenerative relaying," *IEEE Trans. Veh. Technol.*, vol. 62, pp. 721–734, Feb 2013.

[44] *3rd Generation Partnership Project; Technical Specification Group Radio Access Network; Spatial channel model for Multiple Input Multiple Output (MIMO) simulations (Release 10)*, 3GPP TR 25.996 V10.0.0 (2011-03) Std.

[45] A. Fattahi and F. Paganini, "New economic perspectives for resource allocation in wireless networks," in *Proceedings of the 2005 American Control Conference*, June 2005, pp. 3960–3965 vol. 6.

[46] S. M. Perlaza, E. V. Belmega, S. Lasaulce, and M. Debbah, "On the base station selection and base station sharing in self-configuring networks," in *Proceedings of the Fourth International ICST Conference on Performance Evaluation Methodologies and Tools*, ser. VALUETOOLS '09, 2009.

[47] H. Wu, H. Xia, C. Feng, and S. Li, "Interference mitigation in two-tier OFDMA femtocell networks: A potential game approach," in *International Conference on Wireless Communications Signal Processing (WCSP)*, Oct 2012.

[48] P. Dubey, O. Haimanko, and A. Zapechelnyuk, "Strategic complements and substitutes, and potential games," *Games and Economic Behavior*, vol. 54, no. 1, pp. 77 – 94, 2006.

[49] *IST-4-027756 WINNER II D1.1.2 V1.1, WINNER II Channel Models, Part I Channel Models*, Std.

[50] *Further Advancements for E-UTRA Physical Layer Aspects*, 3GPP TR 36.814 V9.0.0 Std., March 2010.

[51] M. Yilmaz, M. Abdallah, K. Qaraqe, and H. Arslan, "Random subcarrier allocation with supermodular game in cognitive heterogeneous networks," in *IEEE Wireless Communications and Networking Conf. (WCNC)*, April 2014, pp. 1450–1455.

[52] P. Mertikopoulos, E. Belmega, A. Moustakas, and S. Lasaulce, "Distributed learning policies for power allocation in multiple access channels," *IEEE J. Sel. Areas Commun.*, vol. 30, pp. 96–106, January 2012.

[53] A. Mishra, V. Shrivastava, S. Banerjee, and W. Arbaugh, "Partially overlapped channels not considered harmful," *SIGMETRICS Perform. Eval. Rev.*, vol. 34, no. 1, pp. 63–74, Jun. 2006.

[54] H. X. Hoque, M.A. and F. Afroz, "Multiple radio channel assignement utilizing partially overlapped channels," in *IEEE Global Telecommunications Conf. (GLOBECOM)*, Nov 2009, pp. 1–7.

[55] V. R. Liu, Y. and C. Li, "Channel assignment exploiting partially overlapping channels for wireless mesh networks," in *IEEE Global Telecommunications Conf. (GLOBECOM)*, Nov 2009, pp. 1–5.

[56] Y. Ding, Y. Huang, G. Zeng, and L. Xiao, "Using partially overlapping channels to improve throughput in wireless mesh networks," *IEEE Trans. Mobile Computing*, vol. 11, no. 11, pp. 1720–1733, Nov 2012.

[57] Y. Xu, Q. Wu, J. Wang, L. Shen, and A. Anpalagan, "Opportunistic spectrum access using partially overlapping channels: Graphical game and uncoupled learning," *IEEE Trans. Commun.*, vol. 61, pp. 3906–3918, September 2013.

[58] P. Duarte, Z. Fadlullah, A. Vasilakos, and N. Kato, "On the partially overlapped channel assignment on wireless mesh network backbone: A game theoretic approach," *IEEE J. Sel. Areas Commun.*, vol. 30, pp. 119–127, January 2012.

[59] M. Klimm, "Competition for resources: The equilibrium existence problem in congestion games," Ph.D. dissertation, 2012.

[60] N. Chamok and M. Ali, "A 5 ghz beam steering array for portable wireless MIMO application," in *Antennas and Propagation Society International Symp. (APSURSI), 2014 IEEE*, July 2014, pp. 1656–1657.

[61] M. Yilmaz, M. Abdallah, K. Qaraqe, and H. Arslan, "On the performance of subcarrier allocation techniques for multiuser OFDM cognitive networks with reconfigurable antennas," in *IEEE Global Communications Conference (GLOBECOM)*, 2014, pp. 1059–1064.

[62] G. E. Bottomley, *Channel Equalization for Wireless Communications: From Concepts to Detailed Mathematics*. Wiley-IEEE Press, July, 2011.

[63] S. Jin, X. Liang, K. K. Wong, X. Gao, and Q. Zhu, "Ergodic rate analysis for multipair massive MIMO two-way relay networks," *IEEE Trans. Wireless Commun.*, vol. 14, no. 3, pp. 1480–1491, 2015.

[64] A. Dey and G. Mumcu, "Microfluidically controlled frequency-tunable monopole antenna for high-power applications," *IEEE Antennas and Wireless Propagation Letters*, vol. 15, pp. 226–229, 2016.

[65] T. Palomo and G. Mumcu, "Microfluidically reconfigurable metallized plate loaded frequency-agile rf bandpass filters," *IEEE Transactions on Microwave Theory and Techniques*, vol. 64, no. 1, pp. 158–165, 2016.

[66] A. A. Gheethan, A. Dey, and G. Mumcu, "Passive feed network designs for microfluidic beam-scanning focal plane arrays and their performance evaluation," *IEEE Transactions on Antennas and Propagation*, vol. 63, no. 8, pp. 3452–3464, 2015.

[67] S. Rangan, T. S. Rappaport, and E. Erkip, "Millimeter-wave cellular wireless networks: Potentials and challenges," *Proceedings of the IEEE*, vol. 102, no. 3, pp. 366–385, March 2014.

[68] M. H. Yilmaz, M. M. Abdallah, H. M. El-Sallabi, J. F. Chamberland, K. A. Qaraqe, and H. Arslan, "Joint subcarrier and antenna state selection for cognitive heterogeneous networks with reconfigurable antennas," *IEEE Transactions on Communications*, vol. 63, no. 11, pp. 4015–4025, Nov 2015.

APPENDICES

Appendix A: Copyright Permissions

The copyright notice for the use of material in Chapter 2 is below.

Title:	Random subcarrier allocation with supermodular game in cognitive heterogeneous networks
Conference Proceedings:	Wireless Communications and Networking Conference (WCNC), 2014 IEEE
Author:	Mustafa Harun Yilmaz
Publisher:	IEEE
Date:	April 2014

Thesis / Dissertation Reuse

The IEEE does not require individuals working on a thesis to obtain a formal reuse license, however, you may print out this statement to be used as a permission grant:

Requirements to be followed when using any portion (e.g., figure, graph, table, or textual material) of an IEEE copyrighted paper in a thesis:

1) In the case of textual material (e.g., using short quotes or referring to the work within these papers) users must give full credit to the original source (author, paper, publication) followed by the IEEE copyright line © 2011 IEEE.
2) In the case of illustrations or tabular material, we require that the copyright line © [Year of original publication] IEEE appear prominently with each reprinted figure and/or table.
3) If a substantial portion of the original paper is to be used, and if you are not the senior author, also obtain the senior author's approval.

Requirements to be followed when using an entire IEEE copyrighted paper in a thesis:

1) The following IEEE copyright/ credit notice should be placed prominently in the references: © [year of original publication] IEEE. Reprinted, with permission, from [author names, paper title, IEEE publication title, and month/year of publication]
2) Only the accepted version of an IEEE copyrighted paper can be used when posting the paper or your thesis on-line.
3) In placing the thesis on the author's university website, please display the following message in a prominent place on the website: In reference to IEEE copyrighted material which is used with permission in this thesis, the IEEE does not endorse any of [university/educational entity's name goes here]'s products or services. Internal or personal use of this material is permitted. If interested in reprinting/republishing IEEE copyrighted material for advertising or promotional purposes or for creating new collective works for resale or redistribution, please go to http://www.ieee.org/publications_standards/publications/rights/rights_link.html to learn how to obtain a License from RightsLink.

If applicable, University Microfilms and/or ProQuest Library, or the Archives of Canada may supply single copies of the dissertation.

Appendix A (Continued)

The copyright notice for the use of material in Chapter 3 is below.

Title: Joint Subcarrier and Antenna State Selection for Cognitive Heterogeneous Networks With Reconfigurable Antennas

Author: Mustafa Harun Yılmaz; Mohamed M. Abdallah; Hassan M. El-Sallabi; Jean-François Chamberland; Khalid A. Qaraqe; Hüseyin Arslan

Publication: Communications, IEEE Transactions on

Publisher: IEEE

Date: Nov. 2015

Thesis / Dissertation Reuse

The IEEE does not require individuals working on a thesis to obtain a formal reuse license, however, you may print out this statement to be used as a permission grant:

Requirements to be followed when using any portion (e.g., figure, graph, table, or textual material) of an IEEE copyrighted paper in a thesis:

1) In the case of textual material (e.g., using short quotes or referring to the work within these papers) users must give full credit to the original source (author, paper, publication) followed by the IEEE copyright line © 2011 IEEE.
2) In the case of illustrations or tabular material, we require that the copyright line © [Year of original publication] IEEE appear prominently with each reprinted figure and/or table.
3) If a substantial portion of the original paper is to be used, and if you are not the senior author, also obtain the senior author's approval.

Requirements to be followed when using an entire IEEE copyrighted paper in a thesis:

1) The following IEEE copyright/ credit notice should be placed prominently in the references: © [year of original publication] IEEE. Reprinted, with permission, from [author names, paper title, IEEE publication title, and month/year of publication]
2) Only the accepted version of an IEEE copyrighted paper can be used when posting the paper or your thesis on-line.
3) In placing the thesis on the author's university website, please display the following message in a prominent place on the website: In reference to IEEE copyrighted material which is used with permission in this thesis, the IEEE does not endorse any of [university/educational entity's name goes here]'s products or services. Internal or personal use of this material is permitted. If interested in reprinting/republishing IEEE copyrighted material for advertising or promotional purposes or for creating new collective works for resale or redistribution, please go to http://www.ieee.org/publications_standards/publications/rights/rights_link.html to learn how to obtain a License from RightsLink.

If applicable, University Microfilms and/or ProQuest Library, or the Archives of Canada may supply single copies of the dissertation.

Appendix A (Continued)

The copyright notice for the use of material in Chapter 5 is below.

Title: Resource Allocation With Partially Overlapping Filtered Multitone in Cognitive Heterogeneous Networks
Author: Mustafa Harun Ylmaz; Hüseyin Arslan
Publication: IEEE Communications Letters
Publisher: IEEE
Date: May 2016
Copyright © 2016, IEEE

LOGIN

If you're a copyright.com user, you can login to RightsLink using your copyright.com credentials. Already **a RightsLink user** or want to learn more?

Thesis / Dissertation Reuse

The IEEE does not require individuals working on a thesis to obtain a formal reuse license, however, you may print out this statement to be used as a permission grant:

Requirements to be followed when using any portion (e.g., figure, graph, table, or textual material) of an IEEE copyrighted paper in a thesis:

1) In the case of textual material (e.g., using short quotes or referring to the work within these papers) users must give full credit to the original source (author, paper, publication) followed by the IEEE copyright line © 2011 IEEE.
2) In the case of illustrations or tabular material, we require that the copyright line © [Year of original publication] IEEE appear prominently with each reprinted figure and/or table.
3) If a substantial portion of the original paper is to be used, and if you are not the senior author, also obtain the senior author's approval.

Requirements to be followed when using an entire IEEE copyrighted paper in a thesis:

1) The following IEEE copyright/ credit notice should be placed prominently in the references: © [year of original publication] IEEE. Reprinted, with permission, from [author names, paper title, IEEE publication title, and month/year of publication]
2) Only the accepted version of an IEEE copyrighted paper can be used when posting the paper or your thesis on-line.
3) In placing the thesis on the author's university website, please display the following message in a prominent place on the website: In reference to IEEE copyrighted material which is used with permission in this thesis, the IEEE does not endorse any of [university/educational entity's name goes here]'s products or services. Internal or personal use of this material is permitted. If interested in reprinting/republishing IEEE copyrighted material for advertising or promotional purposes or for creating new collective works for resale or redistribution, please go to http://www.ieee.org/publications_standards/publications/rights/rights_link.html to learn how to obtain a License from RightsLink.

If applicable, University Microfilms and/or ProQuest Library, or the Archives of Canada may supply single copies of the dissertation.

Appendix A (Continued)

The copyright notice for the use of material in Chapter 6 is below.

Title: Millimeter-Wave Wireless Channel Control using Spatially Adaptive Antenna Arrays
Author: Mustafa Yilmaz; Ertugrul Guvenkaya; Gokhan Mumcu; Huseyin Arslan
Publication: IEEE Communications Letters
Publisher: IEEE
Date: Dec, 2016

Thesis / Dissertation Reuse

The IEEE does not require individuals working on a thesis to obtain a formal reuse license, however, you may print out this statement to be used as a permission grant:

Requirements to be followed when using any portion (e.g., figure, graph, table, or textual material) of an IEEE copyrighted paper in a thesis:

1) In the case of textual material (e.g., using short quotes or referring to the work within these papers) users must give full credit to the original source (author, paper, publication) followed by the IEEE copyright line © 2011 IEEE.
2) In the case of illustrations or tabular material, we require that the copyright line © [Year of original publication] IEEE appear prominently with each reprinted figure and/or table.
3) If a substantial portion of the original paper is to be used, and if you are not the senior author, also obtain the senior author's approval.

Requirements to be followed when using an entire IEEE copyrighted paper in a thesis:

1) The following IEEE copyright/ credit notice should be placed prominently in the references: © [year of original publication] IEEE. Reprinted, with permission, from [author names, paper title, IEEE publication title, and month/year of publication]
2) Only the accepted version of an IEEE copyrighted paper can be used when posting the paper or your thesis on-line.
3) In placing the thesis on the author's university website, please display the following message in a prominent place on the website: In reference to IEEE copyrighted material which is used with permission in this thesis, the IEEE does not endorse any of [university/educational entity's name goes here]'s products or services. Internal or personal use of this material is permitted. If interested in reprinting/republishing IEEE copyrighted material for advertising or promotional purposes or for creating new collective works for resale or redistribution, please go to http://www.ieee.org/publications_standards/publications/rights/rights_link.html to learn how to obtain a License from RightsLink.

If applicable, University Microfilms and/or ProQuest Library, or the Archives of Canada may supply single copies of the dissertation.

Appendix B: List of Acronyms

APSS	Adaptive prior state selection
AWGN	Additive white Gaussian noise
BeS	Best selection
BS	Base station
CDF	Cumulative distribution function
CFO	Carrier frequency offset
CFR	Channel frequency response
CFS	Carrier frequency shift
CIR	Channel impulse response
CoP	Continuous play
FBS	Femto BS
FIP	Finite improvement path
FL	Feedback load
FMT	Filtered multitone
FO	Fully overlapping
FPSS	Fixed prior state selection
FSR	Frequency shift ratio
FUE	Femto user equipment
GF	Gaussian filter
GT	Game theory
HeNB	Enhanced Home Node B
HetNets	Heterogeneous networks
HPBW	Half power beamwidth
IT	Interference temperature
MIMO	Multiple-input multiple-output

Appendix B (Continued)

MUE	Macro user equipment
NE	Nash equilibrium
OFDMA	Orthogonal frequency-division multiple access
OFDM	Orthogonal frequency-division multiplexing
PBS	Primary base station
PCB	Printed circuit board
P'nW	Play&Wait
POCs	Partially overlapping channels
POFMT	Partially overlapping filtered multitone
POTs	Partially overlapping tones
PPP	Poisson point process
PU	Primary user
RA	Reconfigurable antenna
RRCF	Root raised cosine filter
RS	Random state selection
RSS	Received signal strength
SBS	Secondary base station
SG	Supermodular game
SINR	Signal-to-interference-plus-noise ratio
SIR	Signal-to-interference ratio
SISO	Single-input single-output
SU	Secondary user
TDD	Time division duplexing
UE	User equipment

ABOUT THE AUTHOR

Mustafa Harun Yılmaz was born in Bursa, Turkey. He received his B.S. degree from the department of electronic and computer teaching from Gazi University in Ankara, Turkey in 2007 and M.E. degree from Southern University and A&M College in Baton Rouge, Louisiana in 2010. He was with Texas A&M University at Qatar during the summer season in 2013 and 2014.

He has been working towards the Ph.D. degree as a Graduate Research Assistant in the department of Electrical Engineering, University of South Florida in Tampa, Florida since 2011. His research interests are interference coordination, interference management, resource allocation, signal identification and physical layer security, heterogeneous networks and cognitive radio.

He is with National Telecommunications and Information Administration under Department of Commerce in Boulder, Colorado as an electronics engineer.